

Majorana Neutrinos, Neutrino Mass Spectrum, CP-Violation and Neutrinoless Double β -Decay: I. The Three-Neutrino Mixing Case

S. M. Bilenky^(a,b), S. Pascoli^(b,c) and S. T. Petcov^(b,c) ¹

^(a) *Joint Institute for Nuclear Research, Dubna, Russia*

^(b) *Scuola Internazionale Superiore di Studi Avanzati, I-34014 Trieste, Italy*

^(c) *Istituto Nazionale di Fisica Nucleare, Sezione di Trieste, I-34014 Trieste, Italy*

Abstract

Assuming three-neutrino mixing and massive Majorana neutrinos, we study the implications of the neutrino oscillation solutions of the solar and atmospheric neutrino problems and of the results of the CHOOZ experiment for the predictions of the effective Majorana mass in neutrinoless double beta $((\beta\beta)_{0\nu})$ -decay, $|\langle m \rangle|$. The general case of CP-nonconservation is investigated. The predicted values of $|\langle m \rangle|$, which determines the magnitude of the $(\beta\beta)_{0\nu}$ -decay rate, depend strongly on the type of the neutrino mass spectrum, on the solution of the solar neutrino problem, as well as on the values of the two Majorana CP-violating phases, present in the lepton mixing matrix. We find that i) $|\langle m \rangle| \lesssim 0.02$ eV for a hierarchical neutrino mass spectrum, ii) $|\langle m \rangle| \lesssim 0.09$ eV if the spectrum is of the inverted hierarchy type, and iii) $|\langle m \rangle| \leq m$ in the case of three quasi-degenerate neutrinos, $m > 0$ being the common neutrino mass scale which is limited by the bounds from the ${}^3\text{H}$ β -decay experiments, $m < 2.5$ eV. The indicated maximal values of $|\langle m \rangle|$ are reached in the cases i), ii) and iii) respectively, for the large mixing angle (LMA) MSW solution, the small mixing angle (SMA) MSW, and for all current solutions, of the solar neutrino problem. If CP-invariance holds, $|\langle m \rangle|$ is very sensitive to the values of the relative CP-parities of the massive Majorana neutrinos. The cases of neutrino mass spectra which interpolate between the hierarchical or inverted hierarchy type and the quasi-degenerate one are also studied. The observation of the $(\beta\beta)_{0\nu}$ -decay with a rate corresponding to $|\langle m \rangle| \gtrsim 0.02$ eV can provide unique information on the neutrino mass spectrum. Combined with information on the lightest neutrino mass or the type of neutrino mass spectrum, it can give also information on the CP-violation in the lepton sector, and if CP-invariance holds - on the relative CP-parities of the massive Majorana neutrinos.

¹Also at: Institute of Nuclear Research and Nuclear Energy, Bulgarian Academy of Sciences, 1784 Sofia, Bulgaria

1 Introduction

The observation of a significant up-down asymmetry in the rate of (multi-GeV) μ -like events produced by the atmospheric ν_μ and $\bar{\nu}_\mu$ in the Super-Kamiokande experiment [1], brought to a new level the investigation of the neutrino mass and neutrino mixing problem: for the first time model-independent experimental evidence for neutrino oscillations was obtained. Important evidences for existence of neutrino mixing were found in the experiments with solar neutrinos as well: in all five experiments Homestake, Kamiokande, SAGE, GALLEX and Super-Kamiokande, which have provided data on the solar neutrino flux so far [2, 3, 4, 5, 6, 7] (see also [8, 9]), considerably smaller signals than expected [10] were observed. These results are compatible with a depletion of the solar ν_e flux on the way to the Earth, i.e., with a disappearance of the solar ν_e . Indications for $\bar{\nu}_\mu \leftrightarrow \bar{\nu}_e$ oscillations were reported by the accelerator LSND experiment [11].

The existing evidences for nonzero neutrino masses and neutrino mixing will be thoroughly tested in the next generation of neutrino oscillation experiments. The Super-Kamiokande results on the oscillations of the atmospheric neutrinos will be checked in the accelerator long baseline experiments K2K [12], MINOS [13] and in the CERN-Gran-Sasso (CNGS) experiment [14]; K2K is taking data while MINOS and CNGS experiments are under preparation. The solar neutrino experiments SNO [9], which began operation approximately an year and a half ago, and BOREXINO [15], and the reactor antineutrino experiment KamLAND [16], will provide new crucial information on the oscillations of solar neutrinos. Both BOREXINO and KamLAND detectors are under construction and are expected to be operative in 2002. The LSND results on $\bar{\nu}_\mu \leftrightarrow \bar{\nu}_e$ oscillations will be tested in the accelerator experiment MiniBooNE [17] which is under preparation.

The high intensity neutrino beams from a neutrino factory, with known and well-controlled spectra and fluxes, will allow to study the neutrino oscillation phenomena in considerable detail [18]. These studies can provide, in particular, a very precise information on the values of neutrino mass squared differences and of the elements of the neutrino (lepton) mixing matrix. The possibility to build a neutrino factory is extensively investigated at present [19].

There is no doubt that the indicated experimental studies will allow to make a big step forward in the understanding of the patterns of neutrino mass squared differences and of the neutrino mixing. However, no information about the absolute values of the neutrino masses and about the physical nature of the neutrinos with definite mass can be obtained in these experiments.

The problem of the nature of massive neutrinos (see, e.g., [20]) - are they Dirac particles possessing distinctive antiparticles, or Majorana fermions, i.e., truly neutral particles identical with their antiparticles, is one of the fundamental problems in the studies of neutrino mixing. In the minimal version of the Standard Theory the individual lepton charges L_e , L_μ and L_τ are conserved and neutrinos are massless. Massive Dirac neutrinos and neutrino mixing arise in gauge theories in which the lepton charges L_e , L_μ and L_τ are not conserved, but a specific combination of the latter, which could be the total lepton charge $L = L_e + L_\mu + L_\tau$, or, e.g., the charge [21] $L' = L_e - L_\mu + L_\tau$, is conserved. Thus, the existence of massive Dirac neutrinos is associated in gauge theories with massive neutrinos with the presence of a conserved lepton charge. Massive Majorana neutrinos arise if no lepton charge is conserved by the electroweak interactions. Thus, the question of the nature of massive neutrinos is directly related to the question of the fundamental symmetries of the elementary particle interactions.

The relative smallness of the neutrino masses, following from the data, can be naturally explained by the violation of the total lepton charge conservation at a scale which is much larger than the electroweak symmetry breaking scale ² [22]. In this case the neutrinos with definite mass are Majorana particles. Thus, establishing the Majorana nature of the massive neutrinos could imply the existence of a new fundamental scale in physics.

Experiments studying the oscillations of neutrinos cannot answer the question regarding the

²Let us note that this explanation is by no means unique.

nature of the massive neutrinos [23, 24]³. Neutrino oscillations, in particular, are not sensitive to the Majorana CP-violating phases [23, 26] which enter into the expression for the lepton mixing matrix in the case of massive Majorana neutrinos and which are absent if the massive neutrinos are Dirac particles. Thus, the neutrino oscillation experiments cannot provide also information on CP-violation caused by the Majorana CP-violating phases, and in the case of CP-invariance - on the relative CP-parities of the massive Majorana neutrinos.

The Majorana nature of the massive neutrinos can manifest itself in the existence of processes in which the total lepton charge L is not conserved and changes by two units, $\Delta L = 2$. The process most sensitive to the existence of massive Majorana neutrinos (coupled to the electron) is the neutrinoless double β ($(\beta\beta)_{0\nu}$ -) decay of certain even-even nuclei (see, e.g., [27, 20]):

$$(A, Z) \rightarrow (A, Z + 2) + e^- + e^-. \quad (1)$$

If the $(\beta\beta)_{0\nu}$ -decay is generated *only by the left-handed (LH) charged current weak interaction through the exchange of virtual massive Majorana neutrinos*, the probability amplitude of this process is proportional in the case of Majorana neutrinos having masses not exceeding few MeV to the so-called “effective Majorana mass parameter”

$$\langle m \rangle \equiv \sum_{j=1} U_{ej}^2 m_j, \quad (2)$$

where m_j is the mass of the Majorana neutrino ν_j and U_{ej} is the element of neutrino (lepton) mixing matrix.

A large number of experiments are searching for $(\beta\beta)_{0\nu}$ -decay of different nuclei at present (for a rather complete list see, e.g., [28]). No indications that this process takes place were found so far. A rather stringent constraint on the value of the effective Majorana mass parameter was obtained in the ⁷⁶Ge Heidelberg-Moscow experiment [29]:

$$|\langle m \rangle| < 0.35 \text{ eV}, \quad 90\% \text{ C.L.} \quad (3)$$

Taking into account a factor of 3 uncertainty associated with the calculation of the relevant nuclear matrix element (see, e.g., [27, 28]) we get

$$|\langle m \rangle| < (0.35 \div 1.05) \text{ eV}, \quad 90\% \text{ C.L.} \quad (4)$$

The IGEX collaboration has obtained [30]:

$$|\langle m \rangle| < (0.33 \div 1.35) \text{ eV}, \quad 90\% \text{ C.L.} \quad (5)$$

Considerably higher sensitivity to the value of $|\langle m \rangle|$ is planned to be reached in several $(\beta\beta)_{0\nu}$ -decay experiments of a new generation. The NEMO3 experiment [31], scheduled to start in 2001, will search for $(\beta\beta)_{0\nu}$ -decay of ¹⁰⁰Mo and ⁸²Se. In its first stage, after 5 years of data taking, this experiment will reach a sensitivity to values of $|\langle m \rangle| \cong 0.1 \text{ eV}$. A similar sensitivity is planned to be reached with the cryogenic detector CUORE [32] which will search for the $(\beta\beta)_{0\nu}$ -decay of ¹³⁰Te. An order of magnitude better sensitivity, i.e., to $|\langle m \rangle| \cong 10^{-2} \text{ eV}$, is planned to be achieved in the GENIUS experiment [33] utilizing one ton of enriched ⁷⁶Ge. Finally, there is a very interesting proposal [34] to study the $(\beta\beta)_{0\nu}$ -decay of ¹³⁶Xe in a background-free experiment with

³If the massive neutrinos are Majorana particles, e.g., the transitions $\nu_l \rightarrow \bar{\nu}_l$, $l = e, \mu, \tau$ are effectively possible [25]. However, the amplitudes of these transitions are proportional to the ratio m_j/E , m_j and E being the neutrino mass and energy. For the values of the neutrino masses suggested by the existing ³H β -decay data and the data on the oscillations of the solar and atmospheric neutrinos (see Section 2), $m_j \lesssim$ few eV, the transitions $\nu_l \rightarrow \bar{\nu}_l$ are unobservable at present.

detection of the two electrons and the ^+Ba atom in the final state. The estimated sensitivity of this experiment is $|\langle m \rangle| \cong (1 - 5) \times 10^{-2}$ eV.

Having in mind the future progress in the experimental searches for $(\beta\beta)_{0\nu}$ -decay, we derive in the present article the constraints on the effective Majorana mass that can be obtained from the analyzes of the latest neutrino oscillation data. More specifically, assuming three-neutrino mixing and massive Majorana neutrinos, we study in detail the implications of the neutrino oscillation fits of the solar and atmospheric neutrino data and of the results of the reactor long baseline CHOOZ and Palo Verde experiments, for the predictions of the effective Majorana mass parameter $|\langle m \rangle|$, which controls the $(\beta\beta)_{0\nu}$ -decay rate. We consider the possible types of neutrino mass spectrum: hierarchical, with two quasi-degenerate in mass Majorana neutrinos (the third having a different mass), and with three quasi-degenerate Majorana neutrinos. In the case of two quasi-degenerate massive neutrinos, the neutrino mass spectrum can be of three varieties - with inverted hierarchy, with partial hierarchy and with partial inverted hierarchy, and they are also considered in this paper.

The indicated approach for obtaining the values of $|\langle m \rangle|$ which are compatible with solar, atmospheric and accelerator neutrino oscillation data was first used in ref. [35] and in ref. [36]. In ref. [37] it was noticed that in the case of neutrino mass spectrum with inverted hierarchy and the large mixing angle (LMA) MSW solution of the solar neutrino problem, the measurement of $|\langle m \rangle|$ can give information about the CP-violation in the lepton sector, induced by the Majorana CP-violating phases⁴. Various aspects of CP-violation in the lepton sector, generated by the Majorana CP-violating phases, were studied, e.g., in [38, 39, 40, 41]. The approach indicated above was further exploited, e.g., in refs. [42, 43, 44, 45]. In the articles [46, 47, 48], in which the solar and atmospheric neutrino data available in 1998 - 1999 were used, it was concluded, in particular, that the observation of the $(\beta\beta)_{0\nu}$ -decay with a rate within the sensitivity of the next generation of $(\beta\beta)_{0\nu}$ -decay experiments can give information about the neutrino mass spectrum. Further analyzes along the indicated lines were performed more recently in [49, 50, 51, 52, 53].

In the present study we investigate the general case of CP-nonconservation and we use the results of the analyzes of the latest solar and atmospheric neutrino data. For each of the five types of possible neutrino mass spectrum indicated above we give detailed predictions for $|\langle m \rangle|$ for the three solutions of the solar neutrino problem, favored by the current solar neutrino data: the LMA MSW, the small mixing angle (SMA) MSW, the LOW - quasi-vacuum oscillation (LOW-QVO) one. In each case we identify the “just-CP-violation” region of values of $|\langle m \rangle|$: a value of $|\langle m \rangle|$ in this region would unambiguously signal the existence of CP-violation in the lepton sector, caused by Majorana CP-violating phases. Analyzing the case of CP-conservation, we derive predictions for $|\langle m \rangle|$ corresponding to all possible values of the relative CP-parities of the three massive Majorana neutrinos for the five different types of neutrino mass spectrum. The possibility of cancellation between the different terms contributing to $|\langle m \rangle|$ is investigated. We identify the cases when such a cancellation is impossible and there exist non-trivial lower bounds on $|\langle m \rangle|$ and we give these bounds. We find, in particular, that the observation of the $(\beta\beta)_{0\nu}$ -decay with a rate corresponding to $|\langle m \rangle| \gtrsim 0.02$ eV can provide unique information on the neutrino mass spectrum. Combined with data on the mass of the lightest neutrino or/and on the type of neutrino mass spectrum, it can give also information on the CP-violation in the lepton sector, and if CP-invariance holds - on the relative CP-parities of the massive Majorana neutrinos.

In the present article we consider only the mixing of the three flavour neutrinos, involving three massive Majorana neutrinos. We assume that the $(\beta\beta)_{0\nu}$ -decay is induced by the (V-A) charged current weak interaction via the exchange of the massive Majorana neutrinos. Results for the case of four-neutrino mixing will be presented in a separate publication [54].

⁴Let us note that the most recent solar neutrino data from the Super-Kamiokande experiment favors the LMA MSW solution of the solar neutrino problem.

2 Neutrino Masses and Mixing from the Existing Data

We summarize in the present Section the data on the neutrino masses, neutrino mass squared differences and on the neutrino (lepton) mixing which will be used in our further analyzes.

Strong evidences for neutrino oscillations have been obtained in the experiments with atmospheric and solar neutrinos. The Super-Kamiokande atmospheric neutrino data [1, 55] is best interpreted in terms of (dominant) $\nu_\mu \rightarrow \nu_\tau$ and $\bar{\nu}_\mu \rightarrow \bar{\nu}_\tau$ oscillations [55]. Assuming two-neutrino mixing, one obtains a description of the data at 90 (99)% C.L. for the following values of the relevant two-neutrino oscillation parameters - the mass-squared difference Δm_{atm}^2 and the mixing angle θ_{atm} [55]:

$$2.0 (1.5) \times 10^{-3} \text{eV}^2 \leq |\Delta m_{\text{atm}}^2| \leq 6.5 (8.0) \times 10^{-3} \text{eV}^2, \quad (6)$$

$$0.87 (0.75) \leq \sin^2(2\theta_{\text{atm}}) \leq 1. \quad (7)$$

The sign of Δm_{atm}^2 is undetermined by the data. The best fit value of $|\Delta m_{\text{atm}}^2|$ found in [55] is: $|\Delta m_{\text{atm}}^2|_{\text{BF}} = 3.2 \times 10^{-3} \text{eV}^2$.

Global neutrino oscillation analyzes of the most recent solar neutrino data [2, 4, 5, 7, 8] were performed, e.g., in refs. [7, 56, 57, 58]. The new high precision Super-Kamiokande results [7] on the spectrum of the recoil electrons and on the day-night (D-N) effect were included in the analyzes. In refs. [7, 56, 57] the solar neutrino data were analyzed in terms of the hypothesis of two-neutrino oscillations of solar neutrinos, characterized by the two parameters $\Delta m_{\odot}^2 > 0$ and θ_{\odot} (or $\tan^2 \theta_{\odot}$). In ref. [58] a three-neutrino oscillation analysis was performed (see further). The regions of the large mixing angle (LMA) MSW, small mixing angle (SMA) MSW (see, e.g., [59, 60]), of the LOW and the quasi-vacuum oscillation (QVO) solutions of the solar neutrino problem (see, e.g., [56]), allowed by the data at a given C.L. were determined. The studies performed in refs. [7, 56, 57] showed, in particular, that i) a relatively large part of the previously allowed region of the SMA MSW $\nu_e \rightarrow \nu_{\mu(\tau)}$ transition solution is ruled out by the Super-Kamiokande data on the recoil- e^- spectrum and the D-N effect, ii) the LMA MSW $\nu_e \rightarrow \nu_{\mu(\tau)}$ transition solution provides a better description of the data than the SMA MSW solution, and that iii) the purely vacuum oscillation (VO) solution due to the $\nu_e \leftrightarrow \nu_{\mu(\tau)}$ oscillations (see, e.g., [61, 62]), as well as the VO and MSW solutions with solar ν_e transitions into a sterile neutrino (see e.g., [63]), ν_s , are strongly disfavored (if not ruled out) by the data. The Super-Kamiokande collaboration, using a method of analysis which is different from those employed in refs. [56, 57], rules out the SMA MSW $\nu_e \rightarrow \nu_{\mu(\tau)}$ transition solution at 95% C.L. In Tables 1 and 2 we give the results for the different solution regions derived in the two-neutrino $\nu_e \rightarrow \nu_{\mu(\tau)}$ transition/oscillation analyzes in refs. [7, 56]. The Super-Kamiokande collaboration [7] did not produce 99% C.L. results, so we quote and use only their 95% C.L. allowed regions.

Very important constraints on the oscillations of electron (anti-)neutrinos were obtained in the CHOOZ and Palo Verde disappearance experiments with reactor $\bar{\nu}_e$ [64, 65]. This experiment was sensitive to values of $\Delta m^2 \gtrsim 10^{-3} \text{eV}^2$, which includes the corresponding atmospheric neutrino region, eq. (5). No disappearance of the reactor $\bar{\nu}_e$ was observed. Performing a two-neutrino oscillation analysis, the following rather stringent upper bound on the value of the corresponding mixing angle, θ , was obtained by the CHOOZ collaboration ⁵ at 95% C.L. for $\Delta m^2 \geq 1.5 \times 10^{-3} \text{eV}^2$:

$$\sin^2 \theta < 0.09. \quad (8)$$

The precise upper limit in eq. (8) is Δm^2 -dependent. More concretely, it is a decreasing function of Δm^2 as Δm^2 increases up to $\Delta m^2 \simeq 6 \times 10^{-3} \text{eV}^2$ with a minimum value $\sin^2 \theta \simeq 1 \times 10^{-2}$.

⁵The possibility of large $\sin^2 \theta > 0.9$ which is admitted by the CHOOZ data alone is incompatible with the neutrino oscillation interpretation of the solar neutrino deficit (see, e.g., [36, 37, 60, 47]). Let us note also that the CHOOZ limit does not depend on the sign of Δm^2 : we have assumed that $\Delta m^2 > 0$ for convenience.

Table 1: Values of Δm_{\odot}^2 obtained in the analyzes of the solar neutrino data in refs. [7, 56, 58] and used in the present study (see text for details). The best fit values (B.F.V.) in the different solution regions are also given.

		Δm_{\odot}^2 [eV ²]	B.F.V. [eV ²]
Ref. [7] (95% C.L.)	LMA	$2.5 \times 10^{-5} \div 1.3 \times 10^{-4}$	4.0×10^{-5}
	LOW-QVO	$5.6 \times 10^{-8} \div 2.0 \times 10^{-7}$	
Ref. [56] (90 (99%) C.L.)	LMA	$1.6 (1.6) \times 10^{-5} \div 1.0 (1.0) \times 10^{-4}$	4.8×10^{-5}
	SMA	$(4.0 \times 10^{-6} \div 1.0 \times 10^{-5})$	8.0×10^{-6}
	LOW-QVO	$5.5 (0.4) \times 10^{-9} \div 1.4 (2.4) \times 10^{-8}$	1.0×10^{-9}
Ref. [58] (90 (99%) C.L.)	LMA	$1.6 (1.5) \times 10^{-5} \div 2.0 (2.0) \times 10^{-4}$	3.5×10^{-5}
	SMA	$4.0 (3.0) \times 10^{-6} \div 9.0 (10.0) \times 10^{-6}$	
	LOW-QVO	$8.0 (5.0) \times 10^{-10} \div 3.0 (4.0) \times 10^{-7}$	

Table 2: Values of θ_{\odot} obtained in the analyzes of the solar neutrino data in refs. [7, 56, 58] and used in the present study.

		$\tan^2 \theta_{\odot}$	B.F.V.
Ref. [7] (95% C.L.)	LMA	$0.21 \div 0.67$	0.38
	LOW-QVO	$0.3 \div 0.5$	
Ref. [56] (90 (99%) C.L.)	LMA	$0.20 (0.19) \div 0.6 (1.0)$	0.35
	SMA	$(1.2 \times 10^{-4} \div 1.8 \times 10^{-3})$	6.0×10^{-4}
	LOW-QVO	$0.57 (0.42) \div 0.90 (3.0)$	0.70
Ref. [58] (90 (99%) C.L.)	LMA	$0.18 (0.16) \div 1.0 (4.0)$	0.35
	SMA	$2.0 (1.0) \times 10^{-4} \div 2.0 (2.5) \times 10^{-3}$	
	LOW-QVO	$0.4 (0.2) \div 3.0 (4.0)$	

The upper limit becomes an increasing function of Δm^2 when the latter increases further up to $\Delta m^2 \simeq 8 \times 10^{-3}$ eV², where $\sin^2 \theta < 2 \times 10^{-2}$. Let us note that this dependence is accounted for, whenever necessary, in our analysis. The sensitivity to the value of the parameter $\sin^2 \theta$ is expected to be considerably improved by the MINOS experiment [13] in which the following upper limit can be reached:

$$\sin^2 \theta < 5 \times 10^{-3}. \quad (9)$$

As we have already mentioned, a comprehensive 3-flavour neutrino oscillation analysis of the most recent solar neutrino, atmospheric neutrino and CHOOZ data has recently been performed in ref. [58]. The analysis was done under the assumption $\Delta m_{\odot}^2 \ll |\Delta m_{\text{atm}}^2|$, suggested by the results of the two-neutrino oscillation studies [7, 56, 57]. As it follows from eq. (5), the indicated inequality holds for

$$\Delta m_{\odot}^2 \lesssim 2.0 \times 10^{-4} \text{ eV}^2, \quad (10)$$

i.e., for the SMA MSW and LOW-QVO solutions and in most of the LMA MSW solution region found in [7, 56, 57] (see Table 1). Under the condition $\Delta m_{\odot}^2 \ll |\Delta m_{\text{atm}}^2|$, the solar neutrino data

constrain the parameters Δm_{\odot}^2 , θ_{\odot} and θ (see, e.g., [47, 60] and the references quoted therein). It was found in ref. [58] that the LMA MSW, SMA MSW and LOW-QVO solutions of the solar neutrino problem are allowed and the corresponding solution regions were determined. The best fit point was found to lie in the LMA MSW solution region. Although the latter extends to values of $\Delta m_{\odot}^2 \sim (7.0 - 8.0) \times 10^{-4} \text{ eV}^2$, for Δm_{\odot}^2 exceeding the upper bound in eq. (10) the reliability (accuracy) of the results thus derived is questionable. For this reason in our further analysis we will use as a maximal value of Δm_{\odot}^2 for the LMA MSW solution the value given in (10), which is reflected in Table 1 (see below). The atmospheric neutrino data analysis restricts in the case of $\Delta m_{\odot}^2 \ll |\Delta m_{\text{atm}}^2|$ the mass-squared difference $|\Delta m_{\text{atm}}^2|$ and the angles θ_{atm} and θ (see, e.g., [47, 60]). The parameter Δm_{atm}^2 is found in [58] to lie at 90 (99)% C.L. in the following interval:

$$1.4 (1.1) \times 10^{-3} \text{ eV}^2 \leq |\Delta m_{\text{atm}}^2| \leq 6.1 (7.3) \times 10^{-3} \text{ eV}^2 \quad (11)$$

with best fit value given by $|\Delta m_{\text{atm}}^2|_{\text{BF}} = 3.1 \times 10^{-3} \text{ eV}^2$. Note that the upper and the lower limits in eq. (11) depend on the value of $\sin^2 \theta$. More specifically, the upper bound is a decreasing function, while the lower one is an increasing function of $\sin^2 \theta$ and the two bounds reach a common value at $|\Delta m_{\text{atm}}^2| = 2.0 \times 10^{-3} \text{ eV}^2$ for $\sin^2 \theta = 0.04$ (0.08) at 90 (99)% C.L. Combining all the bounds it is possible to constrain further the value of θ . The result at 90 (99)% C.L. reads [58]:

$$\sin^2 \theta < 0.05 (0.08). \quad (12)$$

The best fit value of $\sin^2 \theta$ was found to be [58]: $\sin^2 \theta_{\text{BF}} = 0.005$. The allowed regions for the different parameters can be read from the plots reported in [58] and are given in Tables 1 and 2. We point out that, in general, the various bounds are correlated and such interdependencies, whenever relevant, have been taken into account in our analysis.

In the next few years the constraints on the values of Δm_{\odot}^2 , θ_{\odot} , Δm_{atm}^2 , θ_{atm} and θ will be improved due to the increase of the statistics of the currently running experiments (e.g., SAGE, GNO, Super-Kamiokande, SNO, K2K) and the upgrade of some of them, as well as due to the data from the new experiments BOREXINO, KamLand, MINOS and CNGS. Hopefully, this will lead, for instance, to the identification of a unique solution of the solar neutrino problem instead of the three solutions allowed by the current data.

Let us note that if the three-flavour-neutrino mixing takes place, it would be possible to determine the sign of Δm_{atm}^2 , e.g., by studying the transitions $\nu_{\mu} \rightarrow \nu_e$ ($\nu_e \rightarrow \nu_{\mu}$) and $\bar{\nu}_{\mu} \rightarrow \bar{\nu}_e$ ($\bar{\nu}_e \rightarrow \bar{\nu}_{\mu}$) in the Earth under the condition that the Earth matter effects are non-negligible [66]. A negative Δm_{atm}^2 would correspond to neutrino mass spectrum with inverted hierarchy or to three quasi-degenerate neutrinos. In the inverted mass hierarchy case we adapt the notations as to have $\Delta m_{\text{atm}}^2 > 0$. This leads to a different correspondence between θ_{\odot} , θ_{atm} and θ and the elements of the neutrino mixing matrix in comparison with the case of a hierarchical neutrino mass spectrum. For the quasi-degenerate neutrino mass spectrum which is considered in Section 6, the formulae corresponding to the case of $\Delta m_{\text{atm}}^2 < 0$ can be obtained from those given in Section 6 and corresponding to $\Delta m_{\text{atm}}^2 > 0$, by replacing Δm_{atm}^2 with $|\Delta m_{\text{atm}}^2|$. In what regards the $(\beta\beta)_{0\nu}$ -decay, under the condition $\Delta m_{\odot}^2 \ll |\Delta m_{\text{atm}}^2|$ the results in the two cases coincide.

The Troitzk [67] and Mainz [68] ^3H β -decay experiments, studying the electron spectrum, provide information on the electron (anti-)neutrino mass m_{ν_e} . The data contain features which require further investigation (e.g., a peak in the end-point region which varies with time [67]). The upper bounds given by the authors (at 95% C.L.) read:

$$m_{\nu_e} < 2.5 \text{ eV} \quad [67], \quad m_{\nu_e} < 2.9 \text{ eV} \quad [68]. \quad (13)$$

There are prospects to increase the sensitivity of the ^3H β -decay experiments and probe the region of values of m_{ν_e} down to $m_{\nu_e} \sim (0.3 - 0.4) \text{ eV}$ [69].

Cosmological and astrophysical data provide information on the sum of the neutrino masses. The current upper bound reads (see, e.g., [70] and the references quoted therein):

$$\sum_j m_j \lesssim 5.5 \text{ eV} . \quad (14)$$

The future experiments MAP and PLANCK can be sensitive to [71]

$$\sum_j m_j \cong 0.4 \text{ eV} . \quad (15)$$

In the next Sections we show that the data from the new generation of $(\beta\beta)_{0\nu}$ -decay experiments, which will be sensitive to values of $|\langle m \rangle| \gtrsim (0.01 - 0.10) \text{ eV}$, can provide unique information on the neutrino mass spectrum as well as on the CP-violation in the lepton sector in the case of massive Majorana neutrinos.

3 The Formalism of Neutrino Mixing and $(\beta\beta)_{0\nu}$ -Decay

The explanation of the atmospheric and solar neutrino data in terms of neutrino oscillations requires the existence of mixing of the three left-handed flavour neutrino fields, ν_{lL} , $l = e, \mu, \tau$, in the weak charged lepton current:

$$\nu_{lL} = \sum_{j=1}^3 U_{lj} \nu_{jL}, \quad (16)$$

where ν_{jL} is the left-handed field of the neutrino ν_j having a mass m_j and U is a 3×3 unitary mixing matrix - the lepton mixing matrix. We will assume that the neutrinos ν_j are Majorana particles whose fields satisfy the Majorana condition:

$$C(\bar{\nu}_j)^T = \nu_j, \quad j = 1, 2, 3, \quad (17)$$

where C is the charge conjugation matrix. We will also assume (without loss of generality) that $m_1 < m_2 < m_3$. One of the standard parametrizations of the matrix U reads:

$$U = \begin{pmatrix} c_{12}c_{13} & s_{12}c_{13} & s_{13} \\ -s_{12}c_{23} - c_{12}s_{23}s_{13}e^{i\delta} & -c_{12}c_{23} - s_{12}s_{23}s_{13}e^{i\delta} & s_{23}c_{13}e^{i\delta} \\ s_{12}s_{23} - c_{12}c_{23}s_{13}e^{i\delta} & -c_{12}s_{23} - s_{12}c_{23}s_{13}e^{i\delta} & c_{23}c_{13}e^{i\delta} \end{pmatrix} \text{diag}(1, e^{i\frac{\alpha_{21}}{2}}, e^{i\frac{\alpha_{31}}{2}}) \quad (18)$$

where $c_{ij} \equiv \cos \theta_{ij}$, $s_{ij} \equiv \sin \theta_{ij}$, $0 \leq \theta_{ij} \leq \pi/2$, δ is the so-called Dirac CP-violating phase and α_{21} and α_{31} are the Majorana CP-violating phases [23] (see also, e.g., [20]).

We are interested in the effective Majorana mass parameter

$$|\langle m \rangle| \equiv | m_1 U_{e1}^2 + m_2 U_{e2}^2 + m_3 U_{e3}^2 |, \quad (19)$$

whose value is determined by the values of the neutrino masses m_j and by the elements of the first row of the lepton mixing matrix, U_{ej} . The latter satisfy the unitarity condition:

$$\sum_{j=1}^3 |U_{ej}|^2 = 1. \quad (20)$$

We have

$$U_{ej} = |U_{ej}| e^{\frac{i\alpha_j}{2}}, \quad (21)$$

where α_j , $j = 1, 2, 3$, are three phases. Only the phase differences $(\alpha_j - \alpha_k) \equiv \alpha_{jk}$ ($j > k$) can play a physical role. The mixing matrix in eq. (18) is written taking this into account.

In the general case, one can have

$$C(\bar{\nu}_j)^T = (\xi_j^*)^2 \nu_j, \quad j = 1, 2, 3, \quad (22)$$

where ξ_j , $j = 1, 2, 3$, are three phases. Only two combinations of the six phases α_j and ξ_j represent physical Majorana CP-violating phases. The effective Majorana mass parameter now has the form:

$$|\langle m \rangle| \equiv \left| m_1 U_{e1}^2 \xi_1^2 + m_2 U_{e2}^2 \xi_2^2 + m_3 U_{e3}^2 \xi_3^2 \right|. \quad (23)$$

Obviously, the two physical Majorana CP-violating phases on which $|\langle m \rangle|$ depends are $\alpha_{21} \equiv \arg(U_{e2}^2 \xi_2^2) - \arg(U_{e1}^2 \xi_1^2)$ and $\alpha_{31} \equiv \arg(U_{e3}^2 \xi_3^2) - \arg(U_{e1}^2 \xi_1^2)$. Actually, all CP-violation effects associated with the Majorana nature of the massive neutrinos are generated by $\alpha_{21} \neq k\pi$ and $\alpha_{31} \neq k'\pi$, $k, k' = 0, 1, 2, \dots$. Indeed, under a rephasing of the charged lepton, $l(x)$, and the neutrino, $\nu_j(x)$, fields in the weak charged lepton current, $l(x) \rightarrow e^{i\eta_l} l(x)$ and $\nu_j(x) \rightarrow e^{i\beta_j} \nu_j(x)$, the elements of the lepton mixing matrix and the phase factors in the Majorana condition for the Majorana neutrino fields change as follows:

$$U_{lj} \rightarrow U_{lj} e^{-i(\eta_l - \beta_j)}, \quad l = e, \mu, \tau, \quad j = 1, 2, 3, \quad (24)$$

$$\xi_j \rightarrow \xi_j e^{-i\beta_j}. \quad (25)$$

As was shown in [39], in the lepton sector of the theory under discussion with mixing of three massive Majorana neutrinos there exist three rephasing invariants. The first is the standard Dirac one, J , present in the case of mixing of three massive Dirac neutrinos [72, 39] (see also [73]):

$$J = \text{Im} (U_{\mu 2} U_{e 3} U_{\mu 3}^* U_{e 2}^*). \quad (26)$$

The existence of the other two, S_1 and S_2 , is related to the Majorana nature of the massive neutrinos ν_j [39]:

$$S_1 \equiv \text{Im} (U_{e1} U_{e3}^* \xi_3^* \xi_1), \quad (27)$$

$$S_2 \equiv \text{Im} (U_{e2} U_{e3}^* \xi_3^* \xi_2). \quad (28)$$

A geometrical representation of CP-violation in the lepton sector in terms of unitarity triangles in the case of three-neutrino mixing and presence of Majorana CP-violating phases in the lepton mixing matrix is given in [41]. The two Majorana CP-violating phases α_{21} and α_{31} are determined by the two independent rephasing invariants, $S_{1,2}$. We have:

$$\cos \alpha_{31} = 1 - 2 \frac{S_1^2}{|U_{e1}|^2 |U_{e3}|^2}, \quad (29)$$

$$\cos(\alpha_{31} - \alpha_{21}) = \cos(\alpha_3 - \alpha_2) = 1 - 2 \frac{S_2^2}{|U_{e2}|^2 |U_{e3}|^2}, \quad (30)$$

and

$$\cos \alpha_{21} = \cos(\alpha_{31} - \alpha_{21}) \cos \alpha_{31} + \sin(\alpha_{31} - \alpha_{21}) \sin \alpha_{31}. \quad (31)$$

One can express $|\langle m \rangle|$ in terms of rephasing-invariant quantities as:

$$\begin{aligned} |\langle m \rangle|^2 = & m_1^2 |U_{e1}|^4 + m_2^2 |U_{e2}|^4 + m_3^2 |U_{e3}|^4 \\ & + 2m_1 m_2 |U_{e1}|^2 |U_{e2}|^2 \cos \alpha_{21} + 2m_1 m_3 |U_{e1}|^2 |U_{e3}|^2 \cos \alpha_{31} \\ & + 2m_2 m_3 |U_{e2}|^2 |U_{e3}|^2 \cos(\alpha_{31} - \alpha_{21}). \end{aligned} \quad (32)$$

Note that $|\langle m \rangle|$ depends only on $S_{1,2}$ and does not depend on the Dirac rephasing invariant J . This is a consequence of the specific choice of the rephasing invariants $S_{1,2}$, eq. (28), which is not unique [39]. With this choice the amplitude of the $K^+ \rightarrow \pi^- + \mu^+ + \mu^+$ decay, for instance, which, as like the $(\beta\beta)_{0\nu}$ -decay, is generated by the exchange of the three virtual massive Majorana neutrinos in the scheme under discussion, depends, as can be shown, on all three rephasing invariants S_1 , S_2 and J .

If CP-invariance holds in the lepton sector we have, in particular, $S_1, S_2 = 0$, or $Re(U_{e1}U_{e3}^*\xi_3^*\xi_1) = 0$, $Re(U_{e2}U_{e3}^*\xi_3^*\xi_2) = 0$. In this case the unitarity triangles reduce to lines oriented either along the horizontal or the vertical axis on the plane [41]. In terms of constraints on the phases α_{21} and α_{31} this implies $\alpha_{21} = k\pi$, $\alpha_{31} = k'\pi$ with $k, k' = 0, 1, 2, \dots$

In all our subsequent analyzes we will set for convenience (and without loss of generality) $\xi_j = 1$, $j=1,2,3$, i.e., we will assume that the fields of the Majorana neutrinos ν_j satisfy the Majorana conditions (17). In this case $\alpha_{21} = \alpha_2 - \alpha_1$ and $\alpha_{31} = \alpha_3 - \alpha_1$, where α_j are determined by eq. (21). The CP-invariance constraint on the elements of the lepton mixing matrix of interest reads ⁶ [74, 75] (see also [20]):

$$U_{ej}^* = \eta_j^{CP} U_{ej}, \quad (33)$$

where $\eta_j^{CP} = i\phi_j = \pm i$ is the CP-parity of the Majorana neutrino ν_j with mass $m_j > 0$. In this case $|\langle m \rangle|$ is given by:

$$|\langle m \rangle| \equiv \left| \sum_{j=1}^3 \eta_j^{CP} |U_{ej}|^2 m_j \right| = \left| \sum_{j=1}^3 \phi_j |U_{ej}|^2 m_j \right|. \quad (34)$$

For establishing a direct relation with the mixing angles constrained by the solar neutrino data and the data from the CHOOZ experiment, it proves convenient to express (e.g., in the case of neutrino mass hierarchy) $|U_{e1}|$ and $|U_{e2}|$ in the form:

$$|U_{e1}| = \cos \varphi \sqrt{1 - |U_{e3}|^2}, \quad |U_{e2}| = \sin \varphi \sqrt{1 - |U_{e3}|^2}, \quad (35)$$

where φ is an angle and we have used the relation $|U_{e1}|^2 + |U_{e2}|^2 = 1 - |U_{e3}|^2$. In certain cases (e.g., inverted neutrino mass hierarchy) the analogous relations, $|U_{e2}| = \cos \tilde{\varphi} \sqrt{1 - |U_{e1}|^2}$, $|U_{e3}| = \sin \tilde{\varphi} \sqrt{1 - |U_{e1}|^2}$, are more useful. Depending on the type of the neutrino mass spectrum, we will have either $\varphi = \theta_\odot$, $|U_{e3}|^2 = \sin^2 \theta$, or $\tilde{\varphi} = \theta_\odot$, $|U_{e1}|^2 = \sin^2 \theta$.

The neutrino oscillation experiments, as is well-known, provide information on $\Delta m_{jk}^2 = m_j^2 - m_k^2$ ($j > k$). In the case of 3-neutrino mixing (16) there are two independent Δm^2 parameters: Δm_{31}^2 , for instance, can be expressed as $\Delta m_{31}^2 = \Delta m_{32}^2 + \Delta m_{21}^2$. Correspondingly, as an independent set of three neutrino mass parameters we can choose m_1 , $\sqrt{\Delta m_{21}^2}$ and $\sqrt{\Delta m_{32}^2}$. We have:

$$m_2 = \sqrt{m_1^2 + \Delta m_{21}^2}, \quad (36)$$

⁶This constraint is obtained from the requirement of CP-invariance of the charged current weak interaction Lagrangian \mathcal{L}^{cc} , by choosing the arbitrary phase factors in the CP-transformation laws of the electron and the W -boson fields equal to 1.

$$m_3 = \sqrt{m_1^2 + \Delta m_{21}^2 + \Delta m_{32}^2} . \quad (37)$$

The mass-squared difference inferred from the neutrino oscillation interpretation of the atmospheric neutrino data, Δm_{atm}^2 , is equal to Δm_{31}^2 ,

$$\Delta m_{\text{atm}}^2 = \Delta m_{31}^2 = \Delta m_{21}^2 + \Delta m_{32}^2 , \quad (38)$$

while for the one deduced from the solar neutrino data, Δm_{\odot}^2 , we have two possibilities:

$$\Delta m_{\odot}^2 \equiv \Delta m_{32}^2 \quad \text{or} \quad \Delta m_{\odot}^2 \equiv \Delta m_{21}^2 . \quad (39)$$

Depending on the relative magnitudes of m_1 , $\sqrt{\Delta m_{21}^2}$ and $\sqrt{\Delta m_{32}^2}$, one recovers the different possible types of neutrino mass spectrum:

1. if $m_1 \ll \sqrt{\Delta m_{21}^2} \ll \sqrt{\Delta m_{32}^2}$, one has $m_1 \ll m_2 \ll m_3$, i.e., hierarchical neutrino mass spectrum;
2. $m_1 \ll \sqrt{\Delta m_{32}^2} \ll \sqrt{\Delta m_{21}^2}$ implies $m_1 \ll m_2 \simeq m_3$, i.e., neutrino mass spectrum with inverted hierarchy;
3. for $\sqrt{\Delta m_{21}^2}, \sqrt{\Delta m_{32}^2} \ll m_1$, we have $m_1 \simeq m_2 \simeq m_3$, i.e., quasi-degenerate neutrino mass spectrum;
4. if $\sqrt{\Delta m_{21}^2} \ll \sqrt{\Delta m_{32}^2} \sim \mathcal{O}(m_1)$, one finds $m_1 \simeq m_2 < m_3$, i.e., spectrum with ‘‘partial mass hierarchy’’. This pattern of neutrino masses interpolates between the hierarchical one and the quasi-degenerate one.
5. for $\sqrt{\Delta m_{32}^2} \ll \sqrt{\Delta m_{21}^2} \sim \mathcal{O}(m_1)$, we have $m_1 < m_2 \simeq m_3$, i.e., spectrum with ‘‘partial inverted mass hierarchy’’. This pattern interpolates between the inverted mass hierarchy spectrum and the quasi-degenerate one.

For each of the possible patterns of neutrino masses indicated above, we will study in detail the implications of the data on neutrino oscillations, obtained in the experiments with solar and atmospheric neutrinos and in the CHOOZ experiment, for the searches for $(\beta\beta)_{0\nu}$ -decay.

4 Hierarchical Neutrino Mass Spectrum

The hierarchical neutrino mass spectrum is characterized by the following pattern of the neutrino masses m_j :

$$m_1 \ll m_2 \ll m_3 . \quad (40)$$

This type of neutrino mass spectrum is predicted by the standard versions of the see-saw mechanism of neutrino mass generation [22]. The pattern corresponds to the inequalities ⁷

$$m_1 \ll \sqrt{\Delta m_{21}^2} \ll \sqrt{\Delta m_{32}^2} . \quad (41)$$

Using (40) and (41) it is possible to make the identification (see, e.g., [47, 60]):

$$\begin{aligned} \Delta m_{\odot}^2 &\equiv \Delta m_{21}^2, & \Delta m_{\text{atm}}^2 &\equiv \Delta m_{32}^2, \\ |U_{e1}|^2 &= \cos^2 \theta_{\odot} (1 - |U_{e3}|^2), \\ |U_{e2}|^2 &= \sin^2 \theta_{\odot} (1 - |U_{e3}|^2), \\ |U_{e3}|^2 &\equiv \sin^2 \theta < 0.09 \quad (\text{CHOOZ}). \end{aligned} \quad (42)$$

⁷The case of neutrino mass spectrum with partial hierarchy, $m_1 \simeq m_2 < m_3$ will be treated in Section 7.

We will suppose that Δm_{atm}^2 lies in the interval (5) or (11), Δm_{\odot}^2 and θ_{\odot} take values in the regions given in Tables 1 and 2, and that $|U_{e3}|^2$ satisfies the CHOOZ upper bound. Equations (40) and (42) further imply:

$$m_2 \simeq \sqrt{\Delta m_{\odot}^2}, \quad m_3 \simeq \sqrt{\Delta m_{\text{atm}}^2}. \quad (43)$$

Using eqs. (19), (21), (42) and (43) we can express the effective Majorana mass parameter in terms of the quantities, whose values are determined in the solar and atmospheric neutrino experiments, and of the phase $(\alpha_3 - \alpha_2)$:

$$|\langle m \rangle| \simeq \left| \sqrt{\Delta m_{\odot}^2} (1 - |U_{e3}|^2) \sin^2 \theta_{\odot} + \sqrt{\Delta m_{\text{atm}}^2} |U_{e3}|^2 e^{i(\alpha_3 - \alpha_2)} \right| \quad (44)$$

where the phases $\alpha_{2,3}$ are determined by eq. (21) and we have neglected the contribution of the term $\sim m_1$. Note that although in this case one of three massive Majorana neutrinos effectively “decouples” and does not give a contribution to $|\langle m \rangle|$, the value of $|\langle m \rangle|$ still depends on the Majorana CP-violating phase $\alpha_{32} = \alpha_3 - \alpha_2$. This reflects the fact that in contrast to the case of massive Dirac neutrinos (or quarks), *CP-violation can take place in the mixing of only two massive Majorana neutrinos* [23].

Due to the presence of the first term in eq. (44), one obtains different predictions for $|\langle m \rangle|$ for the LMA, SMA and LOW-QVO solutions of the solar neutrino problem, as the three solutions require different ranges of values of $\sin^2 \theta_{\odot}$ and Δm_{\odot}^2 .

Consider first the case of CP-conservation. There exist two possibilities.

Case A. The neutrinos ν_2 and ν_3 can have the same CP parities, i.e., $\phi_2 = \phi_3$. In this case (with the phase conventions we are using, see Section 3) $\alpha_{32} \equiv \alpha_3 - \alpha_2 = 0$ (or $\alpha_{21} = \alpha_{31} = 0, \pm\pi$), and the effective Majorana mass $|\langle m \rangle|$ is given by:

$$|\langle m \rangle| \simeq \sqrt{\Delta m_{\odot}^2} \sin^2 \theta_{\odot} (1 - |U_{e3}|^2) + \sqrt{\Delta m_{\text{atm}}^2} |U_{e3}|^2. \quad (45)$$

Using the results on Δm_{atm}^2 , Δm_{\odot}^2 , $\sin^2 \theta_{\odot}$ and $|U_{e3}|^2$ obtained in ref. [58] at 90 (99)% C.L. (quoted in Section 2 and in Tables 1 and 2), we find that in the cases of the LMA, SMA and LOW-QVO solutions of the solar neutrino problem $|\langle m \rangle|$ is bounded to lie in the following intervals:

$$6.1 \text{ (5.3)} \times 10^{-4} \text{ eV} \leq |\langle m \rangle| \leq 7.4 \text{ (14)} \times 10^{-3} \text{ eV}, \quad \text{LMA}; \quad (46)$$

$$2.0 \text{ (0.8)} \times 10^{-7} \text{ eV} \leq |\langle m \rangle| \leq 1.9 \text{ (3.6)} \times 10^{-3} \text{ eV}, \quad \text{SMA}; \quad (47)$$

$$6.7 \text{ (0.5)} \times 10^{-5} \text{ eV} \leq |\langle m \rangle| \leq 3.5 \text{ (3.6)} \times 10^{-3} \text{ eV}, \quad \text{LOW-QVO}. \quad (48)$$

For the values of the parameters providing the best fit of the solar and atmospheric neutrino data [58] one finds: $|\langle m \rangle|_{\text{BF}} = 1.8 \times 10^{-3} \text{ eV}$. Note, that in the case of the LMA solution, $|\langle m \rangle|$ can reach $|\langle m \rangle| \cong (1-2) \times 10^{-2} \text{ eV}$. If the LMA solution admits values of $\Delta m_{\odot}^2 \sim (7-8) \times 10^{-4} \text{ eV}^2$, as suggested in [58], $|\langle m \rangle|$ can be as large as $\sim 3 \times 10^{-2} \text{ eV}$. This is the maximal value $|\langle m \rangle|$ can have in the case of hierarchical neutrino mass spectrum. Values of $|\langle m \rangle| \gtrsim 10^{-2} \text{ eV}$ can be tested in the next generation of $(\beta\beta)_{0\nu}$ -decay experiments, as we have discussed in the Introduction.

The maximal allowed values of $|\langle m \rangle|$, $\max(|\langle m \rangle|)$, in the case of the SMA and LOW-QVO solutions are by a factor of $\sim (2-4)$ smaller than that for the LMA solution. This is related to the fact that for the SMA and LOW-QVO solutions

$$\max(|\langle m \rangle|) = \max(\sqrt{\Delta m_{\text{atm}}^2} |U_{e3}|^2), \quad (49)$$

while for the LMA solution $\sqrt{\Delta m_{\odot}^2} \sin^2 \theta_{\odot}$ can be as large as $\sim 1.1 \times 10^{-2}$ eV and both terms in eq. (44) contribute to $\max(|\langle m \rangle|)$.

The minimal allowed values of $|\langle m \rangle|$, $\min(|\langle m \rangle|)$, given in eq. (46) - (48), are exceedingly small. Let us note nevertheless that for the given solution of the solar neutrino problem they correspond to m_1 having a value much smaller than the $\min(|\langle m \rangle|)$ in (46) - (48), i.e., to $m_1 \ll 7.0 \times 10^{-4}$ eV for the LMA solution, etc. If, however, $m_1 \ll \sqrt{\Delta m_{\odot}^2}$, but $m_1 |U_{e1}|^2 = m_1 (1 - |U_{e3}|^2) \cos^2 \theta_{\odot}$ is of the order of, or larger than, some of the $\min(|\langle m \rangle|)$ given in (46) - (48), the corresponding lower bounds will be modified. This can happen in the case of the SMA MSW solution, while $\min(|\langle m \rangle|)$ for the LMA and LOW-QVO solutions are practically stable with respect to “finite” m_1 corrections. Indeed, for the LMA (LOW-QVO) solution, $m_1 \ll \sqrt{\Delta m_{\odot}^2}$ implies $m_1 \lesssim 4.0 (0.025) \times 10^{-4}$ eV and thus $m_1 |U_{e1}|^2 \lesssim 2.0 (0.013) \times 10^{-4}$ eV, which can change the relevant values of $\min(|\langle m \rangle|)$ in eq. (46) (eq. (48)) by not more than $\sim 30\%$. In contrast, in the case of the MSW solution for which $\cos^2 \theta_{\odot} \cong 1$, the inequality $m_1 \ll \sqrt{\Delta m_{\odot}^2}$ is satisfied for $m_1 \lesssim 1.8 \times 10^{-4}$ eV. Correspondingly, $m_1 (1 - |U_{e3}|^2) \cos^2 \theta_{\odot} \lesssim 1.8 \times 10^{-4}$ eV and $\min(|\langle m \rangle|)$ can range from $\sim 1.8 \times 10^{-4}$ eV to 0 eV. Let us note also that in the case of the SMA solution, a value of $|\langle m \rangle| \gtrsim 8.0 \times 10^{-4}$ eV would imply (for a hierarchical neutrino mass spectrum) that

$$\text{SMA, } |\langle m \rangle| \gtrsim 8.0 \times 10^{-4} \text{ eV : } |\langle m \rangle| \simeq \sqrt{\Delta m_{\text{atm}}^2} |U_{e3}|^2. \quad (50)$$

Using the results of the two-neutrino oscillation analyzes of refs. [7, 56] (see Tables 1 and 2), the results on Δm_{atm}^2 from ref. [55], eq. (7), and the upper limit on $|U_{e3}|^2$, obtained in the CHOOZ experiment [64], we get the following intervals of possible values of $|\langle m \rangle|$:

$$\begin{aligned} 0.8 \times 10^{-3} \text{ eV} &\leq |\langle m \rangle| \leq 7.6 \times 10^{-3} \text{ eV}, & \text{LMA [7, 55, 64];} \\ 5.0 \times 10^{-5} \text{ eV} &\leq |\langle m \rangle| \leq 3.6 \times 10^{-3} \text{ eV}, & \text{LOW-QVO [7, 55, 64],} \end{aligned} \quad (51)$$

and

$$\begin{aligned} 6.7 (5.4) \times 10^{-4} \text{ eV} &\leq |\langle m \rangle| \leq 7.4 (8.5) \times 10^{-3} \text{ eV}, & \text{LMA [55, 56, 64];} \\ (2.4 \times 10^{-7} \text{ eV} &\leq |\langle m \rangle| \leq 4.0 \times 10^{-3} \text{ eV}), & \text{SMA [55, 56, 64];} \\ 2.7 (0.6) \times 10^{-5} \text{ eV} &\leq |\langle m \rangle| \leq 3.5 (4.0) \times 10^{-3} \text{ eV}, & \text{LOW-QVO [55, 56, 64],} \end{aligned} \quad (52)$$

where the numbers (the numbers in brackets) correspond to the 90% (99%) C.L. solutions of the ν_{\odot} -problem in [56].

The values of $\max(|\langle m \rangle|)$ for the LMA solution derived in the two-neutrino oscillation analyzes [7, 56] do not exceed 8.5×10^{-3} eV and are smaller than the corresponding one for the LMA solution obtained in the three-neutrino oscillation analysis [58]. This difference is due to the difference in the maximal allowed values of $\sqrt{\Delta m_{\odot}^2} (1 - |U_{e3}|^2) \sin^2 \theta_{\odot}$ in the two cases. The minimal $|\langle m \rangle|$ for the SMA solution in eq. (52) is again unstable with respect to “finite” m_1 corrections and actually can have any value from $\sim 10^{-4}$ eV to 0 eV.

Case B. ν_2 and ν_3 have opposite CP parities, i.e., $\phi_2 = -\phi_3$. We have $\alpha_{32} = \pm\pi$ (or $\alpha_{21} = \alpha_{31} + \pm\pi = 0, \pm\pi$), and the effective Majorana mass parameter is given by:

$$|\langle m \rangle| = \left| \sqrt{\Delta m_{\odot}^2} \sin^2 \theta_{\odot} (1 - |U_{e3}|^2) - \sqrt{\Delta m_{\text{atm}}^2} |U_{e3}|^2 \right|. \quad (53)$$

In this case there exists the possibility of cancellation [76] between the two terms in eq. (53). Correspondingly, one can have $|\langle m \rangle| \simeq 0$ eV for all solutions of the solar neutrino problem.

The 90 (99)% C.L. results of the three-neutrino oscillation analysis of ref. [58] imply the following ranges of allowed values of $|\langle m \rangle|$:

$$\begin{aligned}
0 &\leq |\langle m \rangle| \leq 6.4 (10) \times 10^{-3} \text{ eV}, && \text{LMA;} \\
0 &\leq |\langle m \rangle| \leq 1.8 (3.1) \times 10^{-3} \text{ eV}, && \text{LOW-QVO;} \\
0 &\leq |\langle m \rangle| \leq 1.9 (3.5) \times 10^{-3} \text{ eV}, && \text{SMA.} \quad (54)
\end{aligned}$$

To the best fit values of the parameters found in [58] (the best fit Δm_{\odot}^2 and $\sin^2 \theta_{\odot}$ lie in the LMA solution region), there corresponds $|\langle m \rangle|_{\text{BF}} = 1.2 \times 10^{-3} \text{ eV}$.

The results of the two-neutrino oscillation analyzes of refs. [7] and [56], and of [55, 64] lead to the following possible values of $|\langle m \rangle|$:

$$\begin{aligned}
0 \leq |\langle m \rangle| \leq 4.5 \times 10^{-3} \text{ eV}, &&& \text{LMA [7, 55, 64];} \\
0 \leq |\langle m \rangle| \leq 3.5 \times 10^{-3} \text{ eV}, &&& \text{LOW-QVO [7, 55, 64],} \quad (55)
\end{aligned}$$

and

$$\begin{aligned}
0 \leq |\langle m \rangle| \leq 3.7 (5.0) \times 10^{-3} \text{ eV}, &&& \text{LMA [55, 56, 64];} \\
(0 \leq |\langle m \rangle| \leq 4.0 \times 10^{-3} \text{ eV}), &&& \text{SMA [55, 56, 64];} \\
0 \leq |\langle m \rangle| \leq 3.5 (4.0) \times 10^{-3} \text{ eV}, &&& \text{LOW-QVO [55, 56, 64].} \quad (56)
\end{aligned}$$

We see that the 99% C.L. results of the three-neutrino oscillation analysis [58] allow values of $\max(|\langle m \rangle|) \simeq 10^{-2} \text{ eV}$ for the LMA solution. Using the results of the two-neutrino oscillation analyzes [7, 55, 56, 64] one gets $\max(|\langle m \rangle|) \lesssim 5.0 \times 10^{-3} \text{ eV}$.

The possibility of partial or complete cancellation between the two terms in eq. (53) for $|\langle m \rangle|$ is extremely important in view of the future searches for the $(\beta\beta)_{0\nu}$ -decay. Barring finite m_1 corrections which can be relevant in the case of the SMA solution of the solar neutrino problem, the cancellation can take place if $|U_{e3}|^2$ has a value given by:

$$|\langle m \rangle| = 0 : \quad |U_{e3}|_0^2 = \frac{\sqrt{\Delta m_{\odot}^2} \sin^2 \theta_{\odot}}{\sqrt{\Delta m_{\odot}^2} \sin^2 \theta_{\odot} + \sqrt{\Delta m_{\text{atm}}^2}}. \quad (57)$$

For the ranges of allowed values of Δm_{\odot}^2 , $\sin^2 \theta_{\odot}$ for the three solutions of the ν_{\odot} -problem, and of Δm_{atm}^2 , found in [58], the corresponding values of $|U_{e3}|_0^2$ for which the cancellation can occur belong to the intervals:

$$\begin{aligned}
8.0 (8.0) \times 10^{-3} &\leq |U_{e3}|_0^2 \leq 1.3 (3.7) \times 10^{-1} && \text{LMA,} \\
1.0 (0.3) \times 10^{-5} &\leq |U_{e3}|_0^2 \leq 7.0 (20) \times 10^{-5} && \text{SMA,} \\
8.0 (0.7) \times 10^{-4} &\leq |U_{e3}|_0^2 \leq 0.5 (13) \times 10^{-2} && \text{LOW-QVO.} \quad (58)
\end{aligned}$$

These regions for $|U_{e3}|_0^2$ overlap with the experimentally allowed one and, as we noticed earlier, there can be a complete cancellation between the different contributions in $|\langle m \rangle|$ for all the solutions of the solar neutrino problem. Note, however, that the parameters entering into the expression (57) for $|U_{e3}|_0^2$ are not related, in general, and therefore the complete cancellation of the terms in the expression for $|\langle m \rangle|$ seems to require a fine tuning or the existence of a specific symmetry (see, e.g., [76, 77, 20]). Note also that the cancellation cannot occur for the best fit value of $|U_{e3}|^2 = 0.005$ (LMA) found in [58]. One arrives to analogous conclusions performing this analysis exploiting the two-neutrino oscillation results of refs. [7, 55, 56, 64].

The MINOS experiment [13] currently under preparation will be able to search for $\nu_{\mu} \rightarrow \nu_e$ transitions and can probe values of $|U_{e3}|^2 \geq 5 \times 10^{-3}$. These data can provide information on the

possibility of cancellation of the two terms in $|\langle m \rangle|$ only for the case of the LMA solution of the solar neutrino problem. If it is found that $|U_{e3}|^2 \gtrsim 8 \times 10^{-3}$, the two terms in eq. (53) for $|\langle m \rangle|$ can cancel and one can have $|\langle m \rangle| \cong 0$ eV. If, on the other hand, $|U_{e3}|^2 \lesssim 8 \times 10^{-3}$, there cannot be a complete cancellation. However, the dominant contribution to $|\langle m \rangle|$, eq. (53), would be given by the term $\sqrt{\Delta m_{\odot}^2} (1 - |U_{e3}|^2) \sin^2 \theta_{\odot}$ and in this case $|\langle m \rangle|$ would be relatively small:

$$|U_{e3}|^2 \lesssim 8 \times 10^{-3} : \quad |\langle m \rangle| \sim (\text{few} \times 10^{-4} \div \text{few} \times 10^{-3}) \text{ eV}. \quad (59)$$

Our results are summarized in Fig. 2, Fig. 3 and Fig. 4 in which we show the allowed ranges of $|\langle m \rangle|$ as a function of $|U_{e3}|^2$ for the LMA, LOW-QVO and SMA solutions, respectively, found in ref. [58]. The figures are obtained for any possible values of the CP-violating phase $(\alpha_3 - \alpha_2)$. The regions of allowed values of $|\langle m \rangle|$ in the cases of CP-conservation ($\phi_2 = \pm\phi_3$, or $\alpha_3 - \alpha_2 = 0, \pi$) cover completely that in the case of CP-violation ($(\alpha_3 - \alpha_2) \neq k\pi$, $k = 0, 1, \dots$). This is mainly due to the uncertainties in the value of Δm_{\odot}^2 . With the improvement of the precision on Δm_{\odot}^2 it will be possible to restrict the allowed ranges of values of $|\langle m \rangle|$ in the indicated cases. The latter can lead to a separation between the allowed regions of $|\langle m \rangle|$, corresponding to the cases of CP-conservation and of CP-violation. Let us note also that the cancellation leading to $|\langle m \rangle| \cong 0$ eV can be present in the case of CP-violation as well.

Equation (44) permits to express the cosine of the CP-violating phase $(\alpha_3 - \alpha_2)$ in terms of measurable quantities:

$$\cos(\alpha_3 - \alpha_2) = \frac{|\langle m \rangle|^2 - \Delta m_{\odot}^2 \sin^4 \theta_{\odot} (1 - |U_{e3}|^2)^2 - \Delta m_{\text{atm}}^2 (|U_{e3}|^2)^2}{2\sqrt{\Delta m_{\odot}^2} \sqrt{\Delta m_{\text{atm}}^2} \sin^2 \theta_{\odot} |U_{e3}|^2 (1 - |U_{e3}|^2)}. \quad (60)$$

Thus, if $|\langle m \rangle|$ and $|U_{e3}|^2$ will be found to be nonzero and their values (together with the values of Δm_{\odot}^2 , Δm_{atm}^2 and $\sin^2 \theta_{\odot}$) will be determined experimentally with sufficient precision, one can get direct information about the CP-violation in the lepton sector, caused by Majorana CP-violating phases. In Fig. 5 we show the allowed range of $\cos(\alpha_2 - \alpha_3)$ as a function of $|\langle m \rangle|$ for different values of $|U_{e3}|^2$, using the best fit values for Δm_{atm}^2 , Δm_{\odot}^2 and θ_{\odot} from [58].

Let us note that even if it is found that $\alpha_3 - \alpha_2 = 0, \pm\pi$, this will not necessarily mean there is no CP-violation due to the Majorana CP-violating phases in the lepton sector because the second of the two physical CP-violating phases is not constrained and can be a source of CP-violation in other $\Delta L = 2$ processes.

It follows from the analysis presented in this Section that in the case of 3-neutrino mixing and a hierarchical neutrino mass spectrum, the values of $|\langle m \rangle|$ compatible with the neutrino oscillation/transition interpretation of the solar and atmospheric neutrino data and with the CHOOZ limit are smaller than 5×10^{-3} eV for the SMA and LOW-QVO solutions of the solar neutrino problem. For the LMA solution one can have $\max(|\langle m \rangle|) \cong (1 - 2) \times 10^{-2}$ eV. If the exchange of three relatively light Majorana neutrinos *is the only mechanism generating the $(\beta\beta)_{0\nu}$ -decay*, an observation of the latter with a lifetime corresponding to $|\langle m \rangle| \gtrsim 10^{-2}$ eV would practically rule out a hierarchical neutrino mass spectrum for the SMA and LOW-QVO solutions; an experimentally measured value of $|\langle m \rangle| \gtrsim 2 \times 10^{-2}$ eV would strongly disfavor the hierarchical neutrino mass spectrum for the LMA solution as well. In such a situation one would be led to conclude that at least two of the three massive Majorana neutrinos are quasi-degenerate in mass.

5 Inverted Mass Hierarchy Spectrum

The inverted mass hierarchy spectrum is characterized by the following relation between the neutrino masses m_j :

$$m_1 \ll m_2 \simeq m_3. \quad (61)$$

The identification with the neutrino oscillation parameters probed in the solar and atmospheric neutrino experiments and in CHOOZ reads (see, e.g., [37, 47, 60]):

$$\begin{aligned} \Delta m_\odot^2 &\equiv \Delta m_{32}^2, \\ \Delta m_{\text{atm}}^2 &\equiv \Delta m_{31}^2 \simeq \Delta m_{21}^2, \\ |U_{e1}|^2 &= \sin^2 \theta < 0.09 \quad (\text{CHOOZ}), \\ |U_{e2}|^2 &= \cos^2 \theta_\odot (1 - |U_{e1}|^2), \\ |U_{e3}|^2 &= \sin^2 \theta_\odot (1 - |U_{e1}|^2). \end{aligned} \quad (62)$$

We also have:

$$m_2 \simeq m_3 \simeq \sqrt{\Delta m_{\text{atm}}^2}. \quad (63)$$

The inverted mass hierarchy spectrum can also be defined by the inequalities

$$m_1 \ll (<) \sqrt{\Delta m_{32}^2} \ll \sqrt{\Delta m_{21}^2}. \quad (64)$$

The term $m_1 |U_{e1}^2|$ in the expression for $|\langle m \rangle|$, eq. (19), can be neglected, since $m_1 \ll m_{2,3}$ and $|U_{e1}^2| \ll 1$. This approximation would be valid as long as the sum of the two other terms in eq. (19) exceeds $\sim 5.0 \times 10^{-3}$ eV. Under the assumption that $m_1 |U_{e1}^2|$ gives a negligible contribution to $|\langle m \rangle|$ we have [37, 46]:

$$|\langle m \rangle| \simeq \left| |U_{e2}|^2 m_2 + |U_{e3}|^2 m_3 e^{i(\alpha_3 - \alpha_2)} \right| \quad (65)$$

$$= m_{2,3} \sqrt{1 - 4|U_{e2}|^2 |U_{e3}|^2 \sin^2 \left(\frac{\alpha_3 - \alpha_2}{2} \right)} \quad (66)$$

$$= \sqrt{\Delta m_{\text{atm}}^2} (1 - |U_{e1}|^2) \sqrt{1 - \sin^2 2\theta_\odot \sin^2 \left(\frac{\alpha_3 - \alpha_2}{2} \right)}, \quad (67)$$

where we have used (62) and (63). We see again that even though one of the three massive Majorana neutrinos “decouples”, the value of $|\langle m \rangle|$ depends on the Majorana CP-violating phase $(\alpha_3 - \alpha_2)$ [23]. In contrast, there cannot be CP-violation effects in the mixing of *only two* massive Dirac neutrinos.

It follows, e.g., from eq. (67) that $|\langle m \rangle|$ satisfies the inequalities [37, 46]:

$$\sqrt{\Delta m_{\text{atm}}^2} (1 - |U_{e1}|^2) |\cos 2\theta_\odot| \leq |\langle m \rangle| \leq \sqrt{\Delta m_{\text{atm}}^2} (1 - |U_{e1}|^2). \quad (68)$$

The upper and the lower limits in (68) correspond respectively to the CP-conserving cases $\phi_2 = \phi_3$ ($\alpha_3 - \alpha_2 = 0$, or $\alpha_{21} = \alpha_{31} = 0, \pm\pi$) and $\phi_2 = -\phi_3$ ($\alpha_3 - \alpha_2 = \pm\pi$, or $\alpha_{21} = \alpha_{31} + \pi = 0, \pm\pi$).

If CP-invariance holds in the leptonic sector, the parameters which determine $|\langle m \rangle|$ are i) Δm_{atm}^2 , on the possible values of which there’s a general agreement, ii) $(1 - |U_{e1}|^2) > 0.91$ and

iii) $|\cos 2\theta_\odot|$, if $\phi_2 = -\phi_3$, whose allowed range varies with the analysis (see Table 2). Consider the two cases of CP-conservation.

Case A. If ν_2 and ν_3 have the same CP parities, $\phi_2 = \phi_3$ ($\alpha_{32} = 0$, or $\alpha_{21} = \alpha_{31} = 0, \pm\pi$), the effective Majorana mass $|\langle m \rangle|$ does not depend on $|\cos 2\theta_\odot|$,

$$|\langle m \rangle| = \sqrt{\Delta m_{\text{atm}}^2} (1 - |U_{e1}|^2). \quad (69)$$

Exploiting the 90% (99%) C.L. results of ref. [58] we find that $|\langle m \rangle|$ can take the values

$$3.7 \text{ (3.3)} \times 10^{-2} \text{ eV} \leq |\langle m \rangle| \leq 6.8 \text{ (8.1)} \times 10^{-2} \text{ eV}.$$

The ‘‘best fit’’ value is found to be

$$|\langle m \rangle|_{\text{BF}} = 5.6 \times 10^{-2} \text{ eV}.$$

For the results obtained in ref. [55] and ref. [64] we get:

$$4.4 \text{ (3.6)} \times 10^{-2} \text{ eV} \leq |\langle m \rangle| \leq 8.1 \text{ (8.9)} \times 10^{-2} \text{ eV}.$$

All indicated values of $|\langle m \rangle|$ can be probed in the next generation of $(\beta\beta)_{0\nu}$ -decay experiments like GENIUS, EXO, etc.

Case B. For ν_2 and ν_3 having opposite CP parities, $\phi_2 = -\phi_3$ ($\alpha_{32} = \pm\pi$, or $\alpha_{21} = \alpha_{31} + \pm\pi = 0, \pm\pi$), we have

$$|\langle m \rangle| = \sqrt{\Delta m_{\text{atm}}^2} (1 - |U_{e1}|^2) |\cos 2\theta_\odot|.$$

The ranges of values $|\langle m \rangle|$ can have in this case are reported in Table 3. The ‘‘best fit’’ value, according to the results in ref. [58], is $|\langle m \rangle|_{\text{BF}} = 2.1 \times 10^{-2} \text{ eV}$ (with the best fit Δm_\odot^2 and $\sin^2 \theta_\odot$ lying in the LMA solution region). Note that for the SMA solution one has $\cos 2\theta_\odot \simeq 1$ and $|\langle m \rangle|$ has the same value in the two cases $\phi_2 = -\phi_3$ and $\phi_2 = \phi_3$.

Table 3: Values $|\langle m \rangle|$ compatible with the neutrino oscillation/transition interpretation of the solar and atmospheric neutrino data and with the CHOOZ limit in the case of neutrino mass spectrum with inverted hierarchy, eq. (61), CP-conservation and $\phi_2 = -\phi_3$ (see text for details).

Data from		$ \langle m \rangle $ [eV]
Ref. [7, 55, 64] (95% C.L.)	LMA	$7.3 \times 10^{-3} \div 5.7 \times 10^{-2}$
	LOW-QVO	$0.9 \times 10^{-2} \div 4.5 \times 10^{-2}$
Ref. [55, 56, 64] (90% (99%) C.L.)	LMA	$1.1 \times 10^{-2} \text{ (0.0)} \div 5.3 \text{ (5.9)} \times 10^{-2}$
	SMA	$(3.6 \times 10^{-2} \div 8.9 \times 10^{-2})$
	LOW-QVO	$2.2 \times 10^{-3} \text{ (0.0)} \div 2.1 \text{ (3.7)} \times 10^{-2}$
Ref. [58] (90% (99%) C.L.)	LMA	$0 \text{ (0)} \div 4.8 \text{ (5.8)} \times 10^{-2}$
	SMA	$3.7 \text{ (3.3)} \times 10^{-2} \div 6.8 \text{ (8.1)} \times 10^{-2}$
	LOW-QVO	$0 \text{ (0)} \div 3.4 \text{ (5.4)} \times 10^{-2}$

The results derived in the present Section are illustrated and summarized in Figs. 6, 7, 8 and 9. In Figs. 6 and 7 we show the allowed regions of $|\langle m \rangle|$ for the LMA and LOW-QVO solutions,

respectively, as a function of $\sqrt{\Delta m_{\text{atm}}^2}$. It is interesting to note that there is a region, marked by dark-grey color, which can be spanned *only in the presence of CP-violation*, i.e., this is a “just-CP-violation” region. Thus, for the LMA and LOW-QVO solutions of the solar neutrino problem and neutrino mass spectrum of the type (61), an experimentally measured value of $|\langle m \rangle|$ lying in the indicated region will signal the existence of CP-violation in the leptonic sector, caused by Majorana CP-violating phases. A similar region is present and the above conclusion remains valid if we perform the analysis using the results of ref. [56] and ref. [7] for the LMA and LOW-QVO solutions, as Figs. 8 and 9 demonstrate.

It would be practically impossible to obtain information on the CP-violation in the leptonic sector due to the Majorana CP-violating phases by measuring $|\langle m \rangle|$ if the SMA solution of the solar neutrino problem turns out to be the valid one.

For all solutions of the solar neutrino problem we have $|\langle m \rangle| \lesssim (0.08 - 0.09)$ eV for the inverted mass hierarchy neutrino mass spectrum. In large allowed regions of the corresponding parameter space we have $|\langle m \rangle| \gtrsim (0.01 - 0.02)$ eV, which can be tested in the future $(\beta\beta)_{0\nu}$ -decay experiments like GENIUS, EXO, etc.

As the dependence of $|\langle m \rangle|$ on $\cos 2\theta_{\odot}$ is rather strong, in Fig. 10 we plot $|\langle m \rangle|$ versus $\cos 2\theta_{\odot}$. The region of values of $|\langle m \rangle|$, corresponding to the “just-CP-violation”, is marked by the dark-grey color. The uncertainty in the allowed ranges of $|\langle m \rangle|$ for the two different values of the relative CP-parity of ν_2 and ν_3 is due mainly to the uncertainty in the value of Δm_{atm}^2 . If the value of Δm_{atm}^2 is better constrained, and $|\langle m \rangle|$ is found to lie in the regions corresponding to the LMA or LOW-QVO solution, it would be possible to establish in the case of the mass spectrum (61) if CP is violated and to get information on the value of one of the two CP-violating phases ($\alpha_3 - \alpha_2$).

Equation (67) permits to relate the value of $\sin^2(\alpha_3 - \alpha_2)/2$ to the experimentally measured quantities $|\langle m \rangle|$, Δm_{atm}^2 and $\sin^2 2\theta_{\odot}$:

$$\sin^2 \frac{\alpha_3 - \alpha_2}{2} = \left(1 - \frac{|\langle m \rangle|^2}{\Delta m_{\text{atm}}^2 (1 - |U_{e1}|^2)^2} \right) \frac{1}{\sin^2 2\theta_{\odot}}. \quad (70)$$

A more precise determination of Δm_{atm}^2 and θ_{\odot} and a sufficiently accurate measurement of $|\langle m \rangle|$ could allow to get information about the value of $(\alpha_3 - \alpha_2)$, provided the neutrino mass spectrum is of the inverted hierarchy type (61). This is illustrated in Fig. 11 for the cases of the LMA and LOW-QVO solutions. We would like to point out also that, as in the case of a hierarchical neutrino mass spectrum, even if one finds using the $(\beta\beta)_{0\nu}$ -decay data that the phase $(\alpha_3 - \alpha_2) = 0, \pm\pi$ and does not violate CP-invariance, the second phase, $(\alpha_2 - \alpha_1) \equiv \alpha_{21}$, is not constrained and can be a source of CP-violation in other $\Delta L = 2$ processes.

The results derived in the present Section show that in the case of massive Majorana neutrinos and neutrino mass spectrum of the inverted hierarchy type, eq. (61), the description of the solar and atmospheric neutrino data in terms of neutrino oscillations/transitions and the CHOOZ limit imply an upper limit on the effective Majorana mass parameter: $|\langle m \rangle| \lesssim (8 - 9) \times 10^{-2}$ eV. A measured value of $|\langle m \rangle| \gtrsim (2 - 3) \times 10^{-1}$ eV would strongly disfavor, under the general assumptions of the present study (3-neutrino mixing, $(\beta\beta)_{0\nu}$ -decay generated only by the charged (V-A) current weak interaction via the exchange of the three Majorana neutrinos), the possibility of inverted neutrino mass hierarchy.

6 The Case of Three Quasi-Degenerate Neutrinos

The neutrinos $\nu_{1,2,3}$ are quasi-degenerate in mass if

$$m_1 \simeq m_2 \simeq m_3 \equiv m, \quad (71)$$

and

$$m \gg \sqrt{\Delta m_{\text{atm}}^2}. \quad (72)$$

When (71) holds but $m \sim O(\sqrt{\Delta m_{\text{atm}}^2})$, we have a partial hierarchy or partial inverted hierarchy between the neutrino masses. These two possibilities will be considered in the next Section. The possible implications of quasi-degenerate neutrino mass spectrum for $|\langle m \rangle|$ were discussed recently also in [53], but from a somewhat different point of view.

As for the hierarchical neutrino mass spectrum we have:

$$\begin{aligned} \Delta m_{\odot}^2 &\equiv \Delta m_{21}^2, & \Delta m_{\text{atm}}^2 &\equiv \Delta m_{32}^2, \\ |U_{e1}|^2 &= \cos^2 \theta_{\odot} (1 - |U_{e3}|^2), \\ |U_{e2}|^2 &= \sin^2 \theta_{\odot} (1 - |U_{e3}|^2), \\ |U_{e3}|^2 &= \sin^2 \theta < 0.09 \quad (\text{CHOOZ}). \end{aligned} \quad (73)$$

The parameters Δm_{atm}^2 , Δm_{\odot}^2 and θ_{\odot} take values in the regions quoted in Section 2. Equation (73) allows to express eqs. (71) and (72) in the compact form

$$\sqrt{\Delta m_{21}^2} \ll (<) \sqrt{\Delta m_{32}^2} \ll m_1. \quad (74)$$

As can be shown (see, e.g., [48, 60]), the mass scale m effectively coincides with the electron (anti-)neutrino mass m_{ν_e} measured in the ${}^3\text{H}$ β -decay experiments:

$$m = m_{\nu_e}. \quad (75)$$

Thus, the experimental upper bounds in eq. (13) lead to $m < 2.5$ eV .

The quasi-degenerate neutrino mass spectrum under discussion is actually realized for values of the neutrino mass m , which is measured in the ${}^3\text{H}$ β -decay experiments, $m = m_{\nu_e} \gtrsim (0.2 - 0.3)$ eV (see Section 7 for a more detailed discussion). Recently, Karlsruhe, Mainz and Troitzk collaborations proposed a new ${}^3\text{H}$ β -decay experiment KATRIN [69], which is planned to have a record sensitivity of 0.35 eV to the neutrino mass m_{ν_e} . Clearly, the realization of this project could be crucial for the test of the possibility of three quasi-degenerate neutrinos.

It follows from eqs. (71) - (72) and eq. (19) that $|\langle m \rangle|$ can be approximated by ⁸:

$$|\langle m \rangle| \simeq m |\cos^2 \theta_{\odot} (1 - |U_{e3}|^2) e^{i\alpha_1} + \sin^2 \theta_{\odot} (1 - |U_{e3}|^2) e^{i\alpha_2} + |U_{e3}|^2 e^{i\alpha_3}|. \quad (76)$$

If CP is conserved, we have the following possibilities, depending on the relative CP-parities of the neutrinos ν_j .

Case A. For $\phi_1 = \phi_2 = \pm\phi_3$ (i.e., $\alpha_{21} = 0$, $\alpha_{31} = 0, \pm\pi$), we get a very simple expression for $|\langle m \rangle|$:

$$|\langle m \rangle| \simeq m (1 - |U_{e3}|^2 \pm |U_{e3}|^2), \quad (77)$$

i.e., $|\langle m \rangle|$ does not depend on Δm_{\odot}^2 , θ_{\odot} and Δm_{atm}^2 . Note that if $\phi_1 = \phi_2 = \phi_3$, $|\langle m \rangle| = m$. Using the CHOOZ limit [64] on $|U_{e3}|^2$ one finds the range of allowed values of $|\langle m \rangle|$:

$$0.8 m \leq |\langle m \rangle| \leq 1.0 m. \quad (78)$$

⁸Under the assumption that the terms $\sim |U_{e3}|^2$ give a negligible contribution in $|\langle m \rangle|$, this case was considered briefly recently in [78].

The above result and the bound on $|\langle m \rangle|$ obtained in the Heidelberg-Moscow experiment [29], eq. (4), imply

$$m < (0.4 \div 1.2) \text{ eV} , \quad (79)$$

which is compatible with the ^3H beta-decay limit on m .

Case B. If $\phi_1 = -\phi_2 = \pm\phi_3$ (i.e., $\alpha_{21} = \pm\pi$, $\alpha_{31} = 0, \pm\pi$), $|\langle m \rangle|$ is given by:

$$|\langle m \rangle| \simeq m |\cos 2\theta_\odot (1 - |U_{e3}|^2) \pm |U_{e3}|^2|. \quad (80)$$

Now $|\langle m \rangle|$ depends $\cos 2\theta_\odot$ and thus varies with the solution of the solar neutrino problem. For the LMA and LOW-QVO solutions, the expression for $|\langle m \rangle|$ in the case of $\cos 2\theta_\odot > 0$ and $\phi_1 = -\phi_2 = \phi_3$ coincides with that for $\cos 2\theta_\odot < 0$ and $\phi_1 = -\phi_2 = -\phi_3$. The allowed intervals of values of $|\langle m \rangle|/m$ for the three solutions of the solar neutrino problem derived in [7, 56, 58] are reported in Table 4.

Table 4: Values of $|\langle m \rangle|/m$ for the quasi-degenerate neutrino mass spectrum, eq. (71), CP-conservation and $\phi_1 = -\phi_2 = \pm\phi_3$ (see text for details).

Data from		$ \langle m \rangle /m$	
		$\phi_1 = -\phi_2 = \phi_3$	$\phi_1 = -\phi_2 = -\phi_3$
Ref. [7] (95% C.L.)	LMA	0.21 \div 0.68	0.10 \div 0.65
	LOW-QVO	0.3 \div 0.58	0.18 \div 0.54
Ref. [56] (90% (99%) C.L.)	LMA	0.25 (0) \div 0.68 (0.70)	0.12 (0) \div 0.65 (0.67)
	SMA	(1.0)	(0.8 \div 1.0)
	LOW-QVO	0.05 (0) \div 0.33 (0.49)	0 (0) \div 0.26 (0.42)
Ref. [58] (90% (99%) C.L.)	LMA	0 (0) \div 0.70 (0.74)	0 (0) \div 0.68 (0.72)
	SMA	1.0 (1.0)	0.9 (0.8) \div 1.0 (1.0)
	LOW-QVO	0 (0) \div 0.50 (0.69)	0 (0) \div 0.48 (0.67)

Several remarks are in order.

1. In the case of the LMA solution, the 99% C.L. results of the analysis in ref. [58] and [56] do not exclude the possibility of a cancellation between the different contributions in $|\langle m \rangle|$, so that

$$0 \leq |\langle m \rangle| \lesssim 0.7 m.$$

The results of ref. [7] for the same solution does not allow a complete cancellations to occur and one has

$$0.2 \times 10^{-2} m \leq |\langle m \rangle| \leq 0.7 m.$$

2. The results of all three analyzes for the SMA solution agree. The case under discussion cannot be distinguished from the $\phi_1 = \phi_2 = \pm\phi_3$ one since $\cos 2\theta_\odot \simeq 1$.

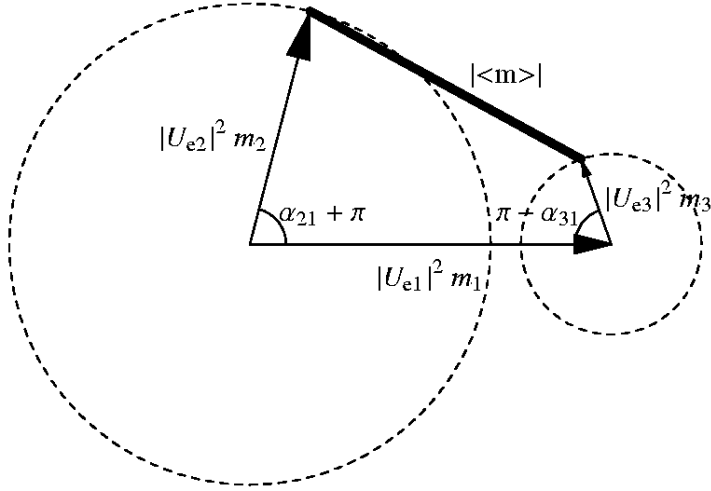


Figure 1: The effective Majorana mass $|\langle m \rangle|$ represented as the absolute value of the vector sum of the three contributions in eqs. (19) and (21), each of which is expressed as a vector in the complex plane (see text for details). The CP-violating phases α_{21} and α_{31} shown in the figure can vary between 0 and 2π .

3. In the LOW-QVO solution case, the results of the analyzes [56, 58] do not exclude the possibility of cancellations between the different contributions in $|\langle m \rangle|$, as well as of having $\cos 2\theta_\odot < 0$, so that:

$$0 \leq |\langle m \rangle| \leq 0.5 \div 0.7 m.$$

In contrast, according to the results of the analysis [7], $\cos 2\theta_\odot > 0$ and one finds a relatively large lower bound on $|\langle m \rangle|$.

The regions of allowed values of $|\langle m \rangle|$, corresponding to the LMA and the LOW-QVO solutions of ref. [58], are shown as a function of m in Figs. 12 and 13, respectively. One can have $|\langle m \rangle| \gtrsim 0.1$ eV for values of $m \geq 0.1$ eV. Taking into account the ${}^3\text{H}$ β -decay upper bound $m < 2.5$ eV, we find that $\max(|\langle m \rangle|) \simeq 1.7$ eV. This implies that $|\langle m \rangle|$ can have the maximal value allowed by the limit (4): $\max(|\langle m \rangle|) < (0.35 - 1.05)$ eV.

If CP-parity is not conserved, one has to take into account the two relevant CP-violating phases α_{21} and α_{31} in the expression for $|\langle m \rangle|$. The effective mass $|\langle m \rangle|$ can be computed using a graphical method [50, 52]. Each of the three contributions to $|\langle m \rangle|$ can be represented by a vector, \mathbf{n}_j , $j = 1, 2, 3$, in the complex plane, as sketched in Fig. 1: $\mathbf{n}_1 = m_1 |U_{e1}|^2 (1, 0)$, $\mathbf{n}_2 = m_2 |U_{e2}|^2 (\cos \alpha_{21}, \sin \alpha_{21})$, $\mathbf{n}_3 = m_3 |U_{e3}|^2 (\cos \alpha_{31}, \sin \alpha_{31})$. The two phases α_{21} and α_{31} can take values from 0 to 2π and the effective Majorana mass $|\langle m \rangle|$ is given by the modulus of the sum of the three vectors: $|\langle m \rangle| = |\mathbf{n}_1 + \mathbf{n}_2 + \mathbf{n}_3|$.

In order to have a complete cancellation between the three terms in $|\langle m \rangle|$, eq. (76), the following condition has to be satisfied (see also [52]):

$$|m_1 U_{e1}^2| < |m_2 U_{e2}^2| + |m_3 U_{e3}^2|. \quad (81)$$

The relation (71) between the masses m_j , eq. (72) and the identification (73) imply that this inequality reduces to a condition on the angle θ_\odot and on $|U_{e3}|^2$:

$$\cos^2 \theta_\odot < \frac{1}{2(1 - |U_{e3}|^2)}. \quad (82)$$

Using the results of the different data analyzes which are summarized in Section 2 and in Tables 1 and 2, we can conclude that:

1. a complete cancellation between the three terms in $|\langle m \rangle|$, eq. (76), is impossible for the SMA solution of the solar neutrino problem;
2. the results on the possible values of θ_{\odot} in [58] and [56] (Table 2) show that there can be a complete cancellation both in the case of the LMA and LOW-QVO solutions;
3. according to the analysis of ref. [7], there can be a cancellation in the LOW-QVO case but not in the LMA one.

The lower and upper limits on $|\langle m \rangle|$ can be found taking respectively $\alpha_{21} = \alpha_{31} = \pm\pi$ (e.g. $\phi_1 = -\phi_2 = -\phi_3$) and $\alpha_{21} = \alpha_{31} = 0$ (e.g. $\phi_1 = \phi_2 = \phi_3$). Recalling the limits already found in the CP-conserving cases, the bounds holding in the CP-violating one are reported in Table 5.

Table 5: Values of $|\langle m \rangle| / m$, corresponding to the different solutions of the solar neutrino problem, neutrino oscillation interpretation of the atmospheric neutrino data and the CHOOZ limit, in the case of quasi-degenerate neutrino mass spectrum, eq. (71), and CP-nonconservation (see text for details).

Data from		$ \langle m \rangle / m$
Ref. [7] (95% C.L.)	LMA	$0.10 \div 1.0$
	LOW-QVO	$0.18 \div 1.0$
Ref. [56] (90 (99%) C.L.)	LMA	$0.12 (0) \div 1.0 (1.0)$
	SMA	$(0.8 \div 1.0)$
	LOW-QVO	$0 (0) \div 1.0 (1.0)$
Ref. [58] (90 (99%) C.L.)	LMA	$0 (0) \div 1.0 (1.0)$
	SMA	$0.9 (0.8) \div 1.0 (1.0)$
	LOW-QVO	$0 (0) \div 1.0 (1.0)$

We see that in the case of CP-violation we can have $|\langle m \rangle| \geq 0.1$ eV as well. The upper bound on m following from the ^3H β -decay data implies $|\langle m \rangle| < 2.5$ eV, while the results (4) of the Heidelberg-Moscow $(\beta\beta)_{0\nu}$ -decay experiment (including a factor of 3 uncertainty in the value of the relevant nuclear matrix element) limit further the maximal value of $|\langle m \rangle|$ to $\max(|\langle m \rangle|) < (0.35 - 1.05)$ eV. Let us remind the reader that, as our results in Sections 4 and 5 showed, one has $\max(|\langle m \rangle|) \lesssim 0.02$ eV if the neutrino mass spectrum is hierarchical, eq. (40), while in the case of inverted mass hierarchy, eq. (61), $\max(|\langle m \rangle|) \lesssim (0.08 - 0.09)$ eV. Thus, the observation of the $(\beta\beta)_{0\nu}$ -decay with a rate which corresponds to $|\langle m \rangle| \gtrsim (0.20 - 0.30)$ eV, would be a very strong experimental evidence in favor of the quasi-degenerate neutrino mass spectrum: this would practically rule out the neutrino mass spectrum of the hierarchical type and would strongly disfavor (if not rule out) that of the inverse mass hierarchy type. The above conclusion would be valid, of course, only if the $(\beta\beta)_{0\nu}$ -decay is generated by the charged current weak interaction with left-handed currents and three-neutrino mixing, via the exchange of three massive Majorana neutrinos.

The improvement of the sensitivity of the ^3H β -decay experiments would allow one to test further the pattern of neutrino masses (71) - (72). The $(\beta\beta)_{0\nu}$ -decay experiments could distinguish between the different CP-parity configurations of the massive neutrinos ν_j and furthermore either

establish the existence of CP-violation in the leptonic sector or put an upper bound on its possible magnitude. This is illustrated in Fig. 14 and in Fig. 15 where we show $|\langle m \rangle|/m$ as a function of $\cos 2\theta_\odot$. The dark grey region is the “just-CP-violation” region which can be spanned by the values of $|\langle m \rangle|/m$ *only if the CP-symmetry is violated*.

If θ_\odot , $|U_{e3}|^2$, m and $|\langle m \rangle|$ are known with a sufficient accuracy, it would be possible to tightly constrain the allowed values of the two CP-violating Majorana phases α_{21} and α_{31} as they must satisfy the relation:

$$\begin{aligned} \frac{|\langle m \rangle|^2}{m^2} - (\cos^4 \theta_\odot (1 - |U_{e3}|^2)^2 + \sin^4 \theta_\odot (1 - |U_{e3}|^2)^2 + |U_{e3}|^4) = \\ 2 \cos^2 \theta_\odot |U_{e3}|^2 (1 - |U_{e3}|^2) \cos \alpha_{31} + 2 \sin^2 \theta_\odot \cos^2 \theta_\odot (1 - |U_{e3}|^2)^2 \cos \alpha_{21} \\ + 2 \sin^2 \theta_\odot |U_{e3}|^2 (1 - |U_{e3}|^2) \cos(\alpha_{21} - \alpha_{31}). \end{aligned} \quad (83)$$

In Fig. 16 we exhibit the allowed values of $\cos \alpha_{21}$ and $\cos \alpha_{31}$ for a given value of $|\langle m \rangle|/m$: for the parameters entering into the expression (83) we use their best fit values from ref. [58] (which lie in the LMA solution region, etc.), $|U_{e3}|^2 = 0.005$ and $|U_{e3}|^2 = 0.08$ and we allow $|\langle m \rangle|$ to vary respectively in the intervals $|\langle m \rangle| = 0.40 m \div 0.70 m$ and $|\langle m \rangle| = 0.20 m \div 0.50 m$.

7 The Partial Mass Hierarchy and Partial Inverted Mass Hierarchy Cases

The partial mass hierarchy and the partial inverted mass hierarchy spectra are characterized respectively by the following relations between the three neutrino masses:

$$m_1 \simeq m_2 < m_3, \quad \text{or} \quad \Delta m_{21}^2 = \Delta m_\odot^2 \ll \Delta m_{32}^2 = \Delta m_{\text{atm}}^2 \sim \mathcal{O}(m_1^2), \quad (84)$$

and

$$m_1 < m_2 \simeq m_3, \quad \text{or} \quad \Delta m_{32}^2 = \Delta m_\odot^2 \ll \Delta m_{21}^2 = \Delta m_{\text{atm}}^2 \sim \mathcal{O}(m_1^2). \quad (85)$$

The pattern (84) ((85)) interpolates between the hierarchical (inverted mass hierarchy) neutrino mass spectrum and the quasi-degenerate one. The two intermediate types of neutrino mass spectrum (84) and (85) were discussed also in [52]. We will consider in the subsequent analysis values of m_1 from the interval: $0.02 \text{ eV} \leq m_1 \leq 0.2 \text{ eV}$. These values of m_1 are determined by the values of Δm_{atm}^2 , obtained in the analyzes of the atmospheric neutrino data, by requiring that $1/5 \Delta m_{\text{atm}}^2 |_{\text{MIN}} \leq m_1^2 \leq 5 \Delta m_{\text{atm}}^2 |_{\text{MAX}}$. For $m_1 > 0.2 \text{ eV}$ one recovers the quasi-degenerate neutrino mass spectrum. If $m_1 \ll 0.02 \text{ eV}$, we get the hierarchical or the inverted mass hierarchy spectrum. We will consider values of m_1 not smaller than 0.02 eV also because for $m_1 \ll 0.02 \text{ eV}$ the contributions of the term $\sim m_1$ in $|\langle m \rangle|$ amounts to a relatively small correction.

7.1 Spectrum with Partial Mass Hierarchy

Using eqs. (19) and (84) and neglecting corrections $\sim \Delta m_\odot^2/m_1^2$, one can express the effective Majorana mass parameter $|\langle m \rangle|$ in the form:

$$|\langle m \rangle| = m_1 \left| \cos^2 \theta_\odot (1 - |U_{e3}|^2) e^{i\alpha_1} + \sin^2 \theta_\odot (1 - |U_{e3}|^2) e^{i\alpha_2} + \sqrt{1 + \frac{\Delta m_{\text{atm}}^2}{m_1^2}} |U_{e3}|^2 e^{i\alpha_3} \right|. \quad (86)$$

If CP is conserved, there are several different possibilities for the values of the relative CP-parities of the three Majorana neutrinos $\nu_{1,2,3}$.

Case A. The three neutrinos $\nu_{1,2,3}$ have the same CP-parities, $\phi_1 = \phi_2 = \phi_3$ (i.e., $\alpha_{21} = \alpha_{31} = 0$). The effective Majorana mass $|\langle m \rangle|$ is given by:

$$|\langle m \rangle| \cong m_1 (1 - |U_{e3}|^2 + \sqrt{1 + \frac{\Delta m_{\text{atm}}^2}{m_1^2}} |U_{e3}|^2). \quad (87)$$

Note that (in the approximation we are working) $|\langle m \rangle|$ does not depend on the value of θ_\odot . Therefore, for all analyzes of the solar neutrino data $|\langle m \rangle|$ is bounded to lie in the interval:

$$2.0 \times 10^{-2} \text{ eV} \lesssim |\langle m \rangle| \lesssim 2.0 \times 10^{-1} \text{ eV} . \quad (88)$$

These values of $|\langle m \rangle|$ can be probed in the future $(\beta\beta)_{0\nu}$ -decay experiments [31, 32, 33, 34].

Case B. If $\phi_1 = \phi_2 = -\phi_3$ (i.e., $\alpha_{21} = 0$, $\alpha_{31} = \pm\pi$), $|\langle m \rangle|$ has the form:

$$|\langle m \rangle| \cong m_1 (1 - |U_{e3}|^2 - \sqrt{1 + \frac{\Delta m_{\text{atm}}^2}{m_1^2}} |U_{e3}|^2). \quad (89)$$

The three terms in the brackets in (89) can mutually compensate each other if $|U_{e3}|^2$ has a value determined by the condition

$$|U_{e3}|_0^2 = \frac{1}{1 + \sqrt{\frac{\Delta m_{\text{atm}}^2}{m_1^2}}}. \quad (90)$$

Using $\max(\Delta m_{\text{atm}}^2) = 8 \times 10^{-3} \text{ eV}^2$ (see eq. (5)) and $\min(m_1) = 0.02 \text{ eV}$, we find that the term in the right-hand side of eq. (77) $(1 + \sqrt{\Delta m_{\text{atm}}^2 / m_1^2})^{-1} \gtrsim 0.18$. Thus, condition (90) cannot be satisfied by the experimentally allowed values of $|U_{e3}|^2$. Correspondingly, cancellation in eq. (89) is impossible and there exists a non-trivial lower bound on $|\langle m \rangle|$:

$$1.6 (1.5) \times 10^{-2} \text{ eV} \leq |\langle m \rangle| \leq 2.0 (2.0) \times 10^{-1} \text{ eV} . \quad (91)$$

The predictions for $|\langle m \rangle|$ in this case can be tested in the next generation of $(\beta\beta)_{0\nu}$ -decay experiments as well.

The dependence of $|\langle m \rangle|$ on $|U_{e3}|^2$ for $\phi_1 = \phi_2 = \phi_3$ and $\phi_1 = \phi_2 = -\phi_3$ is shown in Fig. 17. The figure is obtained for the 90 (99)% C.L. results of the analysis of ref. [58] and taking into account the dependence of the allowed values of Δm_{atm}^2 on the value of $|U_{e3}|^2$. Since in both cases $|\langle m \rangle|$ does not depend on θ_\odot and Δm_\odot^2 , the results exhibited in Fig. 17 are valid for all the different solutions of the solar neutrino problem.

Case C. For $\phi_1 = -\phi_2 = \phi_3$ (i.e., $\alpha_{21} = \pm\pi$, $\alpha_{31} = 0$), the effective mass $|\langle m \rangle|$ is given by:

$$|\langle m \rangle| \cong m_1 \left| \cos 2\theta_\odot (1 - |U_{e3}|^2) + \sqrt{1 + \frac{\Delta m_{\text{atm}}^2}{m_1^2}} |U_{e3}|^2 \right|. \quad (92)$$

Now $|\langle m \rangle|$ depends on $\cos 2\theta_\odot$ and we will get different predictions for $|\langle m \rangle|$ for the different solutions of the solar neutrino problem. Since for the SMA solution one has $\cos 2\theta_\odot \cong 1$, the results for $|\langle m \rangle|$ corresponding to the SMA solution practically coincide with those in the Case 1 considered above and given in eq. (88). According to the 99% C.L. results of ref. [58], for the LMA

and LOW-QVO solutions $\cos 2\theta_\odot$ can be either positive or negative and therefore there can be a cancellation for any allowed value of $|U_{e3}|^2$. The intervals of allowed values of $|\langle m \rangle|$ read:

$$2.2 \times 10^{-3} \text{ (0.0) eV} \leq |\langle m \rangle| \leq 1.3 \text{ (1.4)} \times 10^{-1} \text{ eV}, \quad \text{LMA}, \quad (93)$$

$$0 \text{ (0)} \leq |\langle m \rangle| \leq 7.0 \text{ (11)} \times 10^{-2} \text{ eV}, \quad \text{LOW-QVO}, \quad (94)$$

$$2.0 \text{ (2.0)} \times 10^{-2} \text{ eV} \leq |\langle m \rangle| \leq 2.0 \text{ (2.0)} \times 10^{-1} \text{ eV}, \quad \text{SMA}. \quad (95)$$

Since for the LMA solution the corrections $\sim \Delta m_{21}^2/m_1^2 = \Delta m_\odot^2/m_1^2$ can be as large as $\sim 2.3 \times 10^{-3}$ eV, the (99% C.L.) lower limit, $\min(|\langle m \rangle|) = 0$ eV, quoted above, can actually be any value between $\sim 2.3 \times 10^{-3}$ eV and 0 eV. In contrast, from the analysis of ref. [7] it follows that $\cos 2\theta_\odot > 0$ for the LMA and LOW-QVO solutions. Thus, according to the results of [7], cancellation of the two-contributions in eq. (92) is excluded for both the LMA and the LOW-QVO solutions, leading to the following intervals of possible values of $|\langle m \rangle|$:

$$4.0 \times 10^{-3} \text{ eV} \leq |\langle m \rangle| \leq 1.4 \times 10^{-1} \text{ eV} \quad \text{LMA}, \quad (96)$$

$$6.6 \times 10^{-3} \text{ eV} \leq |\langle m \rangle| \leq 1.2 \times 10^{-1} \text{ eV} \quad \text{LOW-QVO}. \quad (97)$$

Case D. For $\phi_1 = -\phi_2 = -\phi_3$ (*i.e.*, $\alpha_{21} = \alpha_{31} = \pm\pi$), the expression for $|\langle m \rangle|$ can be written as:

$$|\langle m \rangle| \simeq m_1 \left| \cos 2\theta_\odot (1 - |U_{e3}|^2) - \sqrt{1 + \frac{\Delta m_{\text{atm}}^2}{m_1^2} |U_{e3}|^2} \right|. \quad (98)$$

Most of the observations made for the previous case hold also for this one. The results obtained in ref. [58] imply the following allowed intervals of values of $|\langle m \rangle|$:

$$8.0 \times 10^{-4} \text{ (0.0) eV} \leq |\langle m \rangle| \leq 1.2 \text{ (1.3)} \times 10^{-1} \text{ eV}, \quad \text{LMA}, \quad (99)$$

$$0 \text{ (0)} \leq |\langle m \rangle| \leq 5.0 \text{ (14)} \times 10^{-2} \text{ eV}, \quad \text{LOW-QVO}, \quad (100)$$

$$1.6 \text{ (1.5)} \times 10^{-2} \text{ eV} \leq |\langle m \rangle| \leq 2.0 \text{ (2.0)} \times 10^{-1} \text{ eV}, \quad \text{SMA}. \quad (101)$$

The dependence of $|\langle m \rangle|$ on $|U_{e3}|^2$ for the two cases $\phi_1 = -\phi_2 = \pm\phi_3$ is shown in Fig. 18 and in Fig. 19, respectively. The 90 and 99% C.L. results of ref. [58] were used for the figures (in particular, the dependence of Δm_{atm}^2 and θ_\odot on $|U_{e3}|^2$ was taken into account).

In order to illustrate the dependence of $|\langle m \rangle|$ on θ_\odot , we plot in Fig. 20 the ratio $|\langle m \rangle|/m_1$ versus $\cos 2\theta_\odot$ for the four CP-conserving cases discussed above. The region marked with dark-grey scale corresponds to “just-CP-violation”. A value of $|\langle m \rangle|/m_1$ in this region would signal the existence of CP-violation in the leptonic sector, induced by the Majorana CP-violating phases: $|\langle m \rangle|/m_1$ cannot take a value in the indicated region if CP-parity is conserved.

Note that, as we have shown in Section 5, if the neutrino mass spectrum is of the inverted hierarchy type, one typically has $\max(|\langle m \rangle|) \lesssim 0.06$ eV, with the largest allowed value of $|\langle m \rangle| \lesssim (0.08 - 0.09)$ eV possible only in the case of the SMA solution of the ν_\odot -problem. This has to be compared with $\max(|\langle m \rangle|) = \max(m_1) \cong 0.2$ eV one finds for the partial mass hierarchy spectrum under study.

If the CP-symmetry is violated, the two CP-violating phases entering into the expression (86) for $|\langle m \rangle|$, α_{21} and α_{31} , must obey the following relation:

$$\begin{aligned}
|\langle m \rangle|^2 &= m_1^2 \cos^4 \theta_\odot (1 - |U_{e3}|^2)^2 - m_1^2 \sin^4 \theta_\odot (1 - |U_{e3}|^2)^2 - (m_1^2 + \Delta m_{\text{atm}}^2) |U_{e3}|^4 = \\
&= 2 m_1^2 \cos^2 \theta_\odot \sin^2 \theta_\odot (1 - |U_{e3}|^2)^2 \cos \alpha_{21} + 2 m_1 \sqrt{m_1^2 + \Delta m_{\text{atm}}^2} \cos^2 \theta_\odot |U_{e3}|^2 (1 - |U_{e3}|^2) \cos \alpha_{31} \\
&\quad + 2 m_1 \sqrt{m_1^2 + \Delta m_{\text{atm}}^2} \sin^2 \theta_\odot |U_{e3}|^2 (1 - |U_{e3}|^2) (\cos \alpha_{21} \cos \alpha_{31} + \sin \alpha_{21} \sin \alpha_{31}).
\end{aligned} \tag{102}$$

One could constrain α_{21} and α_{31} once the values of all other observables in eq. (102) are measured with a sufficiently good precision. In Fig. 21 and Fig. 22 we illustrate this possibility by plotting $\cos \alpha_{21}$ versus $\cos \alpha_{31}$ for the best fit values of Δm_\odot^2 , θ_\odot , Δm_{atm}^2 and $|U_{e3}|^2$ found in [58] (see Section 2), $m_1 = 0.02; 0.2$ eV, and for $|U_{e3}|^2 = 0.08$, best fit values of the remaining three parameters and $m_1 = 0.02; 0.2$ eV, respectively. Let us note, however, that obtaining experimental information about the mass m_1 ($\simeq m_2$) which in the case under study is supposed to have a value $\sim (0.02 - 0.20)$ eV, seems at present to be extremely difficult.

7.2 Spectrum with Partial Inverted Hierarchy

In this case $|U_{e1}|^2 = \sin^2 \theta$ and is constrained by the CHOOZ limit. The general expression for $|\langle m \rangle|$ has the form

$$|\langle m \rangle| = \left| m_1 |U_{e1}|^2 e^{i\alpha_1} + (1 - |U_{e1}|^2) \sqrt{m_1^2 + \Delta m_{\text{atm}}^2} (\cos^2 \theta_\odot + \sin^2 \theta_\odot e^{i(\alpha_3 - \alpha_2)}) e^{i\alpha_2} \right|. \tag{103}$$

For relatively small values of $|U_{e1}|^2$, e.g., $|U_{e1}|^2 \lesssim 0.01$, the term $m_1 |U_{e1}|^2 \lesssim 2 \times 10^{-3}$ eV and neglecting it we get the following simple expression for $|\langle m \rangle|$:

$$|\langle m \rangle| \cong \left| \cos^2 \theta_\odot + \sin^2 \theta_\odot e^{i(\alpha_3 - \alpha_2)} \right| \sqrt{m_1^2 + \Delta m_{\text{atm}}^2}. \tag{104}$$

In the CP-conserving case, there are two major possibilities for the values of the neutrino CP-parities.

Case A. If $\phi_2 = \phi_3 = \pm \phi_1$ (i.e., $\alpha_{21} = \alpha_{31} = 0, \pm\pi$), the effective Majorana mass parameter $|\langle m \rangle|$ is given by:

$$|\langle m \rangle| = \sqrt{m_1^2 + \Delta m_{\text{atm}}^2} (1 - |U_{e1}|^2) \pm m_1 |U_{e1}|^2, \tag{105}$$

where $m_1 |U_{e1}|^2 \leq 1.8 \times 10^{-2}$ eV. A cancellation between the two terms in (105) is impossible and one has a non-trivial lower bound on $|\langle m \rangle|$. The allowed values of $|\langle m \rangle|$ do not depend on θ_\odot and therefore are the same for all solutions of the ν_\odot -problem and the different analyzes of the solar neutrino data. They depend very weakly on $|U_{e1}|^2$. We have:

$$2.8 (1.8) \times 10^{-2} \text{ eV} \leq \lesssim |\langle m \rangle| \leq \lesssim 2.1 (2.2) \times 10^{-1} \text{ eV}.$$

Case B. For $\phi_2 = -\phi_3 \pm \phi_1$ (i.e., $(\alpha_3 - \alpha_2) = \pm\pi$, $\alpha_{21}, \alpha_{31} = 0, \pm\pi$), $|\langle m \rangle|$ takes the form:

$$|\langle m \rangle|_\pm \simeq \left| \cos 2\theta_\odot \sqrt{m_1^2 + \Delta m_{\text{atm}}^2} (1 - |U_{e1}|^2) \pm m_1 |U_{e1}|^2 \right|. \tag{106}$$

For the SMA solution we have $\cos 2\theta_\odot \cong 1$ and the results for $|\langle m \rangle|$ are equivalent to those in the Case 1. For the LMA and LOW-QVO solutions the values $|\langle m \rangle|$ can have depend on the solution and on the data analysis. In Fig. 23 and in Fig. 24 we plot the allowed regions of values of

$|\langle m \rangle|$ versus Δm_{atm}^2 for the LMA and LOW-QVO solutions, respectively, of ref. [58]. Since for both solutions values of $|\cos 2\theta_{\odot}| < 0.09$ are possible (at 90% and 99% C.L.) [58], and we can have also $|U_{e1}|^2 \cong 0$, one does not get a significant lower bound on $|\langle m \rangle|$. The values of $|\langle m \rangle|$, corresponding to the three solutions of the solar neutrino problem and the different data analyzes in [7], [56] and [58], are reported in Table 6. According to the analysis of ref. [7], $\cos 2\theta_{\odot} > 0.2$ (0.4) for the LMA (LOW-QVO) solution. This leads to the non-trivial lower bounds on the possible values of $|\langle m \rangle|$ for the indicated solutions, cited in Table 6.

The dependence of $|\langle m \rangle|$ on $\cos 2\theta_{\odot}$ is exhibited in Fig. 25. The uncertainty in the allowed ranges of values of $|\langle m \rangle|$ is mainly due to the relatively large interval of possible values of m_1 we consider.

If CP-is not conserved and $|U_{e1}|^2$ is shown to be sufficiently small, so that for $m_1 \leq 0.2$ eV the term $m_1|U_{e1}|^2$ in eq. (103) can be neglected, one has the following simple relation between $\sin^2(\alpha_3 - \alpha_2)/2$ and the observables $|\langle m \rangle|$, $\sin^2 2\theta_{\odot}$ and $m_1^2 + \Delta m_{\text{atm}}^2$:

$$\sin^2 \frac{\alpha_3 - \alpha_2}{2} = \frac{1}{\sin^2 2\theta_{\odot}} \left(1 - \frac{|\langle m \rangle|^2}{m_1^2 + \Delta m_{\text{atm}}^2} \right). \quad (107)$$

The allowed ranges of $\sin^2(\alpha_3 - \alpha_2)/2$ as a function of $|\langle m \rangle| / \sqrt{m_1^2 + \Delta m_{\text{atm}}^2}$ are reported in Fig. 26 for the LMA and LOW-QVO solutions [58], respectively. Obviously, knowing $|\langle m \rangle|$, $\sin^2 2\theta_{\odot}$ and $(m_1^2 + \Delta m_{\text{atm}}^2)$ experimentally would allow to get information about the CP-violation caused by the Majorana CP-violating phases. We note that this conclusion is not valid for the SMA solution of the solar neutrino problem since for this solution $\sin^2 \theta_{\odot} \ll 1$ and (see eq. (104))

$$|\langle m \rangle| \cong \sqrt{m_1^2 + \Delta m_{\text{atm}}^2}, \quad \text{SMA MSW.} \quad (108)$$

Table 6: Values of $|\langle m \rangle|$, corresponding to the different solutions of the solar neutrino problem, neutrino oscillation interpretation of the atmospheric neutrino data and the CHOOZ limit. The results are obtained for the mass spectrum with partial inverted hierarchy, eq. (85), CP-conservation, $\phi_2 = -\phi_3 \pm \phi_1$, negligible $m_1|U_{e1}|^2$, and $0.02 \text{ eV} \leq m_1 \leq 0.20 \text{ eV}$ (see text for further details).

Data from		$ \langle m \rangle $ [eV]
Ref. [7] (95% C.L.)	LMA	$0 \div 1.4 \times 10^{-1}$
	LOW-QVO	$1.0 \times 10^{-2} \div 1.1 \times 10^{-1}$
Ref. [56] (90 (99%) C.L.)	LMA	$0 (0) \times 10^{-2} \div 1.4 (1.5) \times 10^{-1}$
	SMA	$(1.8 \times 10^{-2} \div 2.2 \times 10^{-1})$
	LOW-QVO	$0 (0) \times 10^{-3} \div 0.5 (1.1) \times 10^{-1}$
Ref. [58] (90 (99%) C.L.)	LMA	$0 (0) \div 1.4 (1.5) \times 10^{-1}$
	SMA	$2.8 (1.8) \times 10^{-2} \div 2.1 (2.2) \times 10^{-1}$
	LOW-QVO	$0 (0) \div 1.0 (1.4) \times 10^{-1}$

However, the measurement of $|\langle m \rangle|$ in this case would allow to determine m_1 and thus the whole neutrino mass spectrum.

8 Conclusions

Assuming three-neutrino mixing and massive Majorana neutrinos, we have studied in detail the implications of the neutrino oscillation solutions of the solar and atmospheric neutrino problems and of the data of the reactor long baseline CHOOZ and Palo Verde experiments [64, 65], for the predictions of the effective Majorana mass $|\langle m \rangle|$, which determines the $(\beta\beta)_{0\nu}$ -decay rate. The results of the neutrino oscillation fits of the latest solar and atmospheric neutrino data [7, 55, 56, 58] have been used in our analysis. We have considered essentially all possible types of neutrino mass spectrum compatible with the existing data: hierarchical, neutrino mass spectrum with inverted hierarchy, with partial hierarchy, with partial inverted hierarchy, and with three quasi-degenerate neutrinos. In the present study we have investigated the general case of CP-nonconservation. The $(\beta\beta)_{0\nu}$ -decay effective Majorana mass $|\langle m \rangle|$ depends, in general, on two physical (Majorana) CP-violating phases. For each of the five types of neutrino mass spectrum indicated above we have derived detailed predictions for the values of $|\langle m \rangle|$ for the three solutions of the solar neutrino problem, favored by the current solar neutrino data: the LMA MSW, the SMA MSW and the LOW-QVO one. In each of these cases we have identified the “just-CP-violation” region of values of $|\langle m \rangle|$ whenever it existed: a value of $|\langle m \rangle|$ in this region would unambiguously signal the presence of CP-violation in the lepton sector. Analyzing the case of CP-conservation, we have derived predictions for $|\langle m \rangle|$ corresponding to all possible sets of values of the relative CP-parities of the three massive Majorana neutrinos. This was done for all different types of neutrino mass spectrum we have considered. We have investigated the possibility of cancellation between the different terms contributing to $|\langle m \rangle|$. The cases when such a cancellation is impossible and there exists a non-trivial lower bound on $|\langle m \rangle|$ were identified and the corresponding lower bounds were given.

More specifically, if the neutrino mass spectrum is hierarchical, only the contributions to $|\langle m \rangle|$ due to the exchange of the two heavier Majorana neutrinos $\nu_{2,3}$ can be relevant and $|\langle m \rangle|$ depends only on one CP-violating phase, α_{32} . For the SMA and LOW-QVO solutions of the solar neutrino problem one has $|\langle m \rangle| \lesssim 4.0 \times 10^{-3}$ eV. For the LMA solution we get $|\langle m \rangle| \lesssim 8.5 \times 10^{-3}$ eV if one uses the results of the analyzes in [7, 56], while the results of the 3-neutrino mixing analysis of [58] allow a somewhat larger value of $|\langle m \rangle| \lesssim (1.0 - 2.0) \times 10^{-2}$ eV. The maximal values of $|\langle m \rangle|$ correspond to CP-conservation and ν_2 and ν_3 having identical CP-parities, $\phi_2 = \phi_3$. If $\phi_2 = -\phi_3$, the allowed maximal values of $|\langle m \rangle|$ are somewhat smaller. For all three solutions there are no significant lower bounds on $|\langle m \rangle|$: the lower bound in any case does not exceed 8.0×10^{-4} eV. Deep mutual compensations between the terms contributing to $|\langle m \rangle|$, corresponding to the exchange of different virtual massive Majorana neutrinos, are possible. Such cancellation can take place both if CP is not conserved and in the case of CP-conservation if $\phi_2 = -\phi_3$. The degree of compensation depends for given values of the solar and atmospheric neutrino oscillation parameters Δm_{\odot}^2 , θ_{\odot} and Δm_{atm}^2 , on the value of $|U_{e3}|^2$, which is constrained by the CHOOZ data. The problem of compensations is most relevant in the case of the LMA MSW solution of the ν_{\odot} -problem, since in this case $|\langle m \rangle|$ can have the largest possible values for the hierarchical neutrino mass spectrum. Due to the relatively large allowed ranges of values of Δm_{\odot}^2 , θ_{\odot} and Δm_{atm}^2 , there are no “just-CP-violation” regions of $|\langle m \rangle|$. A better determination of Δm_{\odot}^2 , θ_{\odot} and Δm_{atm}^2 together with a sufficiently accurate measurement of $|\langle m \rangle|$ could allow to get a direct information on the CP-violating phase α_{32} . These results are summarized in Figs. 2 - 5.

In the case of the neutrino mass spectrum with inverted hierarchy, eqs. (61) - (63), the dominant contribution to $|\langle m \rangle|$ are again due to the two heavier Majorana neutrinos $\nu_{2,3}$ and $|\langle m \rangle|$ is determined by Δm_{atm}^2 , $\sin^2 2\theta_{\odot}$, the CP-violating phase α_{32} and by $|U_{e1}|^2$, which is constrained by the CHOOZ data. The effective Majorana mass can be considerably larger than in the case of a hierarchical neutrino mass spectrum: $|\langle m \rangle| \lesssim (6.8 - 8.9) \times 10^{-2}$ eV. The maximal $|\langle m \rangle|$ corresponds

to CP-conservation and $\phi_2 = \phi_3$ ($\alpha_{32} = 0$); it is possible for all three solutions of the ν_\odot -problem. It varies weakly with the results of the different analyzes being used. For $\phi_2 = -\phi_3$ ($\alpha_{32} = \pm\pi$) the maximal allowed values of $|\langle m \rangle|$ are the same for the SMA MSW solution, while we have $|\langle m \rangle| \lesssim (4.8-5.9) \times 10^{-2}$ eV ($|\langle m \rangle| \lesssim (3.7-5.4) \times 10^{-2}$ eV) for the LMA MSW (LOW-QVO) solution. For all three solutions there exists a significant lower bound of $|\langle m \rangle| \gtrsim (3-4) \times 10^{-2}$ eV if $\phi_2 = \phi_3$. For $\phi_2 = -\phi_3$ one gets an analogous lower bound only in the case of the SMA solution, while for the LMA and LOW-QVO solutions values of $|\langle m \rangle| \ll 10^{-2}$ eV are possible. Both for the LMA and LOW-QVO solutions there exist relatively large “just-CP-violation” regions of $|\langle m \rangle|$, in which $|\langle m \rangle|$ has a relatively large value: $|\langle m \rangle| \cong (2-8) \times 10^{-2}$ eV. There is no such region in the case of the SMA MSW solution. We have also shown that a sufficiently accurate measurement of $|\langle m \rangle|$, Δm_{atm}^2 , $\sin^2 2\theta_\odot$, $(1 - |U_{e1}|^2)$ can allow to get direct information on the value of the CP-violating phase α_{32} . Our results for the case of neutrino mass spectrum with inverted hierarchy are illustrated in Figs. 6 - 11.

For the quasi-degenerate neutrino mass spectrum, eqs. (70) - (72), we have $|\langle m \rangle| \sim m$, where m is the common neutrino mass, information about which can be obtained from the ^3H β -decay experiments [67, 68]: $m < 2.5$ eV. Future astrophysical and cosmological measurements (see, e.g., [70, 71]) might further constrain m . The effective Majorana mass $|\langle m \rangle|$ depends also on θ_\odot , $|U_{e3}|^2$ which is constrained by the CHOOZ data, and on two physical CP-violating phases, α_{21} and α_{31} . The maximal value of $|\langle m \rangle|$ is determined by the value of m , $|\langle m \rangle| \leq m$. It is possible for all three solutions of the solar neutrino problem. Obviously, $|\langle m \rangle|$ is limited by the upper bounds obtained in the ^3H β -decay [67, 68] and in the $(\beta\beta)_{0\nu}$ -decay [29, 30] (see eqs. (3) and (4)) experiments: $|\langle m \rangle| < (0.33 - 1.05)$ eV. If CP-invariance holds and the CP-parities of the three massive Majorana neutrinos satisfy the relation $\phi_1 = \phi_2 = \pm\phi_3$, we have $0.8m \lesssim |\langle m \rangle| \leq m$. We get a similar result for $\phi_1 = -\phi_2 = \pm\phi_3$ in the case of the SMA solution. The existence of a significant lower bound on $|\langle m \rangle|$ for the LMA and the LOW-QVO solutions if $\phi_1 = -\phi_2 = \pm\phi_3$ depends on the $\min|\cos 2\theta_\odot|$. The latter varies with the analysis: using the results of [7] one finds $|\langle m \rangle| \gtrsim (0.1-0.2) m$ ($|\langle m \rangle| \gtrsim (0.2-0.3) m$) for the LMA (LOW-QVO) solution. According to the (99% C.L.) results of the analysis [56, 58] one can have $\cos 2\theta_\odot = 0$ and therefore there is no significant lower bound on $|\langle m \rangle|$ for both solutions. There exist “just-CP-violation” regions for the LMA and LOW-QVO solutions, in which $|\langle m \rangle|$ can be in the range of sensitivity of the future $(\beta\beta)_{0\nu}$ -decay experiments, while in the case of the SMA MSW solution there is no such region. The knowledge of $|\langle m \rangle|$, m , θ_\odot and $|U_{e3}|^2$ would imply a non-trivial constraint on the two CP-violating phases α_{21} and α_{31} . Some of our results for the quasi-degenerate neutrino mass spectrum are presented graphically in Figs. 12 - 16.

We have analyzed also in detail the predictions for $|\langle m \rangle|$ in the case neutrino mass spectrum with partial mass hierarchy eq. (83), and with partial inverted mass hierarchy, eq. (84). These spectra interpolate respectively between the hierarchical and the inverted mass hierarchy spectra and the quasi-degenerate one. Accordingly, the results for $|\langle m \rangle|$ we have found in the case of neutrino mass spectrum with partial hierarchy (partial inverted hierarchy) “interpolate” between the results for the hierarchical (inverted mass hierarchy) and the quasi-degenerate neutrino mass spectra. Most of these results are presented graphically in Figs. 17 - 26.

The quasi-degenerate 3-neutrino mass spectrum can be critically tested in the future ^3H β -decay experiment KATRIN [69], which is planned to have a sensitivity to $m_{\nu_e} \geq 0.35$ eV. For the quasi-degenerate spectrum one finds $m_{\nu_e} = m \gtrsim 0.20$ eV, while for all the other 3-neutrino mass spectra compatible with the neutrino mass and neutrino oscillations data, we have $m_{\nu_e} \lesssim 0.20$ eV.

Actually, the five different types of possible neutrino mass spectrum we have considered correspond, once Δm_\odot^2 and Δm_{atm}^2 are known and the choice $\Delta m_\odot^2 = \Delta m_{21}^2$ or $\Delta m_\odot^2 = \Delta m_{32}^2$ is made, to different ranges of values of the smallest neutrino mass m_1 . At the same time $|\langle m \rangle|$ is a continuous function of m_1 . In Figs. 27 and 28 we show the possible magnitude of $|\langle m \rangle|$ as

a function of m_1 for m_1 varying continuously ⁹ from 10^{-5} eV to 2.5 eV. The results presented in Figs. 27 and 28 are derived for the allowed regions of values of the relevant input oscillation parameters, obtained in [7, 55, 64] and in [58], and for the two possible choices of Δm_{\odot}^2 in the case of 3-neutrino mixing, $\Delta m_{\odot}^2 = \Delta m_{21}^2$ and $\Delta m_{\odot}^2 = \Delta m_{32}^2$. With the notations we use, we can have $\Delta m_{\odot}^2 = \Delta m_{21}^2$ ($\Delta m_{\odot}^2 = \Delta m_{32}^2$) in the cases of hierarchical (inverted hierarchy), partial hierarchy (partial inverted hierarchy), and quasi-degenerate neutrino mass spectra.

To conclude, we have found that the observation of the $(\beta\beta)_{0\nu}$ -decay with a rate corresponding to $|\langle m \rangle| \gtrsim 0.02$ eV, which is in the range of sensitivity of the future $(\beta\beta)_{0\nu}$ -decay experiments, can provide unique information on the neutrino mass spectrum. Combined with information on the lightest neutrino mass or the type of neutrino mass spectrum, it can give also information on the CP-violation in the lepton sector, and if CP-invariance holds - on the relative CP-parities of the massive Majorana neutrinos. A measured value of $|\langle m \rangle| \gtrsim (2-3) \times 10^{-2}$ eV would strongly disfavor (if not rule out), under the general assumptions of the present study (3-neutrino mixing, $(\beta\beta)_{0\nu}$ -decay generated only by the charged (V-A) current weak interaction via the exchange of the three Majorana neutrinos, neutrino oscillation solutions of the solar neutrino problem and atmospheric neutrino anomaly) the possibility of a hierarchical neutrino mass spectrum, while a value of $|\langle m \rangle| \gtrsim (2-3) \times 10^{-1}$ eV would rule out the hierarchical neutrino mass spectrum, strongly disfavor the spectrum with inverted mass hierarchy and favor the quasi-degenerate spectrum.

In the present article we have considered only the mixing of three massive Majorana neutrinos. We have assumed that the $(\beta\beta)_{0\nu}$ -decay is induced by the (V-A) charged current weak interaction via the exchange of the massive Majorana neutrinos between two neutrons in the initial nucleus. Results for the case of four-neutrino mixing will be presented elsewhere [54].

Note added. Our attention was brought to the paper [79] which discusses some of the questions studied in the present article and which appeared while the present article was being prepared for submission for publication.

Acknowledgments.

We would like to acknowledge discussions with L. Wolfenstein, B. Kayser, J. Nieves and P. Pal concerning the Majorana CP-violating phases. S.M.B. would like to thank the Elementary Particle Theory Sector at SISSA for kind hospitality and support. S.T.P. would like to acknowledge the hospitality of the Aspen Center for Physics where part of this work was done. The work of S.T.P. was supported in part by the EEC grant ERBFMRXCT960090 and by the Italian MURST under the program "Fisica Teorica delle Interazioni Fondamentali".

References

- [1] Super-Kamiokande Collaboration, Y. Fukuda *et al.*, Phys. Rev. Lett. **81**, 1562 (1998);
- [2] Homestake Collaboration, talk by K. Lande at *Neutrino 2000*, 19th International Conference on Neutrino Physics and Astrophysics (Sudbury, Canada, 2000), to be published in the Proceedings of the Conference.
- [3] Kamiokande Collaboration, Y. Fukuda *et al.*, Phys. Rev. Lett. **77**, 1683 (1996).
- [4] SAGE Collaboration, J.N. Abdurashitov *et al.*, Phys. Rev. C **60**, 055801 (1999); talk by V. Gavrin at *Neutrino 2000* [2], to be published in the Proceedings.
- [5] GALLEX Collaboration, W. Hampel *et al.*, Phys. Lett. B **447**, 127 (1999).

⁹Similar plots were proposed also in refs. [51, 52].

- [6] Super-Kamiokande Collaboration, Y. Fukuda *et al.*, Phys. Rev. Lett. **82**, 2430 (1999).
- [7] Super-Kamiokande Collaboration, talk by Y. Suzuki in *Neutrino 2000* [2], to be published in the Proceedings.
- [8] GNO Collaboration, M. Altmann *et al.*, Phys. Lett. B **490**, 16 (2000); talk by E. Bellotti at *Neutrino 2000* [2], to be published in the Proceedings.
- [9] SNO Collaboration, A. Hallin *et al.*, Nucl. Phys. A **663-664**, 787 (2000).
- [10] J.N. Bahcall, M.H. Pinsonneault, and S. Basu, astro-ph/0010346.
- [11] LSND Collaboration, talk by G. Mills at *Neutrino 2000* [2], to appear in the Proceedings.
- [12] K2K Collaboration, Y. Oyama *et al.*, hep-ex/9803014; talk by K. Nakamura at *Neutrino 2000* [2]; K2K Web page: <http://pnahep.kek.jp/>.
- [13] MINOS Collaboration, P. Adamson *et al.*, NuMI-L-476 (March 1999); Web page: <http://www-hep.anl.gov/ndk/hypertext/numi.html>.
- [14] A. Ereditato, talk presented at the NOW2000, September 2000, Otranto, Italy (<http://www.ba.infn.it/~now2000>).
- [15] Borexino Collaboration, talk by G. Ranucci at *Neutrino 2000* [2], to appear in the Proceedings.
- [16] KamLAND Collaboration, talk by A. Piepke at *Neutrino 2000* [2], to appear in the Proceedings.
- [17] MiniBooNE Collaboration, talk by A. Bazarko at *Neutrino 2000* [2], to appear in the Proceedings.
- [18] S. Geer, Phys. Rev. **D57** (1998) 6989, (E) *ibid.* **D59** (1999) 039903; A. De Rujula, M.B. Gavela and P. Hernandez, Nucl. Phys. **B547**, 21 (1999); K. Dick, M. Freund, M. Lindner and A. Romanino, Nucl. Phys. **B562**, 29 (1999); M. Campanelli, A. Bueno and A. Rubbia, hep-ph/9905240; V. Barger, S. Geer and K. Whisnant, Phys. Rev. **D61**, 6989 (2000); A. Donini, M.B. Gavela, P. Hernandez and S. Rigolin Nucl. Phys. **B574**, 23 (2000); A. Romanino, Nucl. Phys. **B574**, 675 (2000); V. Barger, S. Geer, R. Raja and K. Whisnant, Phys. Rev. **D62**, 013004 (2000); M. Freund, M. Lindner, S.T. Petcov and A. Romanino, Nucl. Phys. **B578**, 27 (2000); A. Cervera, A. Donini, M.B. Gavela, J.J. Gomez Cadenas, P. Hernandez, O. Mena and S. Rigolin, e-Print Archive: hep-ph/0002108; M. Freund, P. Huber and M. Lindner, Nucl. Phys. **B585**, 105 (2000); V. Barger, S. Geer, R. Raja and K. Whisnant, Phys. Lett. **B485**, 379 (2000), Phys. Rev. **D62**, 073002 (2000), hep-ph/0007181 and hep-ph/0012017; M. Campanelli, A. Bueno and A. Rubbia, Nucl. Phys. **B589**, 577 (2000) and hep-ph/0010308; K. Dick, M. Freund, P. Huber and M. Lindner, hep-ph/008016.
- [19] C. Albright et al., hep-ex/0008064.
- [20] S.M. Bilenky and S.T. Petcov, Rev. Mod. Phys. **59**, 671 (1987).
- [21] S.T. Petcov, Phys. Lett. B **110**, 245 (1982).
- [22] M. Gell-Mann, P. Ramond and R. Slansky, in *Supergravity* (eds. F. Nieuwehuizen and D. Friedman, North Holland, Amsterdam 1979), p. 315; T. Yanagida, in *Unified Theories and the Baryon Number of the Universe*, Proceedings of the Workshop (eds. O. Sawada and A. Sugamoto, KEK, Japan, 1979); R. N. Mohapatra and G. Senjanovic, Phys. Rev. Lett. **44**, 912 (1980); see also J. A. Harvey, P. Ramond and D. B. Reiss, Nucl. Phys. B **199**, 233 (1982).

- [23] S.M. Bilenky, J. Hošek and S.T. Petcov, Phys. Lett. B **94**, 495 (1980).
- [24] P. Langacker *et al.*, Nucl. Phys. B **282**, 589 (1987).
- [25] B. Kayser and R. Shrock, Phys. Lett. B **112**, 137 (1982).
- [26] Yu. Kobzarev *et al.*, Yad. Fiz. **32**, 1590 (1980) [Sov. J. Nucl. Phys. **32**, 823 (1980)]; M. Doi *et al.*, Phys. Lett. B **102**, 323 (1981).
- [27] M. Moe and P. Vogel, Ann. Rev. Nucl. Part. Sci. **44**, 247 (1994); A. Faessler and F. Šimkovic, J. Phys. G **24**, 2139 (1998).
- [28] H. Ejiri, talk at *Neutrino 2000* [2], to appear in the Proceedings.
- [29] L. Baudis *et al.*, Phys. Rev. Lett. **83**, 41 (1999); H. V. Klapdor-Kleingrothaus *et al.*, submitted for publication to Phys. Lett. B and talk given at NOW2000, Otranto, Italy, September 2000 (<http://www.ba.infn.it/~now2000>).
- [30] C.E. Aalseth, F.T. Avignone III *et al.*, Physics of Atomic Nuclei **63**, 1225-1228 (2000).
- [31] NEMO3 proposal, LAL-preprint 94-29 (1994); C. Marquet *et al.*, to appear in Nucl. Phys. B (Proc. Suppl.) **87** (2000).
- [32] E. Fiorini, Phys. Rep. **307**, 309 (1998).
- [33] H. V. Klapdor-Kleingrothaus, J. Hellmig and M. Hirsch, J. Phys. G **24**, 483 (1998); L. Baudis *et al.*, Phys. Rep. **307**, 301 (1998).
- [34] M. Danilov *et al.*, Phys. Lett. B **480**, 12 (2000).
- [35] S. T. Petcov and A. Yu. Smirnov, Phys. Lett. B **322**, 109 (1994).
- [36] S.M. Bilenky, A. Bottino, C. Giunti and C.W. Kim, Phys. Lett. B **356**, 273 (1995) and Phys. Rev. D **54**, 1881 (1996).
- [37] S.M. Bilenky, C. Giunti, C.W. Kim and S.T. Petcov, Phys. Rev. D **54**, 4432 (1996).
- [38] G.C. Branco, L. Lavoura and M.N. Rebelo, Phys. Lett. B **180**, 264 (1986).
- [39] J. F. Nieves and P.P. Pal, Phys. Rev. **D36**, 315 (1987).
- [40] P.J. O'Donnell and U. Sarkar, Phys. Rev. **D52**, 1720 (1995).
- [41] J.A. Aguilar-Saavedra and G.C. Branco, Phys. Rev. **D62**, 096009 (2000).
- [42] S.M. Bilenky, C. Giunti, C.W. Kim and M. Monteno, Phys. Rev. D **57**, 6981 (1998).
- [43] F. Vissani, hep-ph/9708483 and JHEP **06**, 022 (1999).
- [44] H. Minakata and O. Yasuda, Phys. Rev. D **56**, 1692 (1997) and Nucl. Phys. B **523**, 597 (1998); T. Fukuyama, K. Matsuda and H. Nishiura, Phys. Rev. D **57**, 5844 (1998) and hep-ph/9804262.
- [45] V. Barger and K. Whisnant, Phys. Lett. B **456**, 194 (1999).
- [46] S.M. Bilenky, C. Giunti, W. Grimus, B. Kayser and S.T. Petcov, Phys. Lett. B **465**, 193 (1999).
- [47] S.T. Petcov, in *Weak Interactions and Neutrinos*, Proceedings of the 17th International Conference, January 23 - 30, 1999, Cape Town, South Africa (eds. C.A. Dominguez and R.D. Viollier, World Scientific, Singapore, 2000), p. 305 (hep-ph/9907216).

- [48] S.M. Bilenky and C. Giunti, in *Weak Interactions and Neutrinos*, Proceedings of the 17th International Conference, January 23 - 30, 1999, Cape Town, South Africa (eds. C.A. Dominguez and R.D. Viollier, World Scientific, Singapore, 2000), p. 195.
- [49] C. Giunti, Phys. Rev. **D61**, 036002 (2000).
- [50] T. Fukuyama, K. Matsuda, H. Nishiura and N. Takeda, Phys. Rev. **D62**, 93001 (2000) and hep-ph/0007237.
- [51] M. Czakon, J. Gluza and M. Zlarek, hep-ph/0003161; M. Czakon, J. Gluza, J. Studnik and M. Zlarek, hep-ph/0010077.
- [52] H. V. Klapdor-Kleingrothaus, H. Pas and A. Yu. Smirnov, hep-ph/0003219.
- [53] W. Rodejohann, hep-ph/0008044.
- [54] S.M. Bilenky, S. Pascoli and S.T. Petcov, Ref. SISSA 13/2001/EP.
- [55] Super-Kamiokande Collaboration, talk by H. Sobel at *Neutrino 2000* [2], to appear in the Proceedings.
- [56] G.L. Fogli, E. Lisi, D. Montanino, and A. Palazzo, Phys. Rev. **D62**, 113003 (2000).
- [57] P. I. Krastev, talk given at NOW2000, Otranto, Italy, September 2000 (<http://www.ba.infn.it/~now2000>).
- [58] C. Gonzalez-Garcia *et al.*, M. Maltoni, C. Peña-Garay, and J.W.F. Valle, hep-ph/0009350.
- [59] S. T. Petcov, Lecture Notes in Physics, v. **512** (eds. H. Gausterer and C.B. Lang, Springer, 1998), p. 281 (hep-ph/9806466).
- [60] S. M. Bilenky, C. Giunti and W. Grimus, Prog. Part. Nucl. Phys. **43**, 1 (1999) (hep-ph/9812360).
- [61] B. Pontecorvo, Zh. Eksp. Teor. Fiz. **53**, 1717 (1967) [Sov. Phys. JETP **26**, 984 (1968)]; S. M. Bilenky and B. Pontecorvo, Phys. Rep. **41**, 225 (1978).
- [62] P.I. Krastev and S.T. Petcov, Phys. Lett. B **285**, 85 (1992), *ibid.* B **299**, 99 (1993), Phys. Rev. Lett. **72**, 1960 (1994) and Phys. Rev. **D53**, 1665 (1996); V. Barger, R.J.N. Phillips, and K. Whisnant, Phys. Rev. Lett. **69**, 3135 (1992); N. Hata and P. Langacker, Phys. Rev. D **56**, 6107 (1997); B. Faïd, G.L. Fogli, E. Lisi, and D. Montanino, Astropart. Phys. **10**, 93 (1999); see also: S.L. Glashow and L.M. Krauss, Phys. Lett. B **190**, 199 (1987).
- [63] P.I. Krastev and S.T. Petcov Phys. Rev. **D53**, 1665 (1996); P.I. Krastev, Q.Y. Liu and S.T. Petcov, Phys. Rev. **D54**, 7057 (1996).
- [64] M. Appolonio *et al.*, Phys. Lett. **B466**, 415 (1999) (hep-ex/9907037).
- [65] F. Boehm, J. Busenitz et al., Phys. Rev. Lett. **84**, 3764 (2000) and Phys. Rev. **D62**, 072002 (2000).
- [66] P. Lipari, Phys. Rev. **D61**, 113004 (2000); V. Barger, S. Geer, R. Raja and K. Whisnant, Phys. Rev. **D62**, 013004 (2000); M. Freund, M. Lindner, S.T. Petcov and A. Romanino, Nucl. Phys. **B578**, 27 (2000).
- [67] V. Lobashov *et al.*, talk at *Neutrino 2000* [2], to appear in the Proceedings.

- [68] C. Weinheimer *et al.*, talk at *Neutrino 2000* [2], to appear in the Proceedings.
- [69] A. Aseev et al., Int. Workshop on Neutrino Masses in the Sub-eV Range, January 18 - 21, Bad Liebenzell, Germany.
- [70] E. Gawiser, astro-ph/0005475.
- [71] MAP collaboration, <http://map.gsfc.gov/>; PLANCK collaboration, <http://astro.estec.esa.ne/SA-general/Projects/Planck>.
- [72] C. Jarskog, Z. Phys. **C29**, 491 (1985); Phys. Rev. **D35**, 1685 (1987).
- [73] P.I. Krastev and S.T. Petcov, Phys. Lett. B **205**, 64 (1988).
- [74] S. M. Bilenky, N. P. Nedelcheva and S. T. Petcov, Nucl. Phys. B **247**, 589 (1984).
- [75] B. Kayser, Phys. Rev. **D30**, 1023 (1984).
- [76] L. Wolfenstein, Phys. Lett. B **107**, 77 (1981).
- [77] S.T. Petcov, Phys. Lett. B **115**, 401 (1982) and *ibid.* B **110**, 245 (1982).
- [78] H. Pas and T.J. Weiler, hep-ph/0101091.
- [79] D. Falcone and F. Tramontano, hep-ph/0102136.

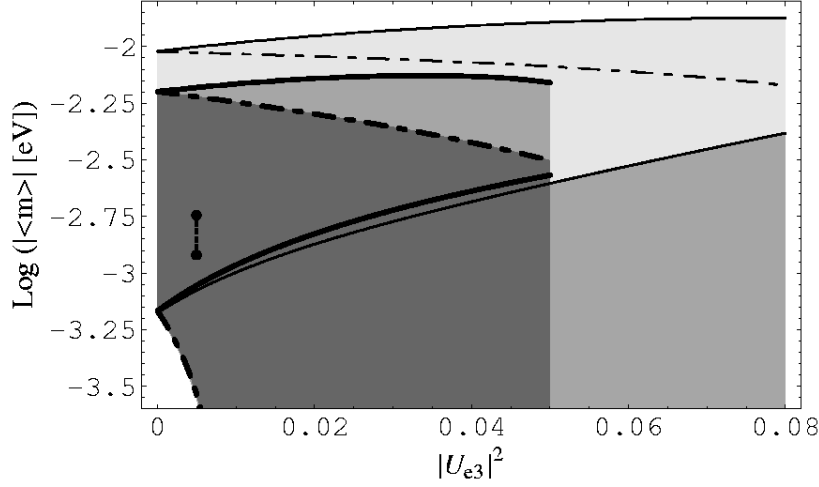


Figure 2: The effective Majorana mass $\langle m \rangle$, allowed by the data from the solar and atmospheric neutrino and CHOOZ experiments, as a function of $|U_{e3}|^2$ in the case of hierarchical neutrino mass spectrum, eq. (40). The values of $\langle m \rangle$ are obtained for Δm_{\odot}^2 , $\sin^2 \theta_{\odot}$ from the LMA MSW solution region, and Δm_{atm}^2 and $|U_{e3}|^2$, derived in [58] at 90% C.L. (medium grey and dark grey regions at $|U_{e3}|^2 < 0.05$) and at 99% C.L. (light, medium and dark grey regions at $|U_{e3}|^2 < 0.08$). The 90% (99%) C.L. allowed regions located *i*) between the two thick (thin) solid lines and *ii*) between the thick (thin) dashed lines and the horizontal axis, correspond to the two cases of CP conservation: *i*) $\phi_2 = \phi_3$, and *ii*) $\phi_2 = -\phi_3$, $i\phi_{2,3}$ being the CP-parities of $\nu_{2,3}$. The values of $\langle m \rangle$, calculated for the best fit values of the input parameters, are indicated by thick dots (CP-conservation) and a dotted line (CP-violation). In the case of CP-violation all the regions marked with different grey colour scales are allowed.

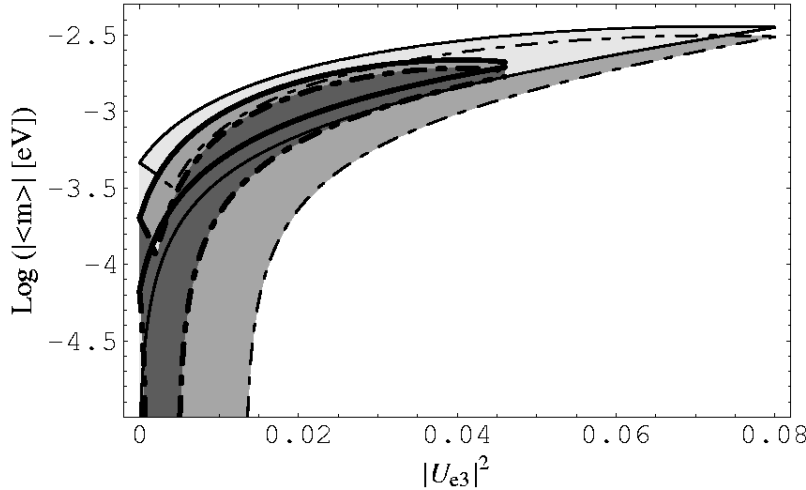


Figure 3: The same as Fig. 2 but for Δm_{\odot}^2 and $\sin^2 \theta_{\odot}$ from the 90% (99%) C.L. region of the LOW-QVO solution of the ν_{\odot} -problem [58]. The regions limited by the two thick (thin) solid and dashed lines correspond to the two cases of CP-conservation: *i*) $\phi_2 = \phi_3$, (regions within the solid lines) and *ii*) $\phi_2 = -\phi_3$ (regions within the dashed lines). In the case of CP-violation, $(\alpha_3 - \alpha_2) \neq k\pi$, $k = 0, 1, \dots$, all the regions marked by different grey color scales are allowed.

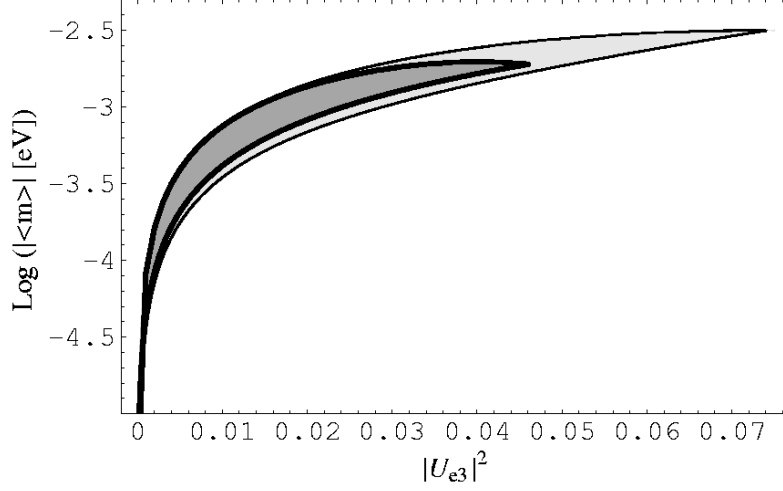


Figure 4: The same as Fig. 2 but for Δm_{\odot}^2 and $\sin^2 \theta_{\odot}$ from the region of the SMA solution of the ν_{\odot} -problem [58] obtained at 90% C.L. (region within the thick solid lines) and at 99% C.L. (region within the thin solid lines). The results shown are derived assuming $m_1 \ll 10^{-4}$ eV. For the range of values of $|\langle m \rangle|$ in the figure, one has in this case $|\langle m \rangle| \sim \sqrt{\Delta m_{\text{atm}}^2} |U_{e3}|^2$ and thus $|\langle m \rangle|$ does not depend on the CP-violating phase ($\alpha_3 - \alpha_2$).

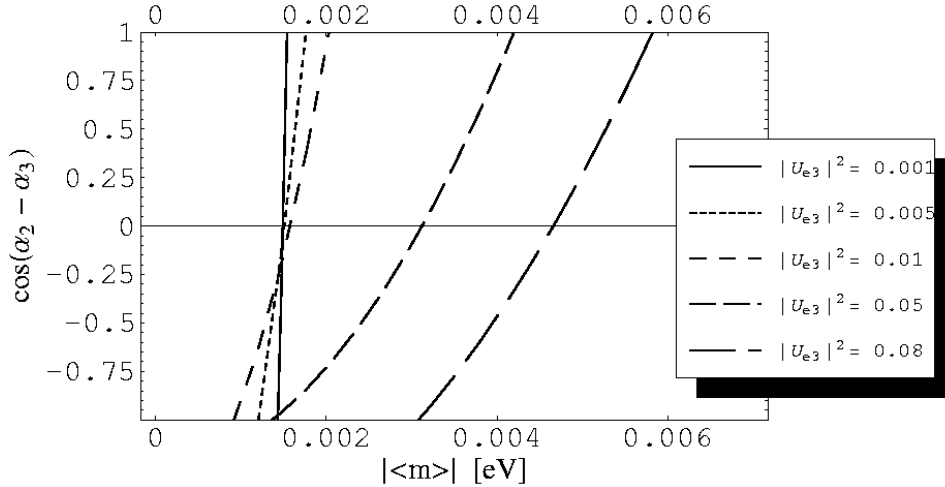


Figure 5: The CP-violation factor $\cos(\alpha_2 - \alpha_3)$, eq. (40) (hierarchical neutrino mass spectrum), as a function of $|\langle m \rangle|$ for different values of $|U_{e3}|^2$ and for the best fit values of the parameters Δm_{\odot}^2 , $\sin^2 \theta_{\odot}$ and Δm_{atm}^2 , found in the analysis [58]. Values of $\cos(\alpha_2 - \alpha_3) = 0, \pm 1$, correspond to CP-invariance.

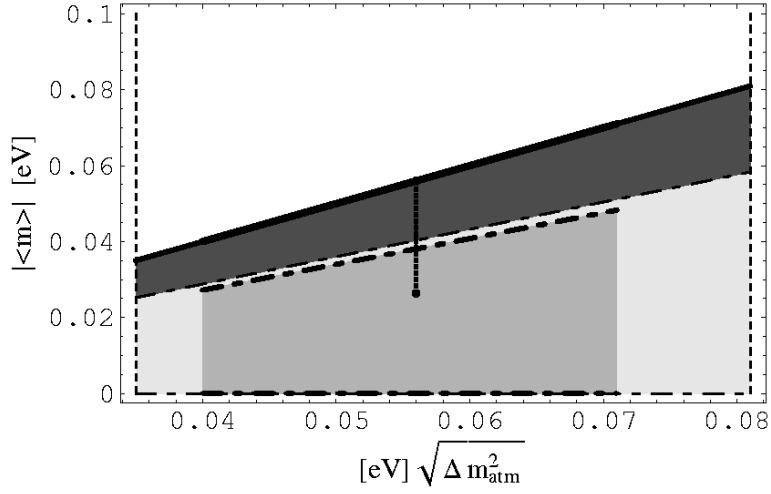


Figure 6: The effective Majorana mass $|\langle m \rangle|$ as a function of $\sqrt{\Delta m_{\text{atm}}^2}$ for the neutrino mass spectrum of the inverted hierarchy type, eq. (61). The allowed regions (in grey) correspond to the LMA solution of ref. [58]. In the case of CP-invariance and for the 90% (99%) C.L. results for the solution region, $|\langle m \rangle|$ can have values *i*) for $\phi_2 = \phi_3$ - in the medium grey (light grey and medium grey) upper region, limited by the doubly thick (thick and doubly thick) solid lines and *ii*) for $\phi_2 = -\phi_3$ - in the medium grey (light grey and medium grey) region limited by the doubly thick (thick and doubly thick) dash-dotted lines. If CP is not conserved, $|\langle m \rangle|$ can lie in any of the regions marked by different grey scales. The dark-grey region corresponds to “just-CP-violation”: $|\langle m \rangle|$ can have value in this region *only if the CP-parity is not conserved*. The values of $|\langle m \rangle|$ corresponding to the best fit values of the input parameters, found in [58], are denoted by dots in the CP-conserving cases and by a dotted line in the CP-violating one.

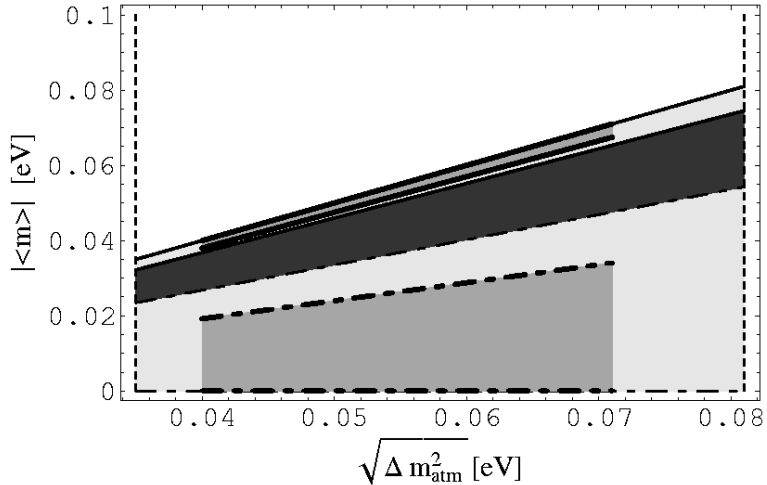


Figure 7: The same as in Fig. (6) for the 90% (99%) C.L. LOW-QVO solution of ref. [58]. The medium grey (light-grey and medium grey) region, bounded by the thick (thick and doubly thick) solid lines, and medium grey (light grey and medium grey) lower region, bounded by the thick (thin) dash-dotted lines, correspond to the two cases of CP-invariance, $\phi_2 = \phi_3$ and $\phi_2 = -\phi_3$, respectively. If CP is not conserved, $|\langle m \rangle|$ can lie in any of the regions marked by different grey scales. The “just-CP-violation” region is shown in dark-grey color: $|\langle m \rangle|$ can have value in this region *only if the CP-symmetry is violated*.

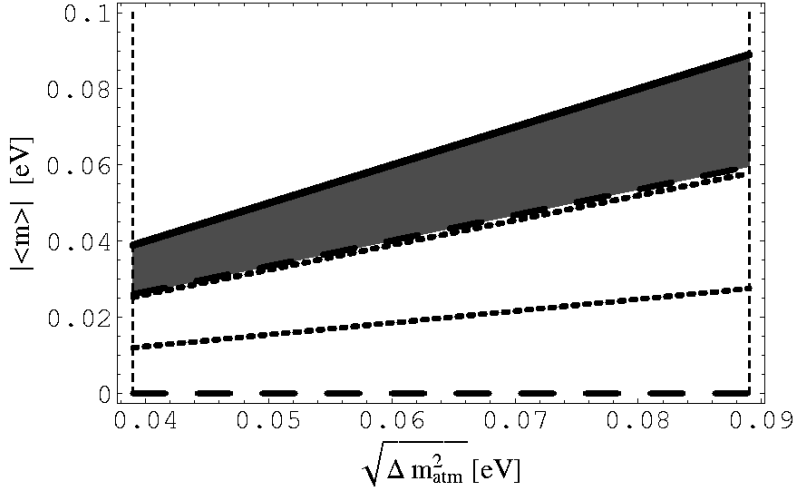


Figure 8: $|\langle m \rangle|$ as a function of $\sqrt{\Delta m_{\text{atm}}^2}$ for the inverted mass hierarchy spectrum and LMA solution of the solar neutrino problem. The figure is obtained using the results of ref. [7] (region between the thick solid line and the lower dotted line) and of ref. [56] (at 99% C.L. - region between the thick solid line and the lower long-dashed line). If CP-invariance does not hold, $|\langle m \rangle|$ spans all the allowed regions indicated (in brackets) above. The values of $|\langle m \rangle|$ in the two CP-conserving cases lie i) on the doubly thick solid line if $\phi_2 = \phi_3$, and ii) for $\phi_2 = -\phi_3$ - between the two dotted lines (dashed lines) for the LMA solution in ref. [7] (ref. [56]). The common “just-CP-violation” region for both analyzes is marked in dark-grey : a value of $|\langle m \rangle|$ in this region would signal CP-violation.

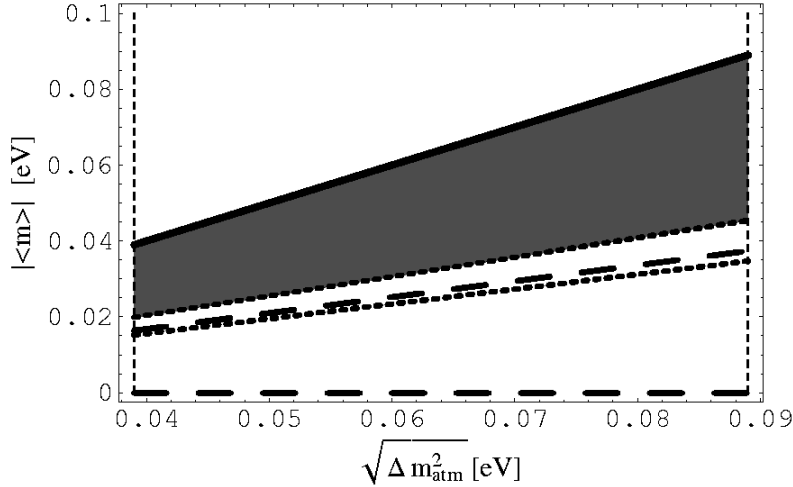


Figure 9: The same as in Fig. 8 for the LOW-QVO solution found in ref. [7] and in ref. [56] (at 99% C.L.). The “just-CP-violation” region, in particular, is marked by dark-grey color.

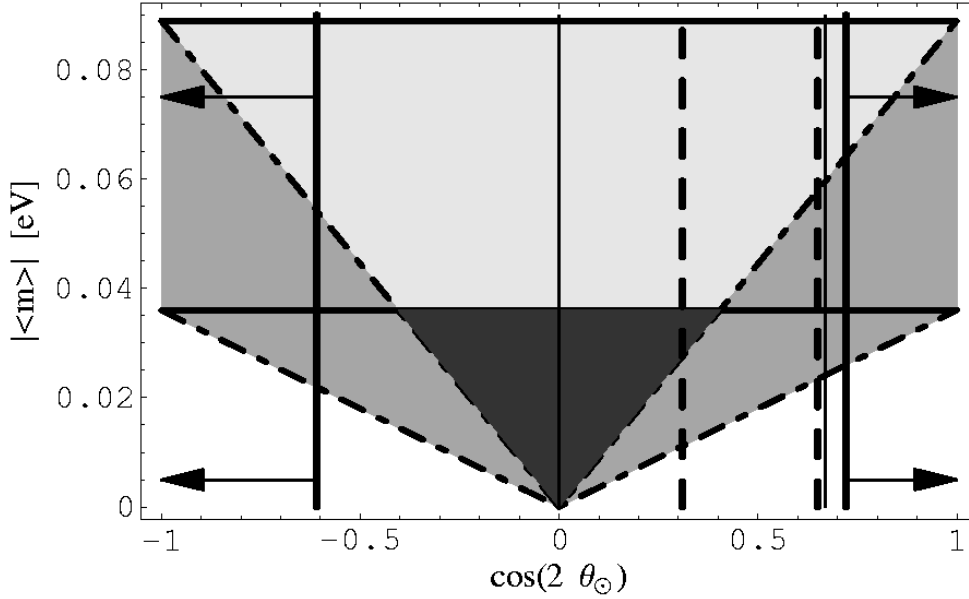


Figure 10: The dependence of $|\langle m \rangle|$ on $\cos 2\theta_\odot$ for the neutrino mass spectrum with inverted hierarchy, eq. (61), and the LMA solution of the solar neutrino problem. The region between the two thick horizontal solid lines (in light grey and medium grey colors) and the two triangular regions between the thick dash-dotted lines (in medium grey color), correspond to the two CP-conserving cases, $\phi_2 = \phi_3$ and $\phi_2 = -\phi_3$, respectively. The “just-CP-violation” region is denoted by dark-grey color. The regions between each of the three pairs of vertical lines of a given type - solid, doubly thick solid and doubly thick dashed, correspond to the intervals of values of $\cos 2\theta_\odot$ for the LMA solution derived (at 99% C.L.) in ref. [7] (region between the two doubly thick dashed lines), ref. [56] (region between the solid lines) and ref. [58].

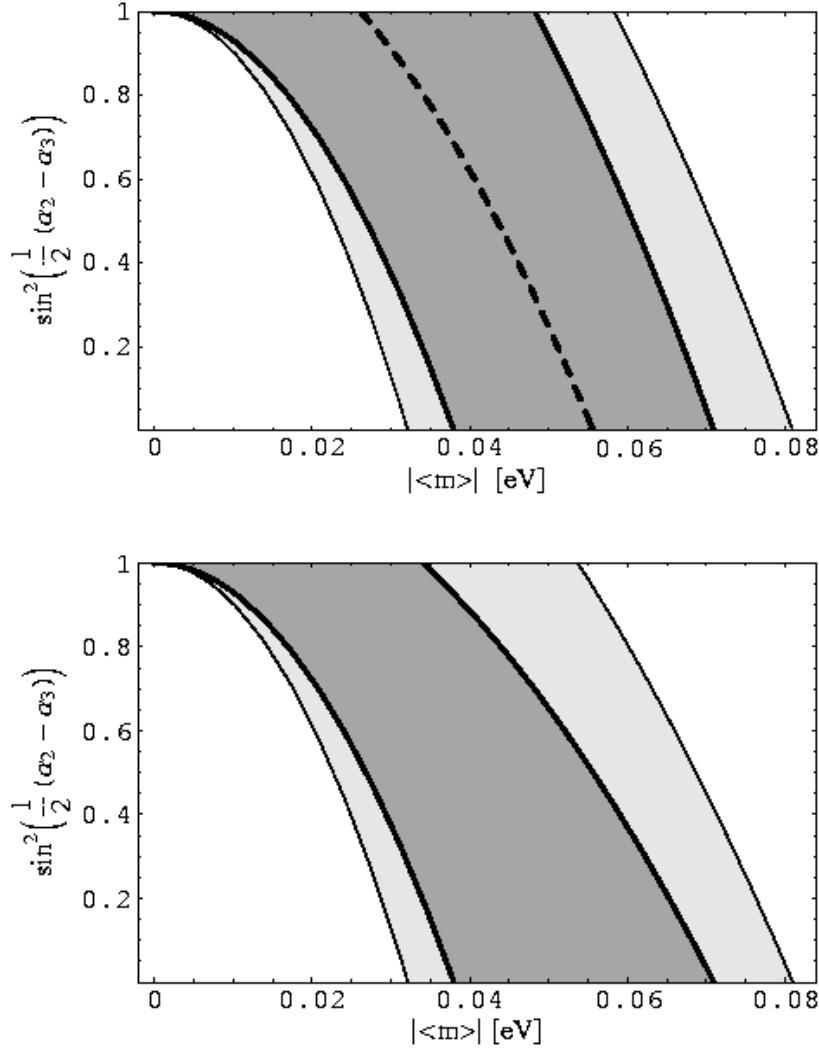


Figure 11: The CP-violation factor $\sin^2(\alpha_2 - \alpha_3)/2$ as a function of $|\langle m \rangle|$ in the case of inverted mass hierarchy spectrum, eq. (61), and the LMA (upper panel) and LOW-QVO (lower panel) solutions of ref. [58], obtained at 90% C.L. (medium grey region with thick contours) and 99% C.L. (light grey and medium grey region limited by ordinary solid lines). The values of $|\langle m \rangle|$, corresponding to the best fit values of the input parameters, found in [58], are indicated by the dashed line. A value of $\sin^2(\alpha_2 - \alpha_3)/2 \neq 0, 1$, would signal CP-violation.

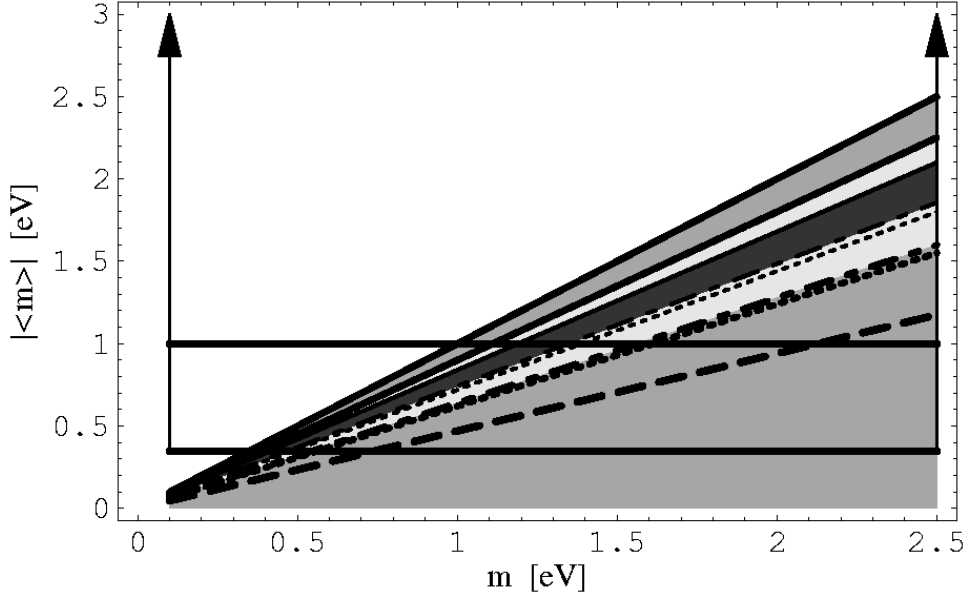


Figure 12: $|\langle m \rangle|$ as a function of the neutrino mass m for the quasi-degenerate neutrino mass spectrum, eqs. (71) - (72), and the LMA solution of the ν_{\odot} -problem of ref. [58] at 90% C.L. (99% C.L.). The regions allowed in the cases of CP-conservation are marked by *i*) $\phi_1 = \phi_2 = \phi_3$ - the thick solid (non-horizontal) line $|\langle m \rangle| = m$, *ii*) $\phi_1 = \phi_2 = -\phi_3$ - medium grey color triangular region between the two doubly thick solid lines (light grey and medium grey color triangular region between the doubly thick and thick solid lines, *iii*) $\phi_1 = -\phi_2 = \pm\phi_3$ (two cases) - medium grey color triangular regions between the doubly thick dashed-dotted line and the horizontal axes and between the doubly thick dotted line and the horizontal axes (light grey and medium grey region between the thin dashed-dotted line and the horizontal axes and between the thin dotted line and the horizontal axes). The “just-CP-violation” region is denoted by dark-grey color. The doubly thick solid line corresponding to $|\langle m \rangle| = m$ and the doubly thick long dashed line indicate the “best fit lines” of values of $|\langle m \rangle|$ for the *i*)-*ii*) and the *iii*) cases, respectively. The two horizontal (doubly thick) lines show the upper limits [29], quoted in eq. (3).

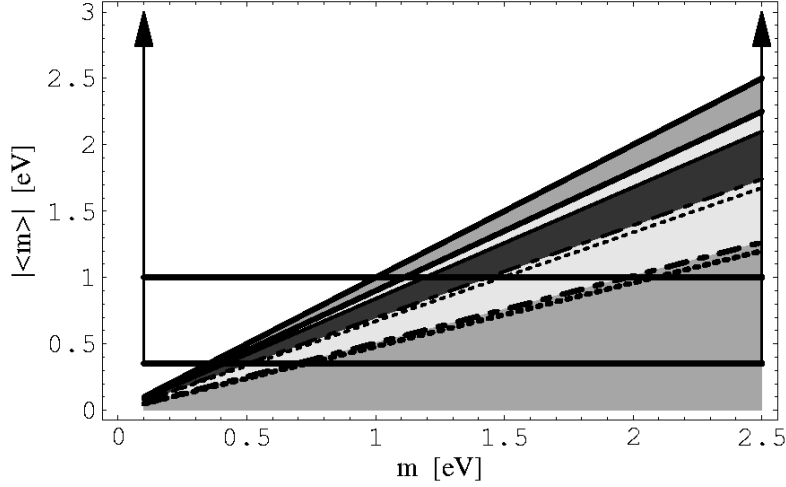


Figure 13: The same as in Fig.(12) for the LOW-QVO solution of the ν_{\odot} -problem [58]. If CP is conserved and at 90% C.L. (99 % C.L.) [58], $|\langle m \rangle|$ should lie in the two medium grey (the two light grey and medium grey) triangular regions: i) for $\phi_1 = \phi_2 = \phi_3$ - on the line $|\langle m \rangle| = m$, ii) for $\phi_1 = \phi_2 = -\phi_3$ - in the upper medium grey (light grey and medium grey) triangular region, iii) if $\phi_1 = -\phi_2 = \pm\phi_3$ - in the lower medium grey (light grey and medium grey) triangular region with dash-dotted ($\phi_1 = +\phi_3$) and dotted ($\phi_1 = -\phi_3$) contours. The “just-CP-violation” region is denoted by dark-grey color.

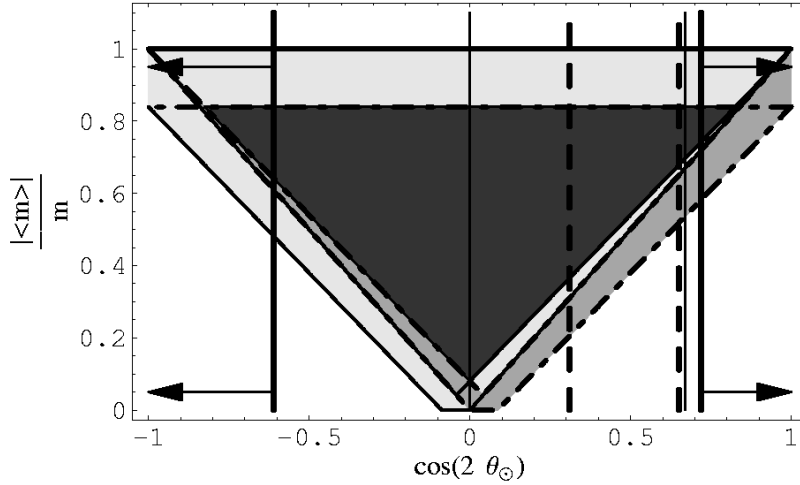


Figure 14: The dependence of $|\langle m \rangle|/m$ on $\cos 2\theta_{\odot}$ for the quasi-degenerate neutrino mass spectrum, eqs. (71) - (72), and the LMA solution of the ν_{\odot} -problem. If CP-invariance holds, the values of $|\langle m \rangle|/m$ lie: i) for $\phi_1 = \phi_2 = \phi_3$ - on the line $|\langle m \rangle|/m = 1$, ii) for $\phi_1 = \phi_2 = -\phi_3$ - in the region between the thick horizontal solid and dash-dotted lines (in light grey and medium grey colors), iii) for $\phi_1 = -\phi_2 = +\phi_3$ - in the light grey polygon with solid-line contours and iv) for $\phi_1 = -\phi_2 = -\phi_3$ - in the medium grey polygon with the dash-dotted-line contours. The “just-CP-violation” region is denoted by dark-grey color. The values of $\cos 2\theta_{\odot}$ between the doubly thick solid, the normal solid and the doubly thick dashed lines correspond to the 99%, 99% and 95% C.L. LMA solution regions in refs. [58], [56] and [7], respectively.

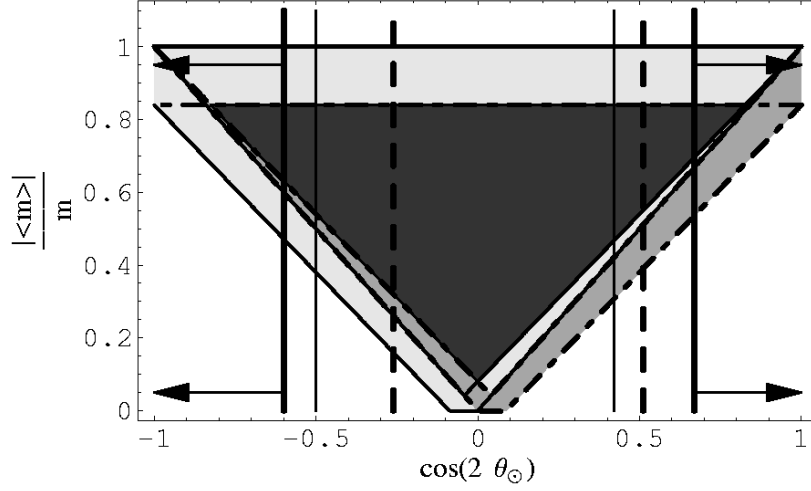


Figure 15: The same as in Fig. (14) for the LOW-QVO solution of the solar neutrino problem. The “just-CP-violating” region, in particular, is denoted by dark-grey color.

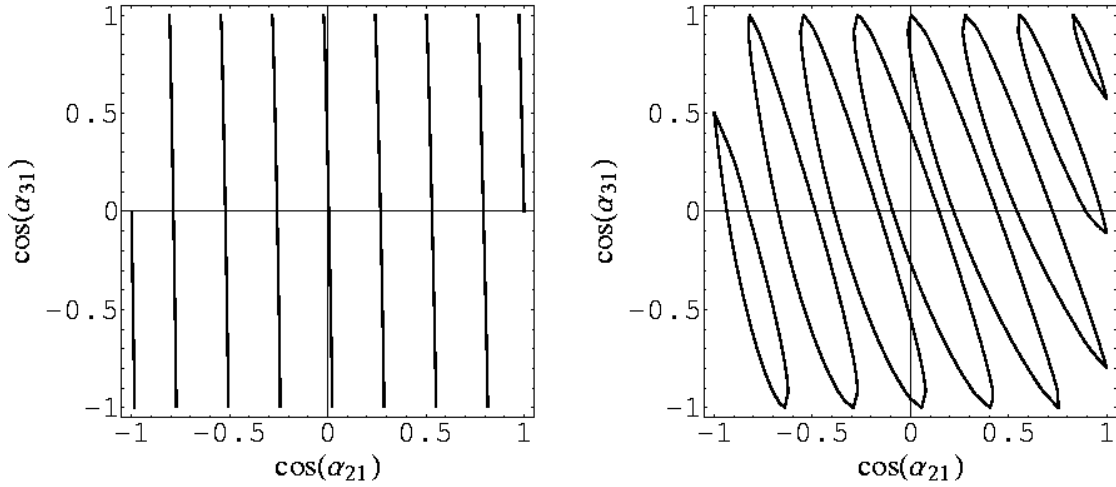


Figure 16: The interdependence of the two CP-violating phases, α_{21} and α_{31} , for a given value of the ratio $|\langle m \rangle|/m$ in the case of quasi-degenerate neutrino mass spectrum. The figures are obtained for $|\langle m \rangle|/m = \sqrt{0.2 + 0.1n}$ eV with $n = 0, 1 \dots 8$ (with increasing $|\langle m \rangle|$ from left to right) and the best fit values of the solar and atmospheric neutrino oscillation parameters from [58], quoted in Section 2 (left-hand plot), and for $|\langle m \rangle|/m = \sqrt{0.24 + 0.10n}$ eV with $n = 0, 1 \dots 7$ (with increasing $|\langle m \rangle|$ from left to right), $|U_{e3}|^2 = 0.08$ and the best fit values of the other solar and atmospheric neutrino oscillation parameters [58] (right-hand plot). The values of $\cos \alpha_{21,31} = 0, \pm 1$, correspond to CP-invariance.

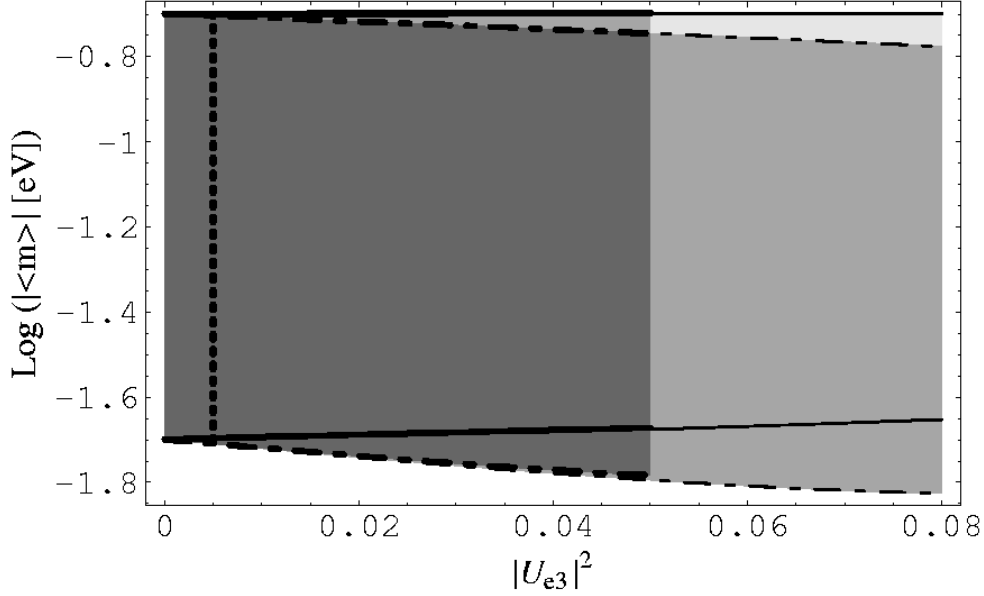


Figure 17: The effective Majorana mass $|\langle m \rangle|$, allowed by the data from the solar and atmospheric neutrino and CHOOZ experiments, as a function of $|U_{e3}|^2$ in the case of partial hierarchy mass spectrum, eq. (84). The values of $|\langle m \rangle|$ are obtained for Δm_{\odot}^2 , $\sin^2 \theta_{\odot}$ from the LMA MSW solution region, and Δm_{atm}^2 and $|U_{e3}|^2$, derived in [58] at 90% C.L. (medium grey and dark grey regions at $|U_{e3}|^2 < 0.05$) and at 99% C.L. (light, medium and dark grey regions at $|U_{e3}|^2 < 0.08$). The 90% (99%) C.L. allowed regions located *i*) between the two thick (thin) solid lines and *ii*) between the two thick (thin) dashed lines, correspond to the two cases of CP conservation: *i*) $\phi_1 = \phi_2 = \phi_3$, and *ii*) $\phi_1 = \phi_2 = -\phi_3$, $i\phi_{2,3}$ being the CP-parities of $\nu_{2,3}$. The values of $|\langle m \rangle|$, calculated for the best fit values of Δm_{\odot}^2 , Δm_{atm}^2 , $\sin^2 \theta_{\odot}$, $|U_{e3}|^2$ and for $0.02 \text{ eV} \leq m_1 \leq 0.2 \text{ eV}$ are indicated by the thick dotted line.

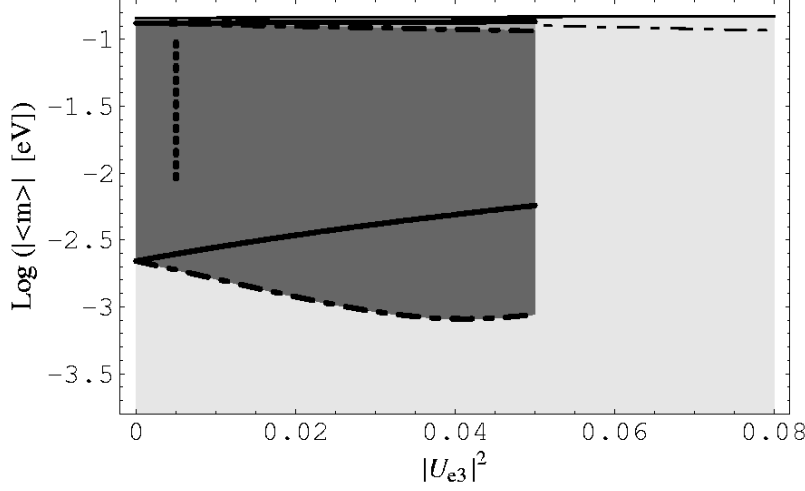


Figure 18: The same as Fig. 17 but for two different sets of values of the relative CP-parities of the massive Majorana neutrinos. The allowed regions are derived using the results of [58] at 90% C.L. (medium grey and dark grey regions at $|U_{e3}|^2 < 0.05$) and at 99% C.L. (light, medium and dark grey regions at $|U_{e3}|^2 < 0.08$). The 90% (99%) C.L. allowed regions located *i*) between the two thick solid lines (between the thin solid line and the horizontal axis) and *ii*) between the two thick dashed lines (between the thin dashed line and the horizontal axis), correspond to the two cases of CP conservation: *i*) $\phi_1 = -\phi_2 = \phi_3$, and *ii*) $\phi_1 = -\phi_2 = -\phi_3$, $i\phi_{2,3}$ being the CP-parities of $\nu_{2,3}$. The values of $|\langle m \rangle|$, calculated for the best fit values of Δm_{\odot}^2 , Δm_{atm}^2 , $\sin^2 \theta_{\odot}$, $|U_{e3}|^2$ and for $0.02 \text{ eV} \leq m_1 \leq 0.2 \text{ eV}$ are indicated by the thick dotted line.

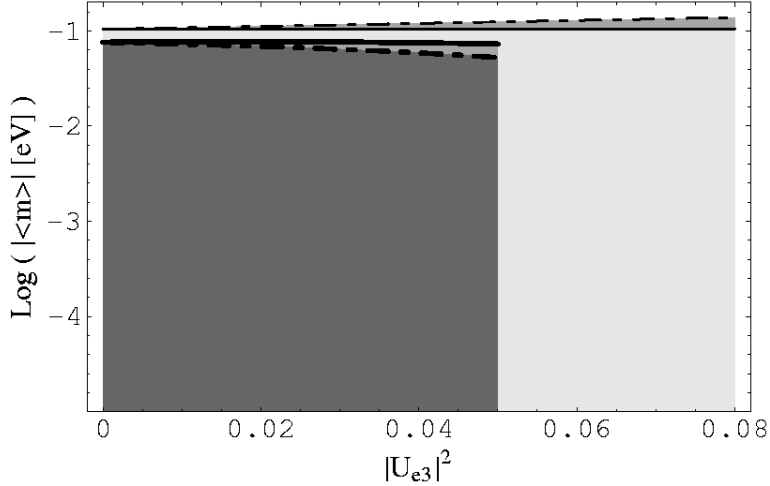


Figure 19: The same as in Fig. 18 but for the LOW-QVO solution of the solar neutrino problem. The 90% (99%) C.L. allowed regions located *i*) between the thick (thin) solid line and the horizontal axis and *ii*) between the thick (thin) dashed line and the horizontal axis, correspond to the two cases of CP conservation: *i*) $\phi_1 = -\phi_2 = \phi_3$, and *ii*) $\phi_1 = -\phi_2 = -\phi_3$, $i\phi_{2,3}$ being the CP-parities of $\nu_{2,3}$.

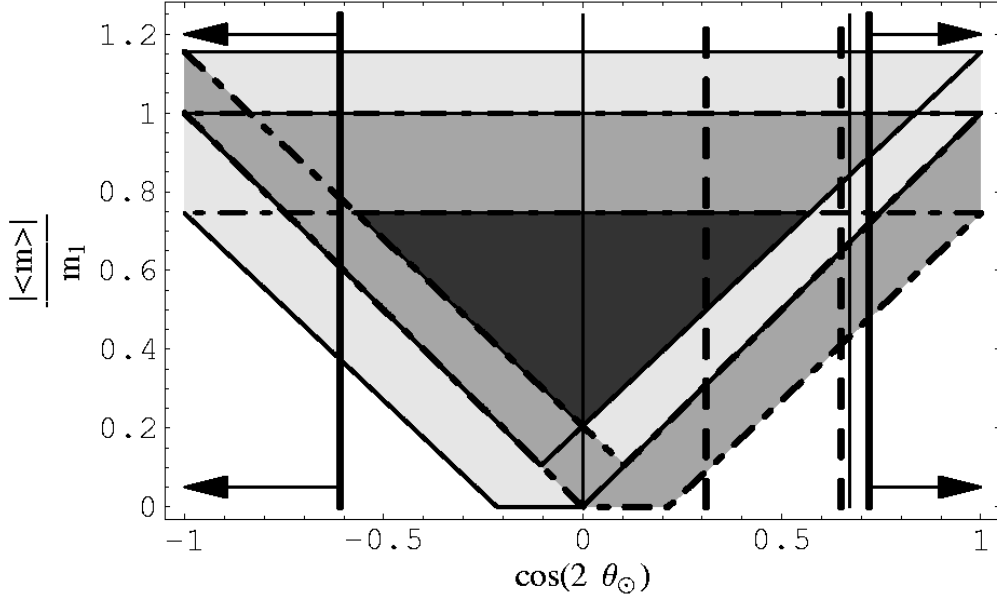


Figure 20: The dependence of $|\langle m \rangle|/m_1$ on $\cos 2\theta_\odot$ for the partial hierarchy mass spectrum, eq. (84), and the LMA solution of the ν_\odot -problem, for the 99% C.L. allowed values of the solar and atmospheric neutrino oscillation parameters and $0.02 \text{ eV} \leq m_1 \leq 0.2 \text{ eV}$. If CP-invariance holds, the values of $|\langle m \rangle|/m_1$ lie: i) for $\phi_1 = \phi_2 = \phi_3$ - in the region between the two thin solid horizontal lines (in light and medium grey), ii) for $\phi_1 = \phi_2 = -\phi_3$ - in the region between the two thick horizontal dash-dotted lines (in light grey and medium grey colors), iii) for $\phi_1 = -\phi_2 = +\phi_3$ - in the light grey polygon with solid-line contours and iv) for $\phi_1 = -\phi_2 = -\phi_3$ - in the medium grey polygon with the dash-dotted-line contours. The “just-CP-violation” region is denoted by dark-grey color. The values of $\cos 2\theta_\odot$ between the doubly thick solid, the normal solid and the doubly thick dashed lines correspond to the 99%, 99% and 95% C.L. LMA solution regions in refs. [58], [56] and [7], respectively.

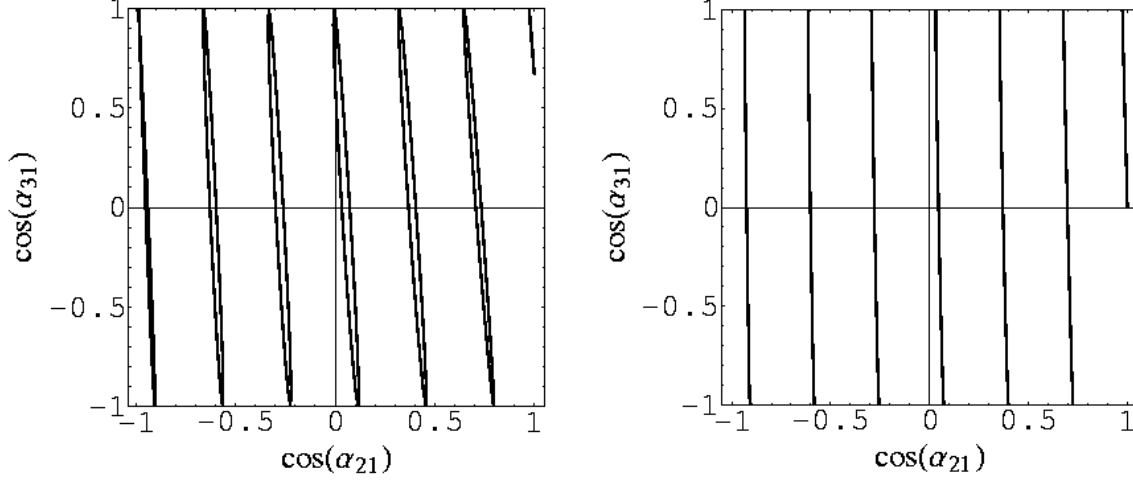


Figure 21: The interdependence of the two CP-violating phases, α_{21} and α_{31} , for a given value of the ratio $|\langle m \rangle|/m_1$ in the case of partially hierarchical neutrino mass spectrum. The figures are obtained for $|\langle m \rangle| = \sqrt{1+0.5n} \times 10^{-2}$ eV with $n = 0, 1 \dots 6$ (with increasing $|\langle m \rangle|$ from left to right), the best fit values of the solar and atmospheric neutrino oscillation parameters from [58], quoted in Section 2, and $m_1 = 0.02$ eV (left-hand plot), and for $|\langle m \rangle| = \sqrt{0.5n} \times 10^{-1}$ eV with $n = 0, 1 \dots 6$ (with increasing $|\langle m \rangle|$ from left to right), the best fit values of the solar and atmospheric neutrino oscillation parameters from [58] and $m_1 = 0.2$ eV (right-hand plot). The values of $\cos \alpha_{21,31} = 0, \pm 1$, correspond to CP-invariance.

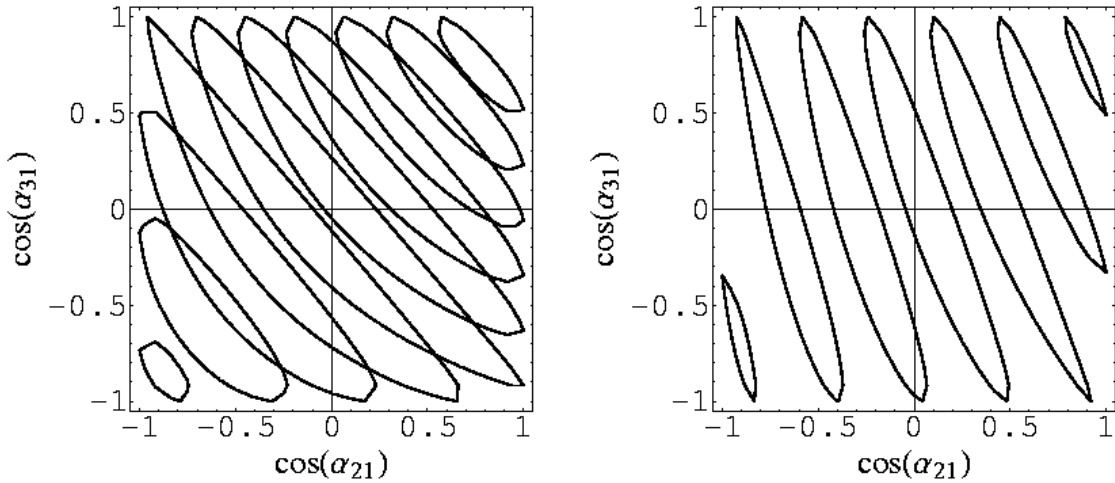


Figure 22: The same as in Fig.(21) but for $|\langle m \rangle| = \sqrt{0.5n} \times 10^{-2}$ eV with $n = 1 \dots 10$ (with increasing $|\langle m \rangle|$ from left to right), $|U_{e3}|^2 = 0.08$, the best fit values of the other solar and atmospheric neutrino oscillation parameters from [58], quoted in Section 2, and $m_1 = 0.02$ eV (left-hand plot), and for $|\langle m \rangle| = \sqrt{1+0.5n} \times 10^{-1}$ eV with $n = 0, 1 \dots 6$ (with increasing $|\langle m \rangle|$ from left to right), $|U_{e3}|^2 = 0.08$, the best fit values of the other solar and atmospheric neutrino oscillation parameters from [58] and $m_1 = 0.2$ eV (right-hand plot). The values of $\cos \alpha_{21,31} = 0, \pm 1$, correspond to CP-invariance.

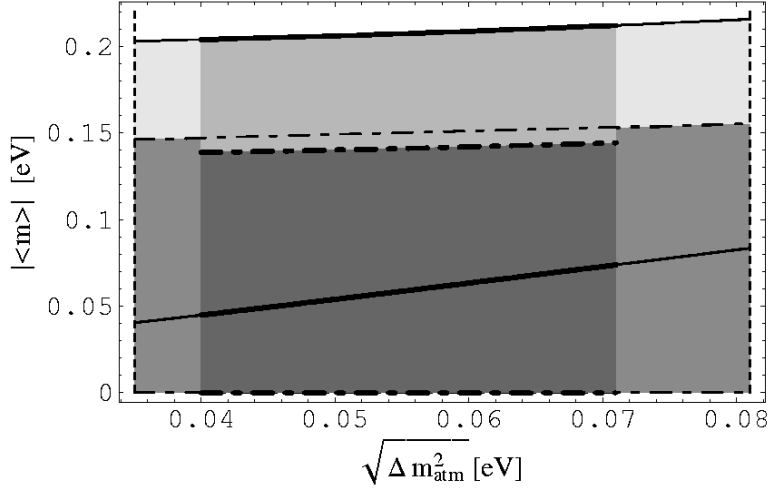


Figure 23: The effective Majorana mass $|\langle m \rangle|$ as a function of $\sqrt{\Delta m_{\text{atm}}^2}$ for the neutrino mass spectrum of the partial inverted hierarchy type, eq. (85). The allowed regions (in grey) correspond to the LMA solution of ref. [58]. In the case of CP-invariance and for the 90% (99%) C.L. solution regions, $|\langle m \rangle|$ can have values *i*) for $\phi_2 = \phi_3$ - in the medium-light and dark grey (light grey, medium-light, medium-dark grey and dark grey) upper region, limited by the doubly thick (thick and doubly thick) solid lines, and ii) for $\phi_2 = -\phi_3$ - in the dark grey (medium-light grey, medium-dark grey and dark grey) region limited by the doubly thick (thick and doubly thick) dash-dotted lines. If CP is not conserved, $|\langle m \rangle|$ can lie in any of the regions marked by different grey scales.

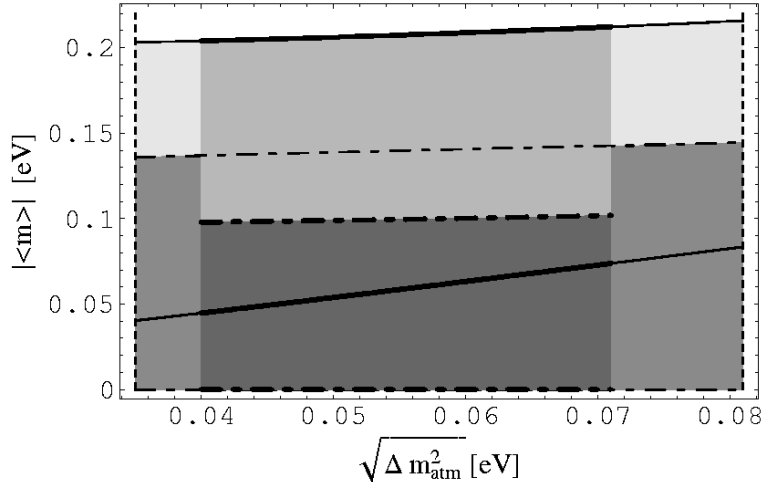


Figure 24: The same as Fig.(23) for the 90% (99%) C.L. LOW-QVO solution of ref. [58].

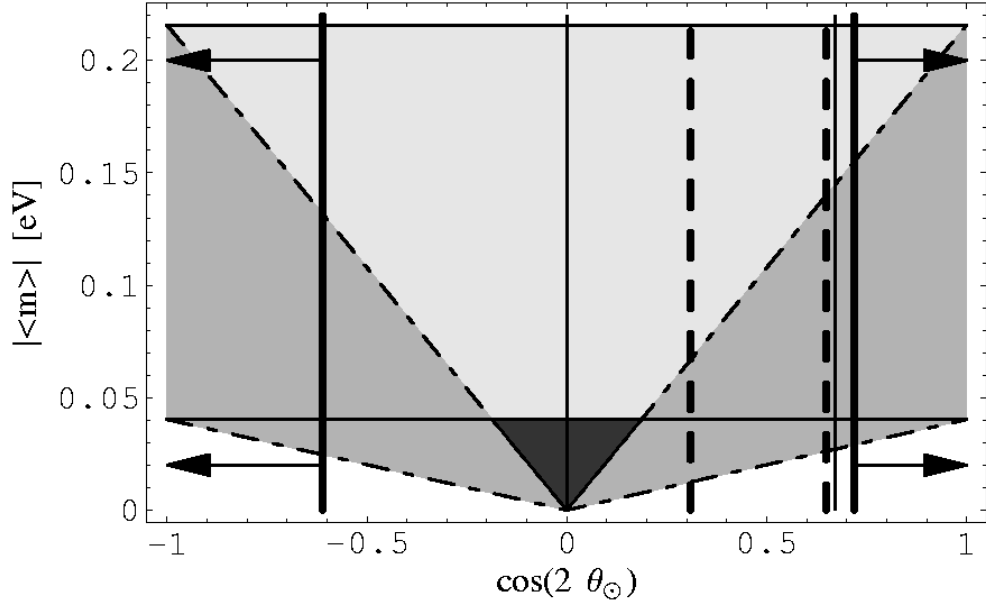


Figure 25: The dependence of $|\langle m \rangle|$ on $\cos 2\theta_\odot$ for the neutrino mass spectrum with partial inverted hierarchy, eq. (85), and the LMA solution of the ν_\odot -problem. The region between the two thick horizontal solid lines (in light grey and medium grey colors) and the two triangular regions between the thick dash-dotted lines (in medium grey color), correspond to the two CP-conserving cases, $\phi_2 = \phi_3$ and $\phi_2 = -\phi_3$, respectively. The “just-CP-violation” region is denoted by dark-grey color. The regions between each of the three pairs of vertical lines of a given type - solid, doubly thick solid and doubly thick dashed, correspond to the intervals of values of $\cos 2\theta_\odot$ for the LMA solution derived (at 99% C.L.) in ref. [7] (region between the two doubly thick dashed lines), ref. [56] (region between the solid lines) and ref. [58].

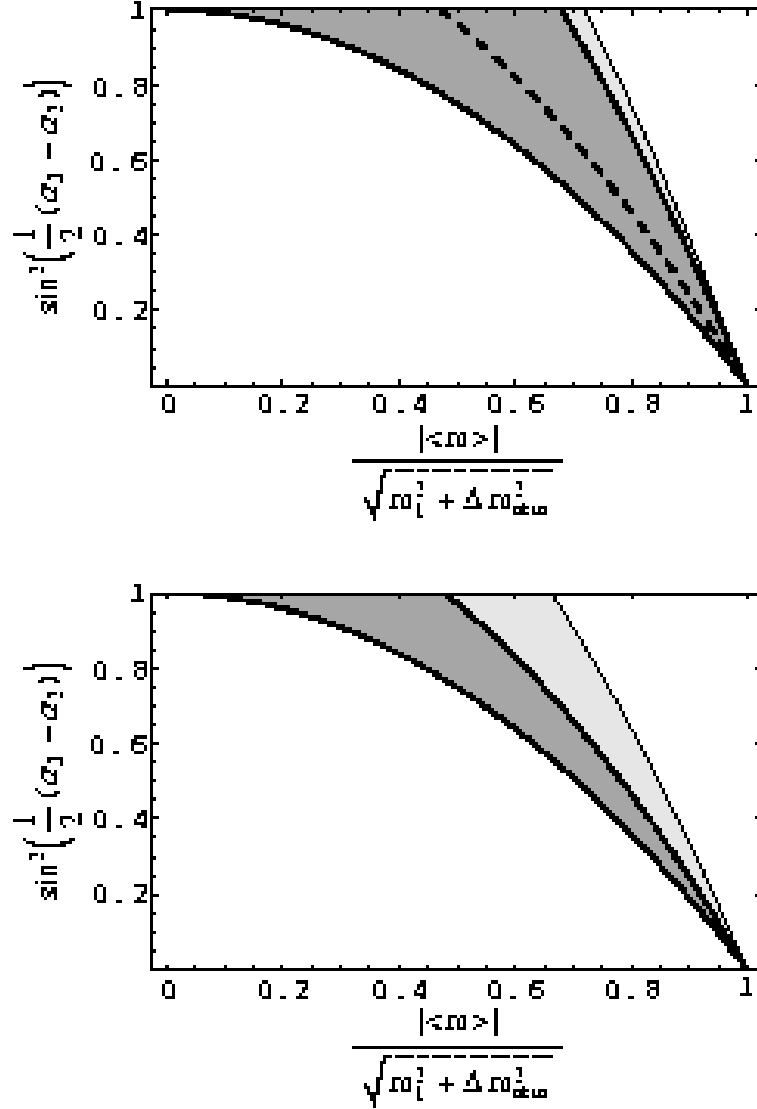


Figure 26: The CP-violation factor $\sin^2(\alpha_2 - \alpha_3)/2$ as a function of $|\langle m \rangle|$ in the case of partially inverted mass hierarchy spectrum, eq. (85), and the LMA (upper panel) and LOW-QVO (lower panel) solutions of ref. [58], obtained at 90% C.L. (medium-grey region with thick contours) and 99% C.L. (light grey + medium grey region limited by ordinary solid lines). The values of $|\langle m \rangle|$, corresponding to the best fit values of the input parameters, found in [58], are indicated by the dashed line. A value of $\sin^2(\alpha_2 - \alpha_3)/2 \neq 0, 1$, would signal CP-violation.

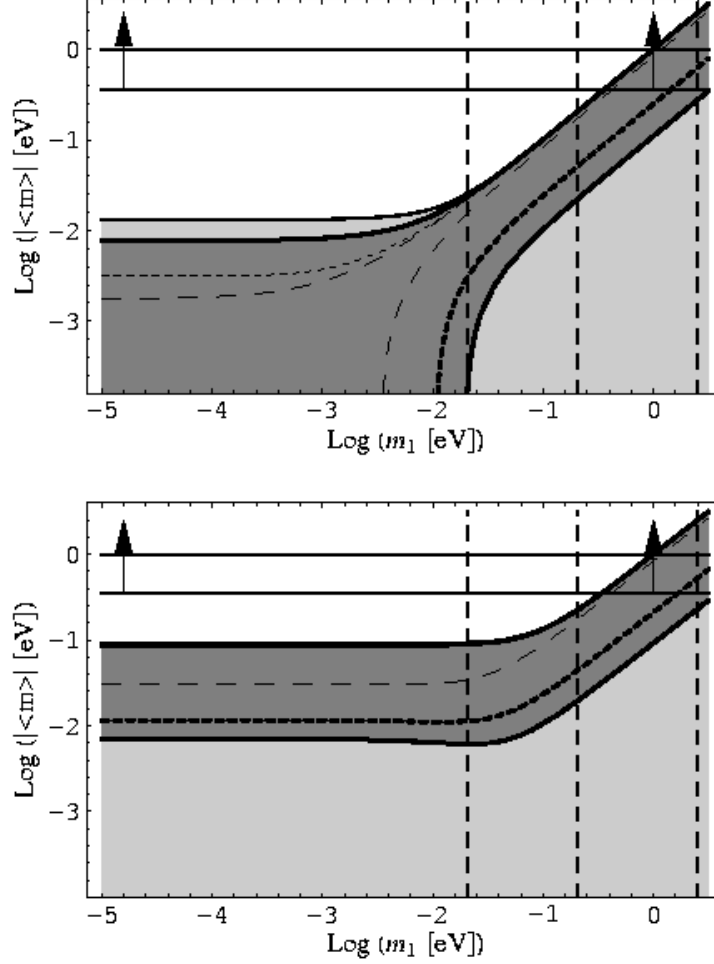


Figure 27: The dependence of $|\langle m \rangle|$ on m_1 in the case of $\Delta m_{\odot}^2 = \Delta m_{21}^2$ (upper panel) and of $\Delta m_{\odot}^2 = \Delta m_{32}^2$ (lower panel). For $\Delta m_{\odot}^2 = \Delta m_{21}^2$ (upper panel), the allowed values of $|\langle m \rangle|$ are obtained *i*) using the 99% C.L. results of ref. [58] for the LMA solution of the ν_{\odot} -problem (light grey and dark grey region between the thick solid line and the axes), for the LOW-QVO solution (light grey and dark grey region between the thin dotted line and the axes), and for the SMA one (the dark grey region between the thin dashed lines) and *ii*) using the results of ref. [7] for the LMA (dark grey region between the two doubly thick solid lines) and for the LOW-QVO (dark grey region between the upper doubly thick solid line and the doubly thick dotted line) solutions. For $\Delta m_{\odot}^2 = \Delta m_{32}^2$ (lower panel), the allowed values are obtained *i*) using the 99% C.L. results of the analysis of ref. [58] for the LMA and LOW-QVO solutions (light grey and dark grey region between the doubly thick line and the axes) and the SMA one (the dark grey region between the upper doubly thick line and the thin dashed one) and *ii*) using the results of ref. [7] for the LMA (dark grey region between the two doubly thick solid lines) and the LOW-QVO (dark grey region between the upper doubly thick solid line and the doubly thick dotted line) solutions. The regions divided by the vertical dashed lines on the upper (lower) panel correspond to *i*) $m_1 \ll 0.02 \text{ eV}$, and if $m_1 \ll \sqrt{\Delta m_{\odot}^2}$ ($m_1 < \sqrt{\Delta m_{\odot}^2} \ll \sqrt{\Delta m_{atm}^2}$) - to a hierarchical (inverted hierarchy) neutrino mass spectrum, *ii*) $0.02 \text{ eV} \leq m_1 \leq 0.2 \text{ eV}$, i.e., spectrum with partial hierarchy (partial inverted hierarchy), and to *iii*) $m_1 \geq 0.2 \text{ eV}$, i.e., quasi-degenerate neutrinos. For both cases the upper bounds from ref. [29], eq. (4), are shown by the horizontal upper doubly thick solid lines.

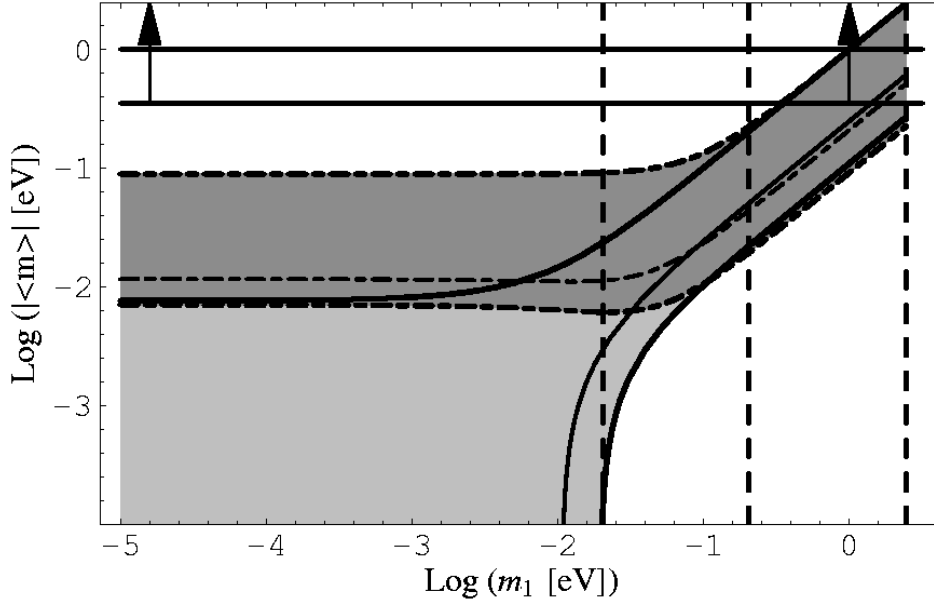


Figure 28: The dependence of $|\langle m \rangle|$ on m_1 *i*) for $\Delta m_{\odot}^2 = \Delta m_{21}^2$ and using the results of the analysis of ref. [7] for the LMA solution (light grey and dark grey region between the two doubly thick solid lines) and for the LOW-QVO solution (light grey and dark grey region between the upper doubly thick solid line and the thick solid line), and *ii*) for $\Delta m_{\odot}^2 = \Delta m_{32}^2$ and in the case of the LMA solution (dark grey region between the two doubly thick dash-dotted lines) and the LOW-QVO solution (dark grey region between the upper doubly thick dashed-dotted line and the thick dashed-dotted line). The upper bounds on $|\langle m \rangle|$ from ref. [29], eq. (4), are shown by the horizontal upper doubly thick solid lines. The regions separated by the vertical dashed lines correspond to *i*) $m_1 \ll 0.02$ eV, and if $m_1 \ll \sqrt{\Delta m_{\odot}^2}$ ($m_1 < \sqrt{\Delta m_{\odot}^2} \ll \sqrt{\Delta m_{atm}^2}$) - to a hierarchical (inverted hierarchy) neutrino mass spectrum, *ii*) 0.02 eV $\leq m_1 \leq 0.2$ eV, i.e., partial hierarchy and partial inverted hierarchy spectrum and to *iii*) the $m_1 \geq 0.2$ eV, i.e., quasi-degenerate spectrum.